STRUCTURAL DESIGN AND ANALYSIS OF AN EXISTING AERODYNAMICALLY OPTIMISED MORTAR SHELL

By
Yohannes Asfaw

A thesis submitted to the school of Graduate Studies of Addis Ababa University in Partial fulfillment of the requirements of the Degree of Masters of Science in Mechanical Engineering (Applied Mechanics Stream).

Advisor

Dr. A. Raman

Department of Mechanical Engineering
Addis Ababa University
Jan, 2008

ADDIS ABABA UNIVERSITY
SCHOOL OF GRADUATE STUDIES
DEPARTMENT OF MECHANICAL ENGINEERING

STRUCTURAL DESIGN AND ANALYSIS OF AN EXISTING AERODYNAMICALLY OPTIMISED MORTAR SHELL

By

Yohannes Asfaw

Approved by Board of Examiners:

Dr.

_____

Chairman, Department Graduate Committee

Dr. A. Raman _____

Advisor

Dr. _____

External Examiner

Dr. _____

Internal Examiner

Acknowledgment

I am gratefully acknowledges the help of my mentor Dr. Raman, who was always ready to give advice. I want to express grateful thanks to Dr. Alem who gave an encouragement to work and finish on this area.

At the end of my thesis I would like to thank all those people who made this thesis possible and an enjoyable experience for me, especially Dr. Berko Zecevic a professor in Bosnian defence technologies university.

I am grateful to the members of the institute for their support and their comradeship especially to my class mates.

I acknowledge the financial support by the Defence industries coordination office and Addis Ababa University research center.

Finally, I would like to express my deepest gratitude for the constant support, understanding and love that I received from my parents during the past years

TABLE OF CONTENT

List of Tables

List of Figures

Abbreviation and accronym

W : weight of projectile

A: area of bore, including grooves

CRH : caliber radius head

C : von karmann constant

C_{root_fin} : chord root fin

C_{tip_fin} : chord tip fin

T_{fin} : thickness of fin

h_{fin} : height of fin

A_{fin} : area of fin

P_{air_o}: 1.013×10^5 pa standard atmospheric air pressure at sea level

P_{air} : 1.013×10^5 pa Air pressure at given altitude

FI: flutter index

V : fragment velocity

M : mass of metal

C : the mass of charge

ρ_{ex} : density of explosive

ρ_m : density of metal

D : detonation velocity of the explosive

N (m): number of fragments heavier than mass m;

m: mass of a fragment ;

M_0: mass of casing ;

M_K: mott distribution factor

F : fragment force at flight

C_D: total drag coefficient;

A_f : face area of fragment

ρ_a : Local air density; and

V_f : fragment velocity.

m_c : mass of powder charge

Q_{ex}: energy of the powder per unit mass

Z: amount of burnt powder

V_b: Co volume of the gas

γ: Relation of the specific thermal capacities $\frac{c_p}{c_v}$

m: mass of the projectile

V: velocity of the projectile

P : Pressure in the barrel (made from propellant gasses)

S : Intersection area in the barrel

ρ: air density

$\dot{i}$: vector velocity

V : scalar magnitude of the vector velocity

$\vec{i} : \frac{\vec{V}}{V}$: a unit vector in the direction of the vector velocity

S: projectile reference area

$\vec{V}$: vector velocity (relative to the ground)

t : time

$\frac{d\vec{V}}{dt}$: vector acceleration

$\sum \vec{F}$: vector sum of all the aerodynamic forces

$\vec{g}$: vector acceleration due to gravity

$\vec{\Lambda}$: vector coriolis acceleration due to the earth's rotation

C_D: drag coefficient

C_{D_o}: zero-yaw drag coefficient (which usually varies with mach number)

$C_{D_{\delta^2}}\delta^2$: yaw drag coefficient (which usually varies with mach number)

α: angle of attack (pitch)

β: angle of side slip (yaw)

$C_{L_{\alpha_0}}$: linear lift force coefficient

$C_{L_{\alpha_2}}\delta^2$: cubic lift force coefficient

C_{M_α}: Overturning moment coefficient

$C_{M_{\alpha O}}$: linear Overturning moment coefficient

$C_{M_{\alpha 2}}$: cubic Overturning moment coefficient

C_{Mq} : pitch damping moment coefficient due to q_t

$C_{M_{\dot{\alpha}}}$: pitch damping moment coefficient due to $\dot{\alpha}_t$

L_N : length of nose cone

S_{fin} : height of fin (semispan)

L_F : length of fin at root cord line

X_R : swept distance of fin

X_B : distance from the tip of the nose to the start of the base of the fins

N_{fin} : number of fins

K_x^{-2} : moment of inertia along the projectile axis

K_y^{-2} : moment of inertia perpendicular to the projectile axis at center of gravity

Abstract

Mortar shell design is one of the most critical components in defence organization of projectile design. Unavilability of data and literature regarding artillery projectiles and rocket warheads, are considered to be one of the main contributors for the failure of manufacturing projectile in a local industry.

The need for this study is to design and fabricate this type of mortar shell in Ethiopia itself. Thus, the primary objective of this thesis is to develop a ballistics model of mortar shell and predicting the performance of mortar casing by ANSYS a finite element analysis package. Initially, the model is designed as a simplistic ballistic model capable of predicting the pressure and thrust generated by a propellant from a given set of input parameters. Its structure was determined on the basis of gun design empirical, experimental investigations of ballistic research laboratories (BRL) and weapon design of ammunition and artilleries of high explosive calibers.

High explosive warhead performances depend on its geometrical shape and dimensions, mass of explosive charge and explosive type, material of warhead case, initiation way and initiation point position, fuse type, round to round variations, etc. These are important parameters in determining the state of projectile features and stresses during the design of projectile. Thus, in this work a parametric study is conducted by varying the casing thickness and its length to study their effect on the fragmentation and stability of mortar projectile for the selected design parameters.

Analysis of stresses and deformation in the casing is an important area of research for projectiles optimal design. This thesis investigates the characteristics of high explosives warhead fragmentation analysis

This research not only gives fragmentation analysis of the shell by continuum method and trajectory calculations, but also gives the stress values for three different loading conditions correspond to launching, hitting the target and subsequent pyro blast.

To estimate the structural stress, three-dimensional model of a mortar shell was made by finite element method using ANSYS. This thesis also considers the study of variation of primary and secondary propellant charge on range. The results obtained by this research are presented and compared with the available literature. This study not only validates the design of the mortar shell, but also helps the Defense Ministry go ahead with its production for its need.

Objectives of the thesis

The specific objective of this thesis work is to determine structure and shell thickness for maximum fragmentation and to analyze mechanical stress due to different loads acting on 120mm mortar shell. The objective includes in general terms the following.

- To determine the basic structure of the mortar shell
- To determine the fragmentation, internal ballistic, range and stability of the mortar shell
- To determine the variation of the mechanical stress and deformation across the shell at three positions
    - at the launching caused by propellant gas pressure and temperature
    - impact at the instant of hitting the target
    - due to developed explosion pressure
- To select the appropriate material and dimension in order to withstand the mechanical stresses before bursting pressure
- To determine and analyze the structural performance of the mortar shell using finite element analysis (FEA)

These objectives will be achieved by employing the following procedures:

- Designing the structural configurations based on the gun design empirical and experimental standards
- Warhead fragmentation analysis
- Creating a 3D modeling of the shell
- Develop finite element solution/ANSYS analysis for the problem.
- Analyzing of FEM results in reference of failure criterion.
- Suggesting appropriate design and method of manufacturing.

Limitation and Scope of the work

Projectile design is a process that entails many complicated procedures which involve many aspects of knowledge, experience and interrelationships between disciplines. These decisions were typically made sequentially by individuals or teams with expertise in various areas of the design process. The design process utilizes a combination of hand estimations, predictions from software codes, and physical testing at each phase of the design process, iteratively, in order to arrive at an optimum configuration. Each discipline involved in the design process has over-time developed its own set of automated tools. Traditionally, projectile designers used a combination of formulas, charts, and rules of thumb and verified their predictions with experiments. These experiments included mechanical testing, wind tunnel testing, flight testing and target effects testing of pit fall and arena fragmentation. Measurements of warhead performances require very complex measuring equipment and measuring process itself is expensive as well. Out of many years of such experimentation, useful references evolved, such as the Army Design Handbook and Pamphlet series, specialized notes, and textbooks. These are not completely ignored in contemporary procedures and codes and will be included in this environment. These basic methods and models will be part of the initial (or rough cut) phase estimates in this system.

Due to unavailability of datas, softwares and test facility, the detail of exterior and intermediate ballistic parts, physical and chemical behaviour of explosives and the effect of fragment with the body of human tissue aren't taking into account in this work.

It has been shown that the development of projectile consists of four stages. In the first stage the basic structural shape dimension are determined based on the required effect of fragment and range causes the internal mechanical response of the mortar shell inside and outside the barrel structures. The second stage consists of the development of fragmentation analysis. This will be done using warhead fragmentation analysis. The present work focuses on the first stage: the determination of the internal and external mechanical response of mortar casing using finite element models.

There have been some efforts made to integrate the various areas of projectile design; the software code ANSYS comes closet to achieving this. Important aspects of these models are: geometry, loading that mimic the actual loading conditions and interface conditions with the barrel structures. The focus in this study will be on designing , anlysing at each design phases and modeling of mortar shell based on gun design method.

Outline of the Thesis

In Chapter 1, we give an overview of mortar projectile, system description and literature review. Chapter 2, Different gun design equations and empirical relations of high explosives are used and a suitable modification to determine the basic structural configuration of the shell at a desired load level is incorporated. Material properties of fabrics is described. In Chapter 3, the thickness of the shell is determined from the fragmentation point of view. Intensive Mott's equation computations have been performed to search for the best fragment velocity and optimum fragment weight. In Chapter 4, here, the primarily concern of basic internal ballistics are studied to determine muzzle velocity, pressure and charge consequence on range. In Chapter 5, Aerodynamic moments and forces for two dimensional domains are presented. A method to compute the static and dynamic stability of a spinning and finned type projectiles is validated. In Chapter 6, modeling and finite element solutions are presented for three conditions of the projectile along its trajectory from launching up to its end effect. In Chapter 7, we draw conclusions from this thesis and suggest possible avenues for future work.

CHAPTER 1

1.1 SYSTEM DESCRIPTION

1.1.1Anatomy and operation of a mortar

Generally 80 mm and higher caliber mortar is an artillery piece having a relatively short mostly smooth bore barrel (in few cases rifled) artillery weapons. It includes a smooth bore barrel resting on a base plate which in turn rests on the ground and fires an explosive projectile in a high arched trajectory. The projectile is fin stabilized and a conventional projectile includes a relatively massive casing containing a propellant and an explosive charge which, upon detonation, causes fragmentation of the casing. Mortars are cannon suitable only for the high-angle fire of shells. It gives high trajectories with short range and are usually loaded from the muzzle. Their primary function was to drop a *shell* or *bomb* behind earthworks or other defenses which could not be penetrated with gun fire. Mortars fired hollow iron spheres or shells filled with small shot, balls or similar anti-personnel devices combined with a small charge of powder which was ignited by a time fuse designed to explode just as it reached the target.

1.1.2 Non cartridge and cartridge based ammunition

Non cartridge based ammunition

In contrast to cartridge-based ammunition, many varieties of non-cartridge based ammunition contain their means of propulsion within the projectile.

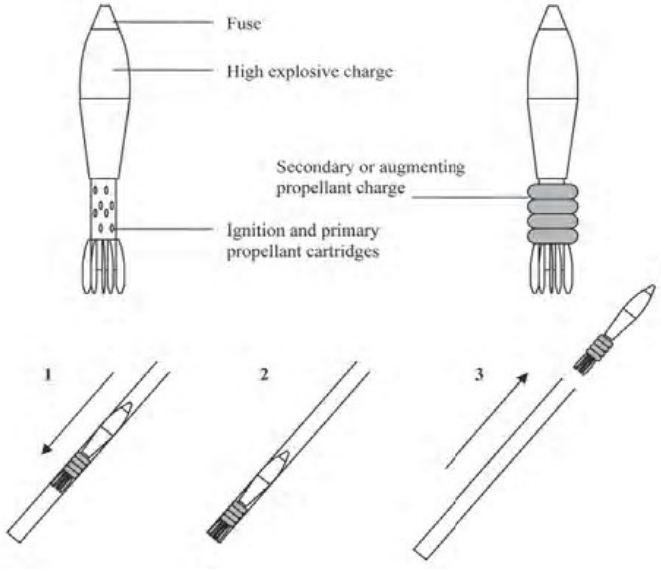

Fig. 1.1 Operational features of mortar artillery

These weapons are commonly referred to as rocket / projectile systems. They also include categories of ammunition such as rocket propelled grenades. Small arms do not operate in this way, but the majority of light weapons operate according to some variation of this principle. The basic configuration of this ammunition differs from system to system but, in all cases, the projectile consists of an explosive warhead and a rocket motor.

Propulsion can be of two types, depending on whether the combustion of gases occurs while the projectile is in the tube or whether it is launched from the tube by a small propelling charge prior to combustion of the main/augumenting. Mortars are different in that they operate in a similar way to firearms by using an integral charge (single combustion) but are not strictly cartridge based. As Figure1.1 illustrates, the mortar bomb is dropped into the tube (1). It strikes a firing pin at the base of the tube (2), which ignites the ignition cartridge and the primary propellant cartridge. This, in turn, ignites the augmenting or secondary propellant charge (if used), which is arranged in bands around the base of the mortar bomb (shown in grey). The expansion of gases in the tube forces the bomb out of the tube (3).

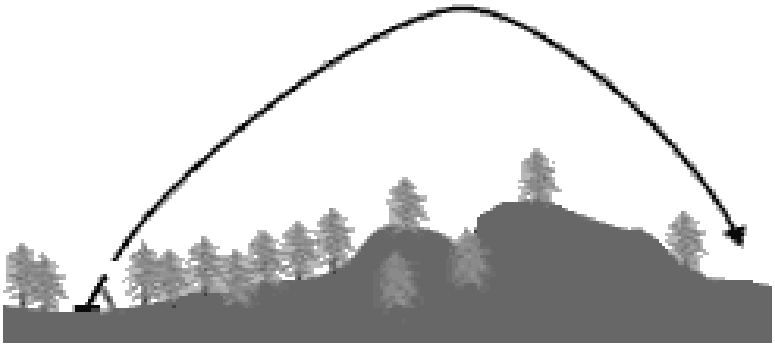

Fig. 1.2 High arched trajectory of mortar artillery

Cartridge-based ammunition

The cartridge is a self-contained unit comprising the cartridge case, the primer, the propellant (powder), and the projectile. All weapons that fire cartridge-based ammunition have a barrel, which is integral to the process of delivering energy, momentum, and direction to the projectile.

The operating principles of all weapons firing cartridge-based ammunition are the same. The cartridge partially seals the firing chamber of the weapon. On firing, a pin strikes the primer at the base of the cartridge (1) and ignites it. This ignites the powder, which burns rapidly and generates expanding gases. The gases are forced down the length of the barrel, pushing the projectile in front of them (2) and eventually out of the barrel (3). Simultaneously, the cartridge case expands, thereby completing the firing chamber seal. The momentum imparted by the process propels the projectile but there is no process within the projectile that sustains movement. As a consequence, the projectile begins to lose velocity shortly after it leaves the barrel.

1.1.3 Unguided ammunition

Unguided ammunition simply follows the trajectory assigned by the firer. Their trajectory cannot be adjusted once they have left the barrel, or launch tube, of the weapon. Unguided weapons are a common feature in most conflicts and include mortars, rocket launchers, RPGs, recoilless rifles, and rifle grenades. Mortars fire ammunition in high arc trajectories designed to hit targets beyond the sight of the firer or behind obstacles (Figure 1.2). The basic design of a direct-fire projectile includes a warhead section and a propellant section. This type of direct-fire weapon was developed to meet the need for a weapon to defeat armored vehicles. The weapons and ammunition are now designed for many different roles, including targeting armored and light vehicles, destroying hard targets such as bunkers or houses, and anti-personnel roles. Because such rocket-propelled ammunition is launched from an unrifled tube, rather than a rifled barrel, no spin is imparted to the projectile on launch. For this reason, stability is achieved through stabilizing fins, which produce a slow rate of roll in flight.

1.1.5 Large caliber ammunition-Types of warhead

Large caliber ammunition may be classified into five major groups: blast (including air and underwater burst), fragmentation, shaped charged, pyrotechnics, and cluster.

Blast

A blast warhead is one that is designed to achieve target damage primarily from blast effect. When a high explosive detonates, it is converted almost instantly into a gas at very high pressure and temperature. Under the pressure of the gases thus generated, the weapon case expands and breaks into fragments. The air surrounding the casing is compressed and a shock (blast) wave is transmitted into it. Typical initial values for a high-explosive weapon are 200 kilo bars of pressure and 5,000 degrees Celsius. The energetic materials used by munitions produce an exothermic reaction defined either as a deflagration or a detonation. A deflagration is an exothermic reaction that propagates from the burning gases to the unreacted material by conduction, convection, and radiation. In this process, the combustion zone progresses through the material at a rate that is less than the velocity of sound in the unreacted material.

Fragmentation

The study of ballistics, the science of the motion of projectiles, has contributed significantly to the design of fragmentation warheads. Specifically, terminalballistics studies attempt to the determine the laws and conditions governing the velocity and distribution of fragments, the sizes and shapes that result from bursting different containers, and the damage aspects of the bursting charge fragmentation.

Approximately 30% of the energy released by the explosive detonation is used to fragment the case and impart kinetic energy to the fragments. The balance of available energy is used to create a shock front and blast effects. The fragments are propelled at high velocity, and after a short distance they overtake and pass through the shock wave. The rate at which the velocity of the shock front accompanying the blast decreases is generally much greater than the decrease in velocity of fragments, which occurs due to air friction. Therefore, the advance of the shock front lags behind that of the fragments. The radius of effective fragment damage, although target dependent, thus exceeds considerably the radius of effective blast damage in an air burst.

Whereas the effects of an idealized blast payload are attenuated by a factor roughly equal to 1/R3 (R is measured from the origin), the attenuation of idealized fragmentation effects will vary as 1/R2 and 1/R, depending upon the specific design of the payload. Herein lies the principle advantage of a fragmentation payload: it can afford a greater miss distance and still remain effective because its attenuation is less.

Anti-personnel fragmentation munitions are designed to destroy or maim personnel or to damage material enough to render it inoperable. In the area of field artillery, the flechette or beehive round is an example of an anti-personnel warhead. The payload in this projectile consists of 8,000 steel-wire, fin-stabilized darts. Upon detonation the darts, or flechettes, are sprayed radially from the point of detonation, normally within sixty feet of the ground. It is extremely effective against personnel in the open or in dense foliage.

Shaped charge

A shaped charge warhead consists basically of a hollow liner of metal material, usually copper or aluminium of conical, hemispherical, or other shape, backed on the convex side by explosive. A container, fuze, and detonating device are included.

When this warhead strikes a target, the fuze detonates the charge from the rear. A detonation wave sweeps forward and begins to collapse the metal cone liner at its apex. The collapse of the cone results in the formation and ejection of a continuous high-velocity molten jet of liner material. Velocity of the tip of the jet is on order of 8,500 meters per sec, while the trailing end of the jet has a velocity on the order of 1,500 meters per sec. This produces a velocity gradient that tends to stretch out or lengthen the jet. The jet is then followed by a slug that consists of about 80% of the liner mass. The slug has a velocity on the order of 600 meters per sec.

Pyrotechnics are typically employed for signaling, illuminating, or marking targets. *Illumination*--these warheads usually contain a flare or magnesium flare candle as the payload, which is expelled by a small charge and is parachuted to the ground. During its descent the flare is kindled. The illuminating warhead is thus of great usefulness during night attacks in pointing out enemy fortifications. Because these flares are difficult to extinguish if accidentally ignited, extreme caution in their handling is required.

Smoke--These munitions are used primarily to screen troop movements and play a vital role in battlefield tactics. A black powder charge ignites and expels canisters that may be designed to emit white, yellow, red, green, or violet smoke.

Markers--White phosphorus is commonly employed as a pay-load to mark the position of the enemy. It can be very dangerous, especially in heavy concentrations. The material can self-ignite in air, cannot be extinguished by water, and will rekindle upon subsequent exposure to air. Body contact can produce serious burns. Copper sulphate prevents its re-ignition.

Cluster munitions are canisters containing dozens or hundreds of small bomblets for use against a variety of targets, such as personnel, armored ve-hicles, or ships. Once in the air, the canisters open, spreading the bomblets out in a wide pattern. The advantage of this type of warhead is that it gives a wide area of coverage, which allows for a greater margin of error in delivery.

1.1.6 Mortar Shell Components At A Glance

Mortar Projectile

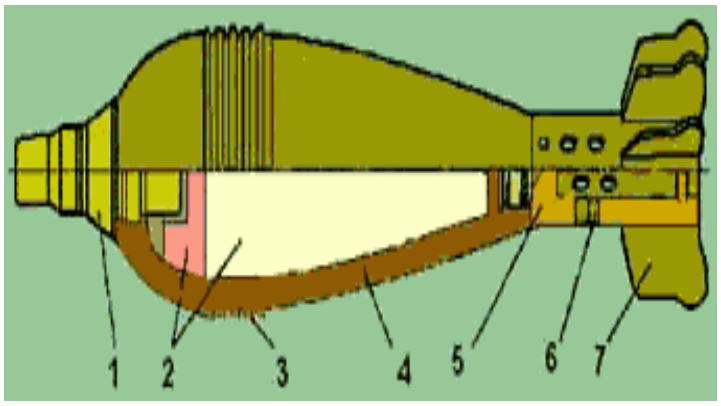

1. The Detonator
2. The Warhead (explosive)
3. The Raised flange
4. The Casing
5. The Stabilizer
6. The Propellant gas channels
7. The Stabilizer wing

Figure 1.3 Mortar shell components

A mortar round is usually a very simple and effective weapon. The construction of one usually consists of an explosive charge, stabilizer, detonator and basic and supplemental charges.

The case is designed to provide maximum fragmentation during the explosion of the charge, which is detonated either by an impact or a proximity fuse. The stabilizer fins are mounted at the rear of the round and provide directional stability during the round's ballistic flight. Such devices are needed, as the round is fired from a low pressure, smooth bore tube. The firing occurs by the ignition of the primary and secondary charges located at the base of the round inside the stabilization package. The expending gases escape from the holes in the tube and propel the round upward through the mortar tube.

1.1.7 Types Of Mortars

Mortars, which are infantry weapons, fall into three main categories depending on their calibers:

• Light infantry—up to 60;

• Medium caliber—81-mm and 82-mm tubes deployed in lieu of light artillery; and

• Heavy—120-mm weapons except for 160-mm and 240-mm mortars .

Mortars are ground emplaced, towed, or vehicle mounted, vehicle-mounted turreted mortars. Mortars have a payload advantage over tube artillery. The 120-mm mortar has a round with a high-explosive capacity close to that of a 155-mm artillery projectile.

Mortars have long been considered area weapons. That is still true. However, “area” does not mean inaccurate: Target information and mortar base plate data must be as accurate as possible to ensure successful engagement of the target. The area effect of the weapon system is a factor of applying the mortar “footprint” and the fragmentation effect of the ammunition. Also, in direct response to developments in “smart” ammunition, the demand is for a mortar to attack a precision target; accordingly, the round must be reasonably expected to arrive in the area of the target thus reducing the workload on the seeker and processor components.

Smaller mortars (up to 81 mm) are commonly used and transported by infantry based mortar sections as a substitute for, or in addition to, artillery.

Ammunition for mortar systems generally come in two main varieties: fin-stabilized and spin-stabilized. The former have short fins on their posterior portion that control their path in flight. The latter use spin (similar to a thrown American Football) to balance and control the mortar shell.

1.1.8 Stabilization

Spin-Stabilized Projectiles

Most guns in use today use spin-stabilized projectiles. Spinning a projectile promotes flight stability. Spinning is obtained by firing the projectiles through a rifled tube. The projectile engages the rifling by means of a rotating band normally made of copper. The rotating band is engaged by the lands and grooves. At a nominal muzzle velocity of 2800 feet per second, spin rates on the order of 250 revolutions per second are encountered. Spin-stabilized projectiles are full bore (flush with the bore walls) and are limited approximately to a 5:1 length-to-diameter ratio. They perform very well at relatively low trajectories (less than 45° quadrant elevation). In high trajectory applications they tend to overstabilize (maintain the angle at which they were fired) and, therefore, do not follow the trajectory satisfactorily.

Spin-stabilised rounds require a rifled barrel. Since mortars on the whole are top-loaded, the mortar bomb has a pre-engraved band that engages with the rifling of the barrel. The increase in accuracy is at a cost in loading time.

Fin-Stabilized Projectiles

These projectiles obtain stability through the use of fins located at the aft end of the projectile. Normally, four to six fins are employed. Additional stability is obtained by imparting some spin (approximately 20 revolutions/second) to the projectile by canting the leading edge of the fins. Fin-stabilized projectiles are very often sub-caliber. A sabot, wood or metal fitted around the projectile, is used to center the projectile in the bore and provide a gas seal. Such projectiles vary from 10:1 to 15:1 in length-to-diameter ratio. Fin-stabilized projectiles are advantageous because they follow the trajectory very well at high-launch angles, and they can be designed with very low drag thereby increasing range and/or terminal velocity. However, fin-stabilized projectiles are disadvantageous because the extra length of the projectile must be accommodated and the payload volume is comparatively low in relation to the projectile length. For projectiles fired without spin or only with a small spin the stabilising influences must be created by aerodynamic forces in this case, the interdependent position of impact of aerodynamic force A and the center of gravity S play a decesive role. when A is positioned infront of S, the moment produced

is destabilising, as described with projectiles with a spin. When A lies behind the center of gravity, the air force moment has a stabilising effect (behaviour of the wind-T, fig.1.4). Thus, spin-free stabilisation involves positioning the point of impact of the air behind the centre of mass. This can be obtained by the following means:

- shift the center of gravity towards the front by redistributing the load (dart stabilization) fig. 1.4a
- shift the point of impact of the air towards the rear by intoducing an aerodynamic forceat the tail ,which can be done in two ways:
    - by increasing the tail drag (drag stabilization) (fig.1.4b) or
    - by increasing the lifting forces at the tail (wing stabilization) (fig.1.4c)

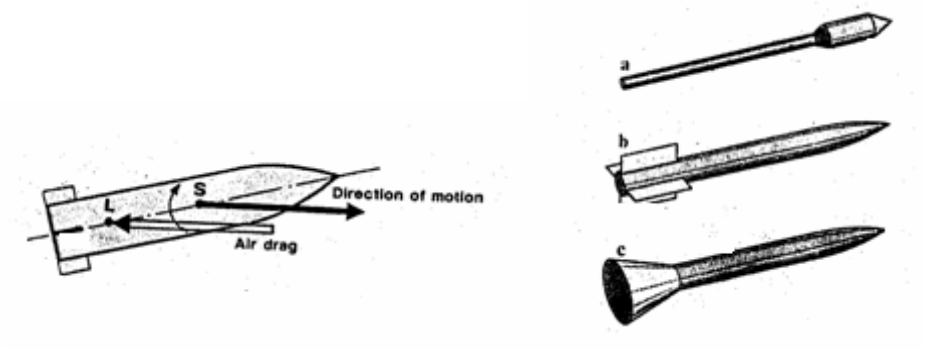

Fig. 1.4. Center of gravity and center of pressurre within a spinless stabilised projectile.
Fig. 1.4 a-c Methods of spinless stabilization, a. dartstabilisation; b. fin stabilisation; c.stabilisation by increasing the tail darg.

1.1.9 Explosives

There are two explosives trains in each conventional round of artillery ammunition; the propelling charge explosion train and the projectile explosive train. The projectile reaches the target area by the power obtained from the propelling charge explosive train. The function of the projectile in the target area depends on the type of projectile explosive train.

The propelling charge explosive train consists of the primer, igniter, and propellant. The propelling charge explosive train is initiated by the primer, which is a small amount of very sensitive explosive. The primer is very sensitive to shock, friction, spark, and heat, and must be kept protected and away from other ammunition components. In separate loading ammunition, the primer is a separate item of issue. The igniter provides hot flaming gases and particles to ignite the propelling charge. The igniter consists of black powder or Clean Burning Igniter (CBI). The igniter is very hygroscopic and subject to rapid deterioration on absorption of moisture. If kept dry, however, it retains its explosive properties indefinitely. The igniter for semi-fixed ammunition is an integral part of the primer. It consists of a perforated tube filled with black powder and is permanently mounted in the cartridge case. In separate loading ammunition, the igniter is in a circular red pancake shaped bag sewn to the base increment of the propellant. When ignited by the primer, the igniter sends hot flaming gases around the charge to ignite the propellant.

A propellant is a large amount of insensitive but powerful explosive that propels the projectile to the target. Semi-fixed ammunition propellant is generally issued with seven increments numbered 1 through 7, and connected by a thin acrylic cord. Each increment is a different size because each increment has a different pre-measured amount of propellant. Increment 1 and 2 are single perforated and increments 3-7 are multi-perforated. Separate loading ammunition propellants are issued as a separate unit of issue in sealed canisters to protect the propellant. The amount of propellant to be fired with artillery ammunition is varied by the number of propellant increments. The charge selected is based on the range to the target and the tactical situation.

1.2 LITERATURE REVIEW

A review of literature was conducted in three key areas of relevance to this thesis : behaviour of projectile in the weapon systems, external and end effect of the projectile, Berko Zecevic et.al [1] recently research shows that design of the HE warhead is process confronted with series of contradictory requirements. Influence of warhead design on lethal efficiency is very complex. Lethal efficiency of HE warhead depends on the form and dimension of the warhead, quantity and type of explosive, warhead case material, warhead case thickness, fuse type, explosive train etc. At warheads natural fragmentation, fragments geometry, their mass and spatial distribution are functions of designed shape of the warhead case(shell), mechanical properties of case material (tensile strength and yield strength) and performances of explosive (physical and energetic). It is essential to have a capability to make warhead performance predictions in the earliest phases of ammunition or warheads preliminary design.

Ponder Timothy C. et.al. [2] had computed a cylindrical warhead design optimization segment of the weapons optimization techniques computer program. This segment enables the user to optimize or parameterize the basic design parameters of a theoretical warhead for a given target or set of targets. The warhead lethality is determined as a function of the basic design parameters: warhead weight, warhead volume, warhead diameter, charge-to-metal ratio, fragment mass, ratio of warhead length to diameter, and fragment height-to-width ratio. This segment can also optimize or parameterize height of burst, terminal velocity, impact angle, and fragment spray angle.

An elongated, aerodynamically improved ballistic projectile fuse, having an overall fuse length greater than its maximum diameter by a factor of approximately two, includes a lightweight aluminum fuse body having forward and rearward portions and an interiorily disposed firing pin with a shearable flange thereon. A steel sleeve mounted in the fuse body is provided for supporting the firing pin with a head portion thereof forwardly directed and exterior to the sleeve and for guiding the firing pin through the fuse body toward the rearward portion thereof subsequent to impact of the fuse with a target. A cap, enclosing the firing pin head, is configured for collapsing and impacting the head upon fuse impact with a target, thereby causing shearing of the firing pin flange and driving of

the firing pin rearwardly toward detonation means disposed within the fuse body rearward portion. The cap is in turn enclosed by a windscreen which provides an aerodynamically streamlined, forward continuation of the fuse body. Means joining the windscreen to the sleeve enables separation there between on target impact, thereby enabling the windscreen to collapse the cap. [3]

An army mortar shell having two sections linked to one another by linkages liable to shear and located to the rear of the sealing band, and where the head of such shell is equipped with a time fuse and inside the shell there are two interlinked chambers containing the charge which is released into the air when said two chambers are separated from one another due to the effect of a cartridge located inside the foremost chamber [4].

Moss et al. [5] provided a good review of 'ballistics', the study of the motion, behavior and effects of projectiles. Their study had a major part of internal, intermediate, external and terminal ballistics. Terminal ballistics has further divided into material and wound ballistics dealing with projectile interaction with inanimate (material) and animate targets respectively. Internal ballistics studies the events inside the weapon when the primer is detonated igniting the propellant. From the wound ballistic aspect it is relevant to know the internal ballistic factors affecting the projectile velocity. Every powder type has its characteristic burning velocity. Burning is actually controlled explosion since no external oxygen is required. It obeys Piobert's law, which states that the surface of a powder granule is burned away before the layer beneath it is ignited. This allows the control of the burning velocity and pressure build-up by using either decreasing, constant or increasing surface area of the powder granule degressive, neutral and progressive powders. Beat vogelsanger [6] study indicates, in addition, special coating of granules may be used. The burning velocity is often reduced in subzero temperatures.

Rinker [7] had computed that when the pressure increases sufficiently high, it pushes the projectile into the barrel. The forces involved cause radial expansion and torsional twist of the barrel as the projectile is forced into the helical rifling. This and the advancing pressure wave in the barrel metal will make the barrel oscillate. Moss et al. also studied an intermediate ballistics that examines the events that take place when the projectile

exits the muzzle in transition from internal to external ballistics The high pressure gases behind the projectile cause turbulence which will to an extent disturb the stability of the projectile. Rinker had further studied that due to small differences in the powder charge and its burning a projectile may exit the barrel at different phases of the oscillation. This will have a deteriorating effect on the accuracy of the projectile the amount of which depends on the oscillation characteristics. Barrel oscillation may also increase the initial yaw of the projectile.

Kneubuehl et. al [8] deal 'external ballistics' was conducted to determine the phenomena of the projectile in flight, is subjected to aerodynamic forces that combined with its construction, internal ballistics and intermediate ballistics may cause yawing, tumbling, precession and nutation of the projectile

Rinker had innovatively researched that a projectile will not fly accurately and straight unless it is stabilised because of minor symmetric flaws in the projectile material or centre of gravity being behind the centre of pressure as is usually the case with aerodynamically efficient forms. There are two principal stabilisation mechanisms: drag and spin. Moss et al studied drag stabilisation which is done by means of a tail cone, tail fins or a drag tail causing increased drag in the rear and thus keeping the projectile straight. spin stabilisation means giving the projectile rapid rotation around its longitudinal axis. This is done either by using a rifled barrel or angled tail fins on the projectile. Spin makes even a tail heavy projectile fly straight provided that the rotation speed is high enough. With too little spin the projectile will start tumbling in mid air and may hit the target at any angle with unpredictable wound ballistic results. J.A Cardes et.al [9] had studied to estimate the minimum rifling twist required to stabilise a given projectile the Greenhill equation is often used because it gives reasonable approximations of the required twist and is very simple to use.

Moss et al. had conducted a research with the gyroscopic stability of a projectile depends on its shape and weight distribution, density of the penetrated substance (usually air) and spin rate induced by the projectile velocity and rifling twist.

Anthony J. Calise et. al [10] described an experimental model and the outcome of the research suggested that according to ICAO-defined standard atmosphere air density at sea

level is 1.225 kg/m3 and density of muscle tissue 1060 g/cm^3 the stability coefficient reveals that the spin rate required to maintain stability in muscle tissue would have to be some 860 000 times faster than in the flight through air. As this is not possible the projectiles will in most cases rapidly lose their stability after entering the tissue and start tumbling.

The gyroscopic stability equation is problematic to use since the axial and transversal moments are ordinarily not published by ammunition manufacturers and would have to be measured using a torsional pendulum.

S D naik [11] recently studies the basic class of problems in stability of an axis-symmetric body; this has been discussed by many researchers. Before 1930, the condition $0 < \delta < 1$ dominated every design in flight dynamics. Fowler attempted the stability of high angle of fire through his β type equations. As awareness of the implications of mathematical modelling to investigate the motion in its full entirety developed during the Second World War, many models were made and linear motion was developed in its completeness. It was investigated that nonlinear motion where the parameter is positive and established that if $1 - 4qs > 0$, the ensuing motion is bounded. It derived the McShane– Murphy stability condition for slowly yawing motion from Fowler's dynamical equations generalised by Rath taking into account the complete aerodynamic force system. The motion of a nonlinear Lock–Fowler missile under the same condition using the Routh–Hurwitz criterion has been discussed.

Moss et al. had innovatively researched that too much spin will result in an over stabilised projectile. It will resist any change in the trajectory and fly eventually at a marked yaw angle since the longitudinal axis of the projectile will not follow the trajectory but will maintain its original angle of elevation. This will result in increased drag and shorter range.

At the very moment when the projectile leaves the barrel gravity starts to pull it downwards. The faster the projectile and the better it retains its velocity the farther it will fly before hitting the ground. The trajectory of the projectile will therefore be curved and depends on the angle of the weapon, projectile mass, velocity, diameter, length and form.

Rinker and Kneubuehl et.al were investigated further a form factor number (*Fform*) is used to describe the projectile form. Rinker, studied that the trajectory also depends on

the prevailing external atmospheric conditions of temperature, air pressure, humidity and the velocity and direction of the wind. The projectile's aerodynamic efficiency i.e. capability to overcome the air resistance and retain its velocity is usually described with ballistic coefficient C_b. The higher the C_b, the better the velocity is retained.

Rinker had stated that a study that crosswind pushes the projectile aside and either up or down depending on the direction of the wind and the spin of the projectile. Crosswind increases the difficulty of accurate shooting. It pushes the projectile aside and either up or down depending on the direction of the wind and the spin of the projectile. Moreover the wind is rarely constant and may vary throughout the trajectory making the estimation of its effects on the projectile rather difficult in an actual situation. The susceptibility of a projectile to crosswind can, for comparison purposes, be estimated using an arbitrary of, 3 m/s transversally to the projectile trajectory.

Kneubuehl had invesigated a projectile behavior in the target and wound ballistics, 'the part of terminal ballistics dealing with what happens when a projectile strikes a living being'. It is characterised by very rapid events, high pressures and great deformation rates. A projectile must have a significant amount of kinetic energy to reach the target, penetrate into it and perform its task.

Jorma Jussila [12] did computations and aimed at analyze the effect of different impact directions following, and to evaluate existing that a projectile impacting the target has an impact mass of *mi* (g) and velocity *vi* (m/s). Impact energy is partially dissipated into the target and performs work upon it. Both the projectile mass but more significantly its velocity determines the amount of kinetic energy. If the energy is not dissipated into the target, it is used somewhere else. The wound ballistic energy equation can be expressed interms of the residual kinetic energy, the impact energy, the energy used by projectile deformation and the energy dissipated into the target tissue. Since impact energy has to be significant, *deformation energy* and *dissipated energy* must be maximised in order to minimise residual energy. The residual energy is a significant factor describing the danger to bystanders when the projectile completely penetrates and exits the primary target continuing its flight. Pirlot also uses the term deformation energy in conjunction with deformation of tissue simulant.

Kinetic energy dissipation (*Ed*) can be increased by projectile instability, deformation and fragmentation. When a rigid tail-heavy projectile hits the target it tends to start tumbling because the rate of spin is insufficient to maintain stability in dense medium like tissue. This increases the cross-sectional area in the direction of penetration which increases the dissipation of kinetic energy. The process is, however, somewhat out of control. The precise depth at which tumbling occurs is difficult to predict as it depends on the yaw angle on impact, properties of the tissue encountered and internal instabilities of the projectile. Controlled deformation can in principle be achieved by a cavity in the tip of the projectile.

Rinker studied the impact of changing the tip of the projectile changes its aerodynamic form factor, possibly reducing the ballistic coefficient *Cb* and shortening the tactical range. Upon impact these projectiles start expanding at the tip. This makes the cross-sectional area larger and increases *Ed*. It will also shift the centre of gravity of the penetrating projectile closer to the tip making a long projectile in theory more stable in penetration. The dimensions and surface angles of the cavity together with the projectile materials and construction determine the rate and type of expansion.

Projectile fragmentation can be controlled by jacket thickness, making prefragmentation incisions in the jacket and by varying the strength of bonding between the projectile core and jacket.

D. Levin [13] studied surface roughness effect on the aerodynamic characteristics of a blunt body. The use of a smooth surface, for small projectiles, may lead to a reduction of drag at zero angle of attack. However, for specific configurations, especially those with blunt aft sections, an adverse normal force characteristic may develop, causing stability problems, similar to the one described by Schneider. On the other hand, a skilful use of the separation-zone motion could serve as a maneuvering tool for unguided projectiles that are required to perform a search motion, and a built-in instability could maintain the desired motion.

CHAPTER 2

2. BASIC STRUCTURAL CONFIGURATION

2.1 Strength and capacity, weight, sectional density, length, cavity and shape

Strength and capacity

The shell has to meet various design features governing its form and dimensions. The external contour is more or less determined by the ballistic requirements. The shell must also have adequate strength to withstand the forces of projection. Shell are therefore made of forged steel to possess the requisite strength of design which is, therefore, the prime factor to determine the dimensions of the shell body in avoiding premature; the internal design of the shell and the quality of the material are, therefore, limited by the factor of strength.

Weight

The weight of projectile determines its kinetic energy, and it, therefore, follows that an increase in the weight of the projectile will give a longer range and flatter trajectory. But this does not mean that the weight can be increased indefinitely, since the safety limits of the maximum stress the gun can sustain have to be considered. Again the increase in the weight of the projectile results in an increase in length, which may upset the balance. The relation between the weight of a projectile, propellant charge, muzzle velocity and pressure, is a part of internal ballistics, but experience has shown that a suitable weight for a projectile is obatainable from the relation $W=d^3 \times K$, where W is the weight of the projectile in kilogram, d the caliber in milimeter and K a constant of about 0.5.

Different types of projectiles for the same gun should practically have the same weight so as to realize the same range, thereby simplifying the compilation of range tables. Variation in length also affects the range and the length is, therefore, usually kept the same. Where it becomes absolutely essential to have a projectile, which is significantly different in weight or length from the standard, matching up in ranging is effected, at least within the 'critical range' zone, by effecting suitable modification to the shape of the head. [14]

Sectional density

The sectional density', which is the weight of the projectile per square milimeter of the bore, has also an important bearing on the design of projectiles. This is given by:-

$$SD = \frac{W}{A}$$

Where W = weight of projectile in kg

A = area of bore, including grooves in square milimeter and is given by

$A = 1.02\frac{\prod}{4}d^2$, where d is the calibre in milimeter.

The sectional density is dependent on the calibre and has an average value of 0.6 of the calibre. The sectional density which determines the distribution of weight and hence the position of *CG* in a projectile is a matter of considerable importance. As a general rule, the centre of gravity of a projectile should be in the longitudinal axis and close to or at the front of the centre of pressure (the point of application of the resultant of the forces due to the resistance of air in flight). Slight variation in the position of the centre of gravity with respect to the centre of pressure has negligible effect on the dispersion, and is therefore permissible in the design.

Length

The length of a projectile is connected with the rate of spin required to stabilize it and the exact length of a particular type is fixed after a series of experiments with different lengths. The length of modern projectile varies generally from 2 to 4 calibers. For certain blunt nose heavy projectiles, a ballistic cap of light weight is attached to minimize the retardation due to air resistance by increasing the *CRH*. This obviously increasing the weight of the projectile without adversely affecting its balance [14].

The limits of length for a conventional gun-fired projectile, which must be observed with respect to stability, is between 4.5 and 6 calibers. If length "x" is reserved for the body, and length "y" is reserved for designing the base, the remaining length can be used for shaping the nose.

Total length of projectile = between 4.5d and 6d

Length of streamlined base = 0.5d (dimensions are approximate.)

Length of body = 1.3d

Length available for shaping the o-give radius = 2.7 d - 73.8mm

Minimum length of 120mm projectile can be = 4.5d = 4.5x120mm=540mm

Maximum length of 120mm projectile can be = 6d = 6x120mm=720mm

Length available for shaping the ogive rdaius, body with streamlined base = 466.8mm

Shape

As the projectile moves along its trajectory in air, there is a systematic loss in its velocity due to the tremendous air resistance, which opposes the motion of the projectile. This opposing force is due to the combined effects of the resistance at the head, the skin friction due both to linear and rotating motions, and the drag acting at the base. The shape of the projectile must therefore, be considered in designing for minimum resistance. An ideal shape would be the one which would minimize the effect of the opposing force, give perfect stability throughout its flight, and realize the maximum range. This is more or less of a practical consideration and the ideal shape is decided after a series of firing trials with projectiles of varying shape.

While the external shape and contour determine the ballistic qualities of the projectile in flight, the internal shape, which has a direct bearing on the wall thickness and choice of material, determines the strength of design of filled projectiles. Since the projectile has to withstand the forces of projection, reach its destination intact, absorb the shocks of impact and avoid premature functioning, a sound design is of the utmost importance.

External shape

In general, the projectile has a an ogival front body and a tail tube suitably positioned near the base. Some projectiles may also be streamlined at the base. Depending on the design, the projectile is screw threaded at the nose or base to take the fuze. The shape of the fuse is also made to follow the same contour of the projectile. Solid shot generally follow the same shape as other projectiles but the head is comparatively blunt effective for effective armour piercing.

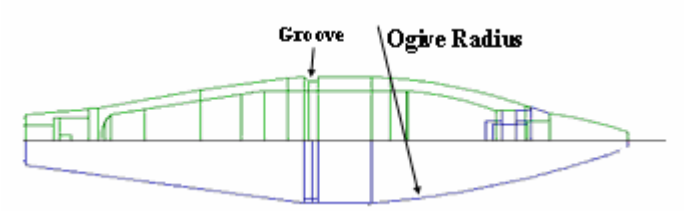

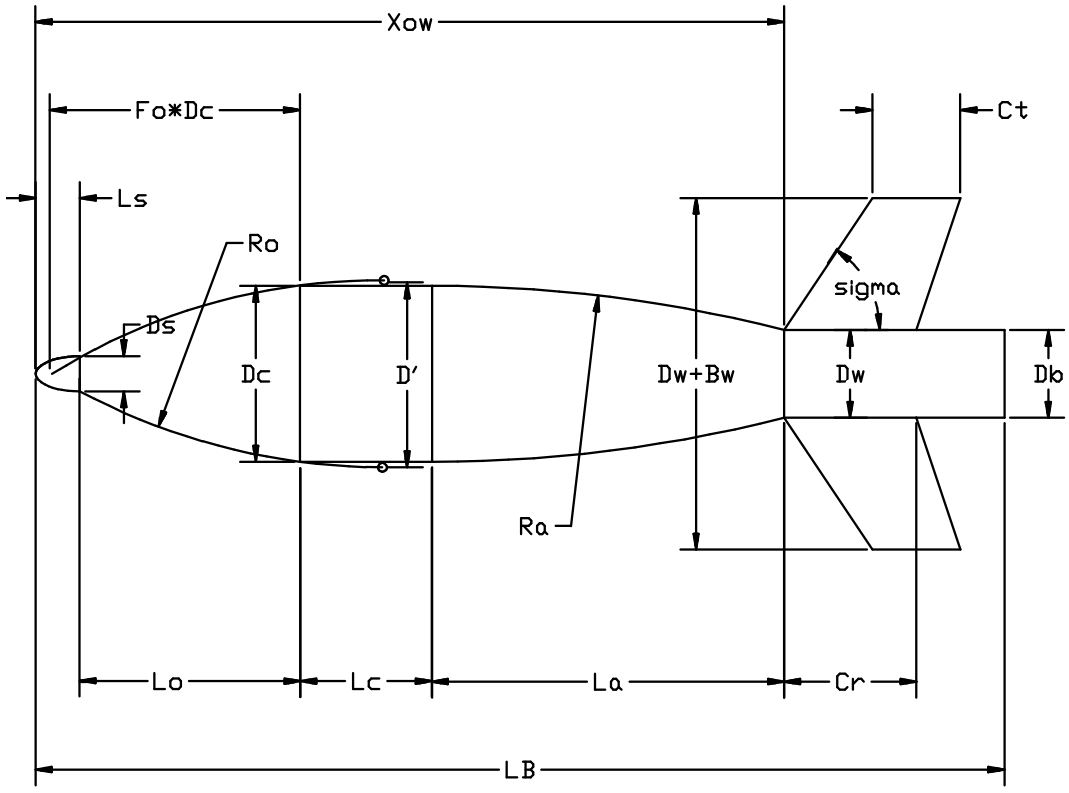

Fig.2.1 Radius of curvature of a mortar shell

Internal shape

The internal walls at the head and the body portion follow the same external contour, with usually the same thickness as at the shoulder, tapering towards the base where the wall thickness is increased. The metal is sometimes thickened towards the fuze hole to get sufficient depth for the fuze. The internal shape is slightly altered as per design requirements, and in some cases the walls are perfectly parallel, tapering towards the nose, and base. The internal surface is perfectly smooth, free from scales butts and sharp edges. The entire surface is copal varnished which on storing sets hard, giving a very smooth surface, there by preventing possible corrosion of the metal and interaction or friction with the filling.

Body

In reference to the entire projectile, the term body specifically denotes the portion between the shoulder of the projectile and the tail tube. This portion is ogive radius in shape, subsequent to a diameter nearly equal to the diameter of the bore across the lands with the windage necessary to ensure free passage through the bore. The solid body, or the walls in case of a hollow projectile, should be well designed to eliminate eccentricity and should be of such material and strength as to withstand the forces of projection and other stresses. For ballistic efficiency, the projectile should have a smooth contour and surface, With its centre of gravity situated towards the front.

Cavity

The projectile should have greatest possible capacity within safety limits of total weight and wall thickness to allow for a maximum quantity of filling. The size and shape will mostly depend on the type of projectile, and should be so designed as to be concentric with the body and be easily adaptable to manufacture and filling. The present trend in shell design is towards thinner wall (or high capacity) using steel of higher yield point.

2.2 Nose cone design

The aerodynamic design of nose cone section of any projectile meant to travel through a compressible fluid medium, the main problem at hand is the determination of the nose

cone geometrical shape. For many applications, such a task requires the definition of solid of revolution shape that experiences minimal resistance to rapid motion through such a fluid medium, which consists of elastic particles [4].

Nose cone shape

Nose cone shape is mainly determined by drag and thermal considerations. For projectiles that attain speeds below Mach 5 (hypersonic) thermal considerations are not very great and thus drag considerations dominate. Most nose cones are either ogive, conical some form of a power series.

Nose cone drag characteristics

For aircraft and rockets, below mach 0.8, the nose pressure drag is essentially zero for all shapes. The major significant factor is friction drag, which is largely dependent upon the wetted area, the surface smoothness of that area, and the presence of any discontinuities in the shape. In strictly subsonic projetiles a short, blunt, smooth elliptical shape is usually best. In the transonic region and beyond, where the pressure drag increases dramatically, the effect of nose shape on drag becomes highly significant. The factors influencing the pressure drag are the general shape of the nose cone, its fineness ratio, and its blufness ratio.

Influence of the general shape

Many refernces on the nose cone design contain empirical data comparing the drag characteristics of various nose shapes in different flight regimes. In many nose cone designs, the greatest concern is flight performance in the transonic region from 0.8 to 1.2 Mach. Although data is not available for many shapes in the transonic region, the table clearly suggests that either the Von Kármán shape, or Power Series shape with $n = 1/2$, would be preferable to the popular Conical or Ogive shapes, for this purpose.

Influence of the fineness ratio

The ratio of the length of a nose cone compared to its the base diameter is known as the ‘Fineness Ratio’. This is sometimes also called the ‘Aspect Ratio’, though that term is

usually applied to wings and fins. The length/diameter relation is also often called the 'Caliber' of a nose cone. At supersonic speeds, the fineness ratio has a very significant affect on nose cone wave drag, particularly at low ratios; but there is very little additional gain for ratios increasing beyond 5:1. As the fineness ratio increases, the wetted area, and thus the skin friction component of drag, is also going to increase. Therefore the minimum drag fineness ratio is ultimately going to be a tradeoff between the decreasing wave drag and increasing friction drag.

Table 2.1 Nose cone shape design matrix

Nose cone shape	Ogive	Cone (n=1)	n=1/4	n=3/4
Drag coefficient	4	3	1	5
Heat transfer	3	2	5	3
Total	7	5	6	8

Nose cone shape and equations

General dimensions

In the following nose cone shape equations , L is the overall length of the nose cone and R is the radius of the base of the nose cone. y is the radius at any point x, as x varies from 0, at the tip of the nose cone, to L. The equations define the 2-dimensional profile of the nose shape. The full body of revolution of the nose cone is formed by rotating the profile around the centerline *(C/L)*. Note that the equations describe the 'perfect' shape; practical nose cones are often blunted or truncated for manufacturing or aerodynamic reasons.

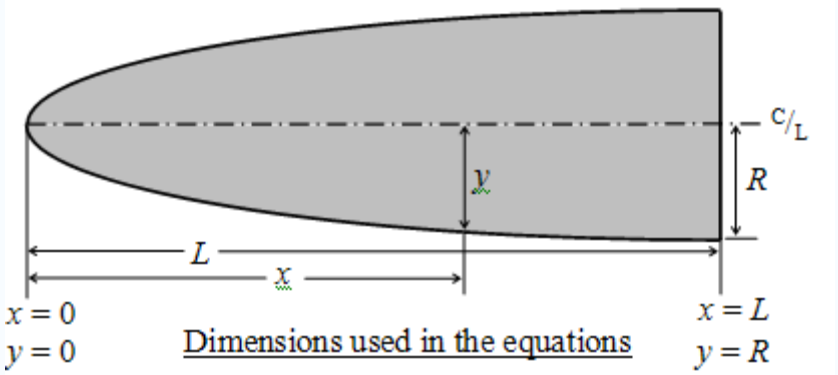

Haack series

Unlike all of the nose cone shapes, the haack series shape (the selected nose shape among other nose design because of its imperceptible) is not constructed from geometric figures. The shapes are instead mathematically derived for the purpose of minimizing drag. While the series is a continuous set of shapes determined by the value of *C* in the equations below, two values of *C* have particular significance : when *C = 0*, the notation *'LD'* signifies minimum drag for the given length and diameter, and when *C = 1/3*, *'LV'* indicates minimum drag for a given length and volume. The Haack series nose cones are not perfectly tangent to the body at their base, however the discontinuity is usually so slight as to be imperceptible. Haack nose tips do not come to a sharp point, but are slightly rounded [4].

$$\theta = \arccos\left(1 - \frac{2x}{L}\right)$$

$$y = \frac{R\sqrt{\theta - \frac{\sin(2\theta)}{2} + C\sin^3\theta}}{\sqrt{\pi}}$$

Where *C*=1/3 for *LV*-haack

C=0 for *LD*-haack (also known as the Von Kármán or the *Von Kármán Ogive*)

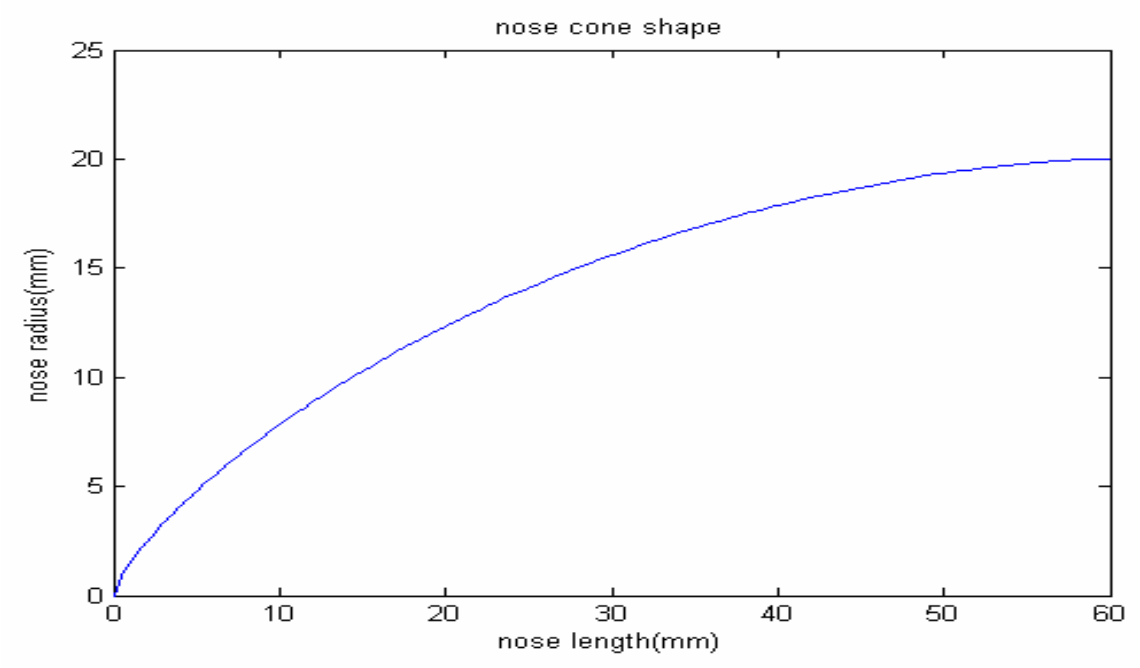

Fig.2.2 Nose cone shape

2.3 Fin Considerations:

The main role of the fins on a projectile is to bring the center of pressure rearward so that the projectile attains stable flight. In general, making the fins larger moves the center of pressure rearward (to a point). It is usually desirable to have the smallest fins that achieve the desired stability, as smaller fins develop less drag. The number of fins also has an effect on stability. The more fins that are used, the smaller they can be made and still keep the center of pressure in the same location. More fins create more drag. Another aspect of fin design is flutter. If not properly designed, the air rushing past the fins can cause large vibrations, which in the worst cases may tear the fins from the projectile. One method for determining flutter is that, a dimensionless flutter index is found that depends on fin geometry; this is then plotted against shear modulus and checked against experimental results [5].

Number of Fins:

The design matrix for number of fins ended in a tie between an eight-fin and a ten-fin design. Both types had their own advantages and disadvantages. The ten-fin method required smaller fins than the eight-fin layout, which translated into less fin flutter. If eight fins were employed, then the fins would create less drag and less manufacturing would be required to attach this amount rather than ten. The amount of drag reduction, however, was not considerable. In the eight-fin arrangement the fins could be made thicker to help with the vibration issues. After some consideration, ten fins were chosen because they create less drag force and use less material.

Table 2.2 Design matrix for number of fins.

Number of fins	*Eight*	*Ten*	*Twelve*
Drag force	5	4	3
Simplicity	4	3	1
Stability	4	5	5
Flutter	3	4	5
Total	16	16	14

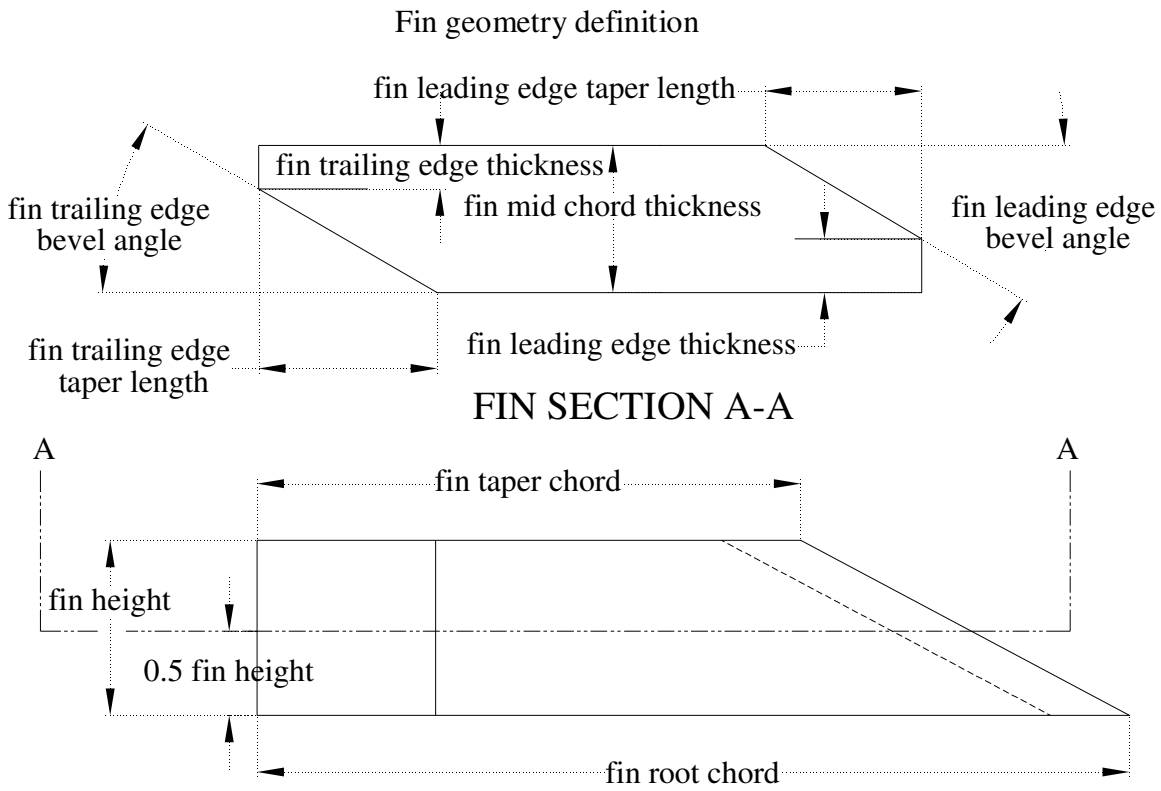

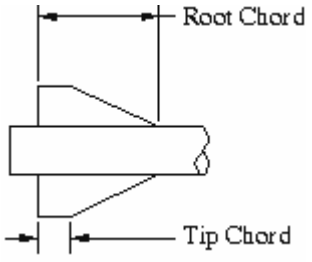

Clipped

Figure 2.3 Geometry and configuration of fin

t_{fin} = 2.6mm h_{fin}= 60mm

C_{root_fin} = 60mm, C_{tip_fin} =20mm

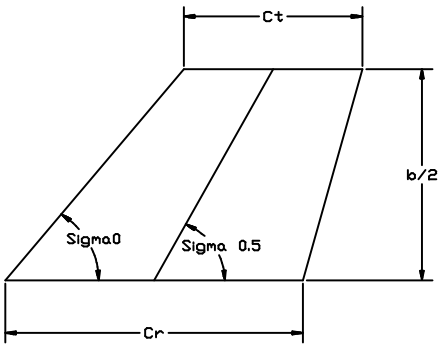

$$\lambda = \frac{C_{tip\_fin}}{C_{root\_fin}}$$

A_{fin}= 3.415mm^2 fin aspect ratio. span/fin ratio

P_{air_o}=1.013x10^5 pa standard atmospheric air pressure at sea level

P_{air} =1.013x10^5 pa Air pressure at given altitude

$$X = \frac{39.3 \cdot A_{fin}{}^3}{\left(\frac{t_{fin}}{C_{root\_fin}}\right)^3 \times \left(A_{fin} + 2\right)}$$

$$FI = X \frac{P_{air}}{P_{air\_o}} \cdot \frac{\lambda + 1}{2} \quad \text{…….. flutter index}$$

The flexural modulus (FI = 2.907x 10^6) is inside the safe part of the graph summary of flutter experience as a guide to the preliminary design of lifting surfaces on finned projectiles.

Fin material alternatives and Fin attachment method:

Steel, aluminum, composite materials, plastic, and wood were all considered as alternatives for fin construction. A steel sheet material was selected mainly because it was easy to manufacture and reasonably priced. This material would also be easily attached with spot welding to the tail tube, creating a strong and seamless interface. The flexibility category referred to how easily the fins' shape could be altered to affect performance.

There are several options for methods of attaching the fins to the tail tube. The weld to collar method was chosen because it offered a strong attachment of the fins, low weight and reasonable cost.

2.4 Material selection

Common shell for modern high-velocity guns may be made of steel or forged steel; those made of cast iron are now generally made for practice, as they are found to break up on impact, even against earthworks, before the fuze has time to act; the bursting charge is, therefore, not ignited or only ignited after the shell has broken up, the effect of the bursting charge being lost in either case. So long as the shell is strong enough to resist the shocks of discharge and impact against earth or thin steel plates, it should be designed to contain as large a bursting charge as possible and to break up into a large number of medium-sized pieces. To prevent the premature explosion of the shell, by the friction of the grains of powder on discharge, it is heated and coated internally with a thick lacquer, which on cooling presents a smooth surface. Besides this the bursting charge of all shell of 4-in. calibre and upwards (also with all other natures except shrapnel) is contained in a flannel or canvas bag. There are two determining factors when selecting steel for mortar shell: compressive strength and impact strength. Compressive strength is defined as the measured force required to break cross-sectional area of steel by pushing at both ends. Basically it measures how much force it takes to push a rod of steel apart. Impact strength is the steel's ability to take a sharp blow without breaking. The criteria that was concentrated in the material selections was that the material should have enough strength to withstand the rated pressure loading, the material should be thermally stable to withstand high temperatures. Cast iron is the most conventional material used in mortar ammunition. It was preferred to take the advantage of the years of study that have been devoted in the investigation of steel-shell wear and corrosion. Gray cast iron for mortar shells are selected for their hot strength properties and as barrels reach high temperatures in launching (450 to 550°C). Pearlitic malleable iron with a typical yield strength of 956 MPa (140 ksi) is used primarily as shell bodies in the manufacture of mortar ammunition, HF-1 steel (in S.A.E) was considered as the material for the mortar shell.

Table 2.3 Composition of HF-1 high-fragmentation steels

Steels	C ,%	Mn, %	P ,%	S, %	Si, %	Cr, %
HF-1	1.00-1.15	1.6-1.9	0.035	0.040	0.70-1.00	-

As a general rule, the design and selection of materials for the projectile is predicted, so far as is consistent with efficient operation, low cost and quantity production. In fact, the co-ordination between design and mass production is of vital importance. This consideration generally leads to the selection of high carbon-manganese, and the adoption of a design which reduces the number of machining operations to the minimum. In designs requiring the maximum attainable weight of bursting charge, greater strength per unit of area will be required, in which case a higher carbon or even nickel steel may be necessary. Semi-steel, cast steel and even cast iron are also used for certain low performance projectiles. The guiding criterion for the selection of material for a particular projectile is the resultant stress due to the various dynamic forces and end effect discussed; and the elastic limit of the material chosen must not be less than this resultant stress, but should preferably be about 25% above so as to provide an adequate factor of safety. Before acceptance, the material is physically tested to ensure that it is up to the required standard, the specification laying down the maximum yield and the breaking strain in (kilo grams per square centimeter tons per square inch), and the minimum final elongation.

Yield strength (min.) .....9846.9 kg./sq.cm. (63 tons/sq. inch).

Breaking strain..... 5985-7560kg./sq.cm.(38-48 tons/sq.inch)

Elongation (min.) ..... 5 %

As an additional safeguard against accepting sub-standard projectiles for filling, the empty projectiles are subjected to a severe firing test in which they are subjected to a pressure more than that obtainable under the worst possible conditions. The projectiles are fired at P_1 proof pressure of the gun, which is 15% more than the normal service charge pressure and the fired projectiles are then recovered for examination. Any abnormal defects noticed in this examination render the lot unacceptable.

Table 2.4 Properties of HF-1 ductile gray cast iron steel

Young's modulus	Poisson's ratio	Coefficient of thermal expansion	Yield strength
175GPa	0.33	13.5μm/m^{0}c	965MPa

CHAPTER 3

General

High explosives shells are employed for fragmentation effect against personnel, aircraft and vehicles with little or no armour protection, or for the demolition of material targets. The fragmentation is achieved by the dispersion of high velocity fragments over a wide area, while the blast or shock wave emanating from the source of detonation, effects destruction of material targets. A typical Artillery shell, generally, combines both these effects to meet tactical requirements.

3. FRAGMENTATION OF MORTAR SHELL

On detonation of the high explosive filling, the projectile body is broken up into a number of pieces of varying sizes, which are thrown outwards at high velocities. The fragmentation is satisfactory when the shell breaks up into a large number of pieces each of which is of optimum size and retains sufficient velocity to disable unprotected, or lightly protected, personnel or soft-skinned vehicles within the specified vulnerable zone. These fragments are effective against personnel and soft targets over a considerable area but have little effect against hard targets. The size and velocity of the fragments depend on the brisance or velocity of detonation of the high explosive filling, the charge weight ratio and the quality of the steel. The effectiveness of fragments is dependent on fragments size and velocity. Fragmentation is considered satisfactory when most of the fragments fall into the middleweight groups i.e., when the number of heavier and lighter fragments is few. It is evident that if the fragments are too large there will not be enough of them, thus minimizing probability of hitting with in a fixed zone; conversely if they are too small, they lose their velocity too quickly and the lethal zone will be reduced. Tests have shown that the optimum size of fragments to achieve maximum effect against personnel and soft targets is approximately 1.4gm and the average velocity of the fragments is of the order of 915 m/sec (3000ft/s) and miminum energy required to cause body failure of human tissue is 80-100J, though it may be possible to effect further increase by the use of more powerful explosives and improved shell design[16].

3.1 Fragment Velocity

In this part, we will examine how fast the explosives can throw pieces of metal, dependent upon the geometry of the charge and metal piece to be thrown; how a cylinder breaks up when it is explosively expanded; how methods are used for estimating the resulting sizes of the fragments from that break up; and finally, how the velocity of a piece of metal will be affected by the air through which it is traveling after it is thrown.
For effective fragmentation on ground impact, it is essential that the shell must detonate instantaneously on impact with the ground. The slower the fuse, the greater the penetration (depending on the type of ground) before the shell detonates, thus resulting in the loss of a number of effective fragments. A quick-action nose fuse is, therefore, required for good fragment effect from percussion bursts.

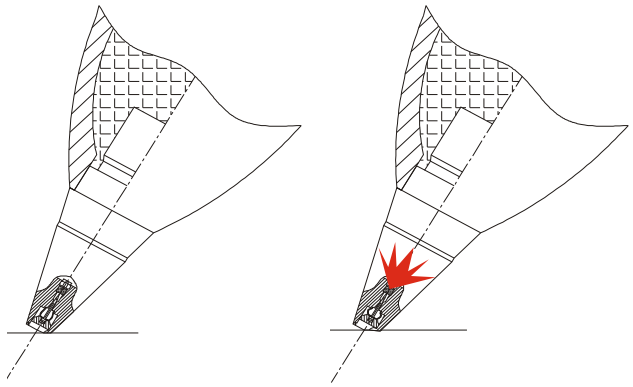

Fig.3.1 Impact from the ground and fuse spark

R.W. Gurney developed a model that described the expansion of a metal cylinder driven by the detonation of an explosive filler charge. The model predicts the initial velocity of the fragments produced by the breakup of the expanding cylinder. His model relied on a partition of an explosive's energy between the metal cylinder and the gases driving it. He assumed a linear velocity gradient I of the expanding gases. The model yielded a deceptively simple relationship between the final metal velocity, the explosive energy, and the ratio of the mass of the driven metal to that of the loaded explosive charge. Gurney equation is simple and long standing, geometry-specific. Fragment velocities are measured using different techniques as electronic, optical or x-ray. If these techniques are

not available, initial velocity of fragments released from explosion of a warhead is approximated by the Gurney formula. The simplest expression of the Gurney formula for symmetrical configurations is:

$$\frac{V}{\sqrt{2E}} = \left(\frac{M}{C} + \frac{1}{2}\right)^{-\frac{1}{2}} \quad \text{.....(3.1)}$$

$$V_f = V_g \, (\rho_{cyl} / \rho_{ex})^{-1/2} \, [(t_{cyl} / R_{ex})^2 + 2 \, (t_{cyl} / R_{ex}) + 0.5 \, (\rho_{ex} / \rho_{cyl})]^{-1/2}$$

Where V: fragment velocity, M: mass of casing, C: mass of exploisve

R_{ex}= radius of the exposives, t_{cyl} = thickness of the cylinder

ρ_{ex}=density of the cylinder, ρ_{cyl}= density of the cylinder

$\sqrt{2E}$ = a constant, the Gurney velocity coefficient, which is specific to a particular explosive. The value of E or $\sqrt{2E}$ is determined experimentally for each explosive. It has also been correlated to several other explosive or detonation properties. Among the extant correlations, a simpler and also more accurate correlation is

$$\sqrt{2E} = \frac{D}{2.97}$$

Where D is the detonation velocity of the explosive.

3.2 Fragment mass distributuion

Prediction of mass fragment distribution is usually performed by application of Mott formula, or Held formula. Each of mentioned formulas has certain limitations. These empirical formulas are based on experimental data gained from many fragmentations in pit and Arena test. There are several theories of how fragments are formed and hence how large or small they would be; one of the earliest is N.F. Mott. The Mott equation has been used for many years for prediction of fragments mass distribution in naturally fragmented warheads and ammunition. Mott explained the sizes of fragments as a function of the rate of cylinder expansion as compared to the rate of a tensile relief to the rate of a tensile relief wave around the cylinder's periphery. It is assumed that the cylinder is placed in greater and greater hoop stress (tensile) as it expands. A fracture eventually will occur at some point. The fracture presents a free surface, and a relief wave can now travel away from it. Fracture can no longer occur in the relived regions,

but tensile stress and plastic flow are still growing in the unrelieved region where a new fracture is free to form. The size of the fragments then are determined by the unbalance between the rate of increasing strain and the rate of relief wave. Other theories give fragment size as a function of a hypothesized critical expansion velocity, or based upon a critical strain rate, a mechanism related to radial, not tangential, stress gradient across the cylinder wall. Mott, however, gives a more tractable mathematical treatment suited to first order engineering, as compared to others. It is essential to have a capability to make warhead performance prediction in the earliest pahse of HE ammunition or warheads preliminary design. Ablity for warhead performances prediction depends on the comprehensive data base of warheads natural fragmentation features, including data on fragment numbers, initial fragment velocities, warhead case material performances, fragment shape features and spatial fragment distributions, etc [1]. Mott's equations are

$$N(m)=\frac{M_0}{2M^2{}_K}e^{\left[-\frac{m^{\frac{1}{2}}}{M_K}\right]} \qquad \text{.....(3.2)}$$

Where $N(m)$ is the number of fragments heavier than mass m;

m, the mass of a fragment (lb);

M_0, the mass of casing (lb); M_K, a distribution factor ($lb^{1/2}$)

B=0.0779(from the detonation properties of steel table),

$$M_K = Bt^{\frac{5}{16}}d^{\frac{1}{8}}\left(1+\frac{t}{d}\right)$$

Where B is a constant that is specific for a given explosive-metal repair;

t is the wall thickness (m) ;

d , casing interior diameter (m)

Now we find M_0, which was the weight of the cylinder before blew it up

$$vol = \pi\left(R_2{}^2 - R_1{}^2\right)\cdot L$$
$$M_0 = \rho \cdot V$$

Table 3.1 Thickness, velocity and number of fragment relations

S. No	Thickness (m)	Inside radius R_2 (m)	Outside radius R_1(m)	Volume of casing	Volume of charge	mass of casing (M) (kg)	mass of charge (C) (kg)	C/M	Fragment velocity (km/s)	Mott distribution factor	Number of fragment greater than 1.4gm
1	0.005	0.055	0.06	0.00075831	0.00398937	4.459832	5.5425668	1.198309	1.79188265	0.022085	862
2	0.006	0.054	0.06	0.000902059	0.003845621	5.49482624	5.30681811	0.971053	1.67359957	0.025552	1081
3	0.007	0.053	0.06	0.001043171	0.003704509	6.51082976	5.07539509	0.808885	1.57094758	0.028875	1297
4	0.008	0.052	0.06	0.001181645	0.003566035	7.50784256	4.84829773	0.687401	1.48055361	0.03207	1507
5	0.009	0.051	0.06	0.001317481	0.003430199	8.48586464	4.62552603	0.593043	1.39998566	0.03515	1710
6	0.01	0.05	0.06	0.00145068	0.003297	9.444896	4.40708	0.517677	1.32743937	0.038124	1907
7	0.011	0.049	0.06	0.001581241	0.003166439	10.3849366	4.19295963	0.456125	1.26154351	0.041	2095
8	0.012	0.048	0.06	0.001709165	0.003038515	11.3059866	3.98316493	0.404938	1.20123448	0.043782	2275
9	0.013	0.047	0.06	0.001834451	0.002913229	12.2080458	3.77769589	0.361726	1.14567264	0.046475	2446
10	0.014	0.046	0.06	0.001957099	0.002790581	13.0911142	3.57655251	0.324783	1.09418486	0.049083	2609
11	0.015	0.045	0.06	0.00207711	0.00267057	13.955192	3.3797348	0.292857	1.04622419	0.051609	2762
12	0.016	0.044	0.06	0.002194483	0.002553197	14.800279	3.18724275	0.265011	1.00134079	0.054055	2906
13	0.017	0.043	0.06	0.002309219	0.002438461	15.6263754	2.99907637	0.240526	0.95916076	0.056423	3041
14	0.018	0.042	0.06	0.002421317	0.002326363	16.433481	2.81523565	0.218845	0.91937027	0.058714	3167
15	0.019	0.041	0.06	0.002530777	0.002216903	17.2215958	2.63572059	0.199528	0.88170363	0.06093	3284
16	0.02	0.04	0.06	0.0026376	0.00211008	17.99072	2.4605312	0.182222	0.84593409	0.06307	3390
17	0.021	0.039	0.06	0.002741785	0.002005895	18.7408534	2.28966747	0.166643	0.81186672	0.065136	3488
18	0.022	0.038	0.06	0.002843333	0.001904347	19.4719962	2.12312941	0.152556	0.77933286	0.067127	3575
19	0.023	0.037	0.06	0.002942243	0.001805437	20.1841482	1.96091701	0.13977	0.74818564	0.069044	3653
20	0.024	0.036	0.06	0.003038515	0.001709165	20.8773094	1.80303027	0.128125	0.71829644	0.070887	3722
21	0.025	0.035	0.06	0.00313215	0.00161553	21.55148	1.6494692	0.117485	0.68955204	0.072655	3780

The following graphs has summarised Table 3.1

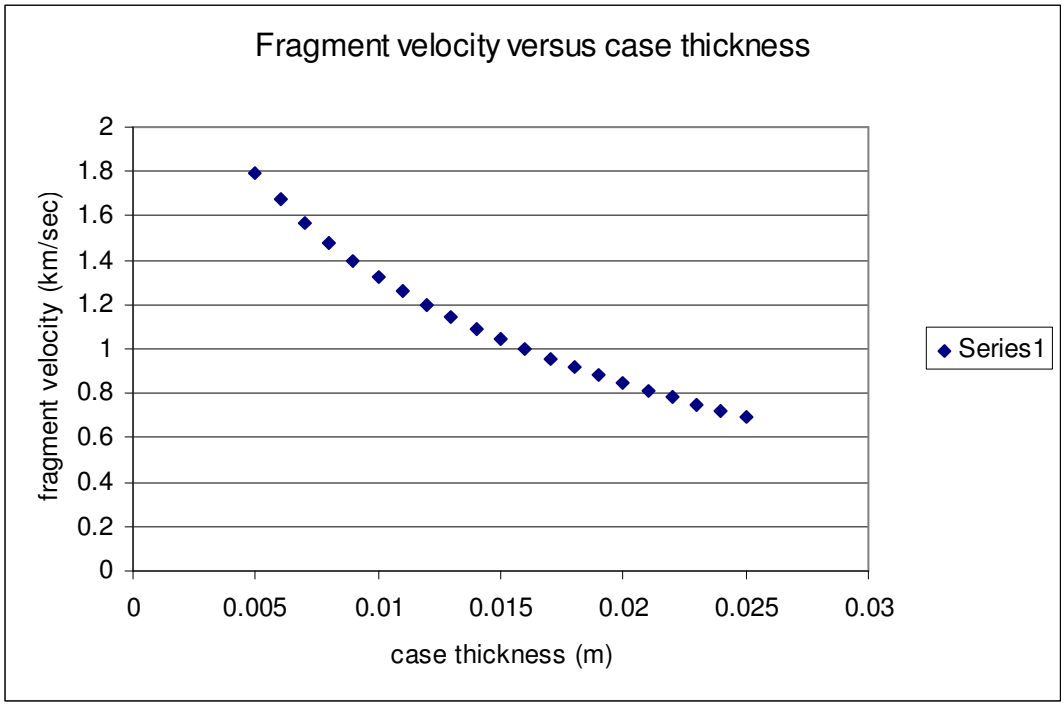

Fig.3.2 Fragment velocity versus casing thickness

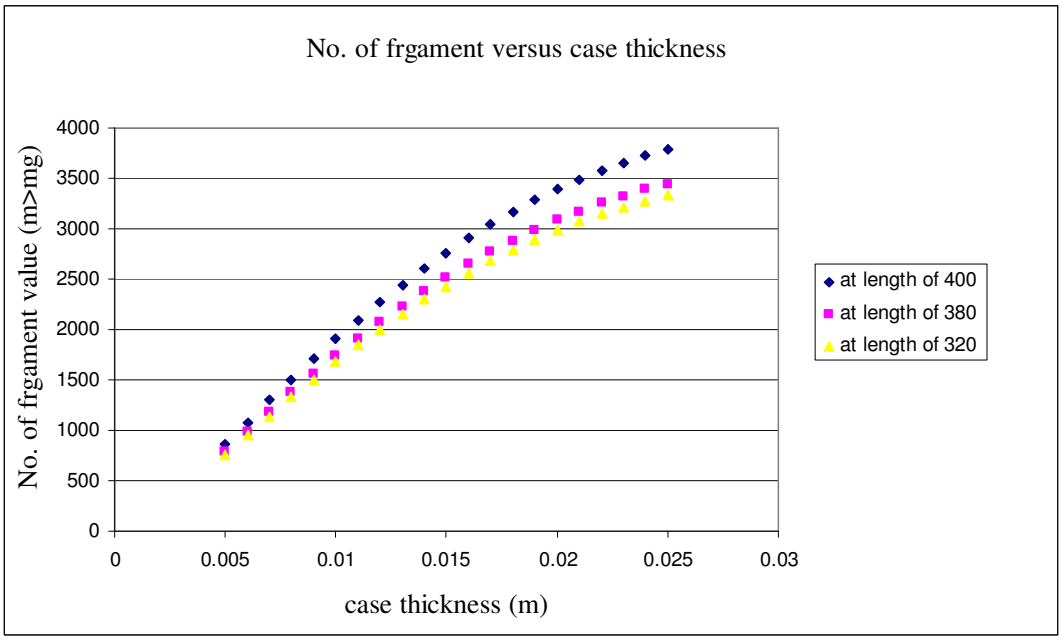

Fig.3.3 Number of fragment versus casing thickness

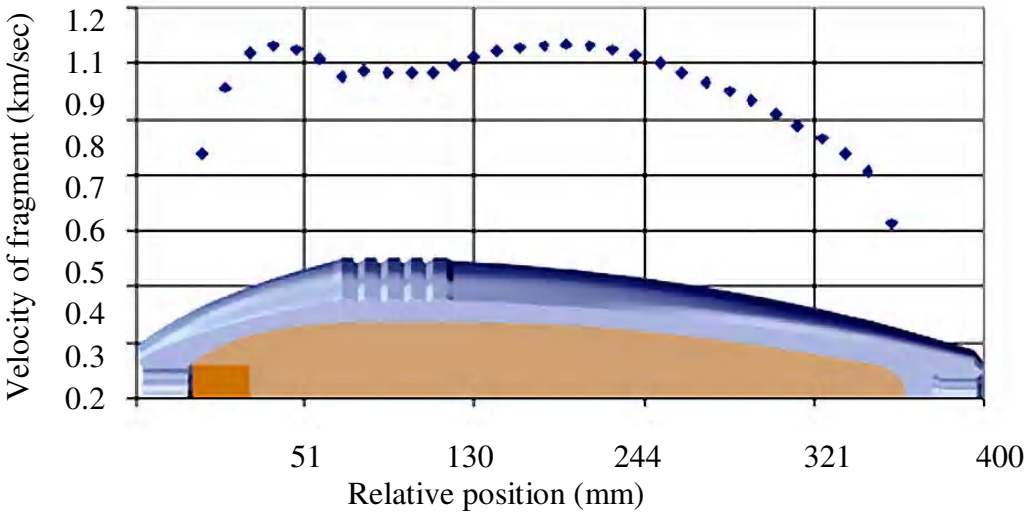

Fig.3.4 Relative fragment of velocity along the shell

The number of fragments, which is greater than 75gm

$$N(75gm) = \frac{15.6kg}{2(0.1114)^2(0.05426)} e^{-\left(\frac{(0.022x75)^{\frac{1}{2}}}{0.1114}\right)} = 1.28$$

There is one fragment whose weight is greater than 75gm. Similarly, for the other size fragments, we find

Table 3.2 Number of fragment for selected fragments

Weight (gm)	Number
Above 75	1
50-75	2
30-50	24
20-30	45
15-20	54
10-15	122
5-10	268
3-5	217
2-3	180
1.4	658

The weight of the largest fragment

$$m = \left[M_K \ln\left(\frac{M_O}{2M_K{}^2} \right) \right]^2 = \left[0.5426 \ln\left(\frac{15.6kg}{2(0.1114)^2} \right) \right]^2$$

$$m = \left[0.5426 \ln\left(\frac{15.6kg}{2(0.1114)^2} \right) \right]^2 = 89gm$$

The volume of this fragment

$$V = \frac{m}{\rho} = \frac{0.089kg}{7200\frac{kg}{m^3}} = 123cm^3$$

The wall thickness of the original cylinder was 17mm, if we assume that the wall thickness was not significantly compressed, that would lead to a square fragment 2.67mm on a side by 17.14mm thick.

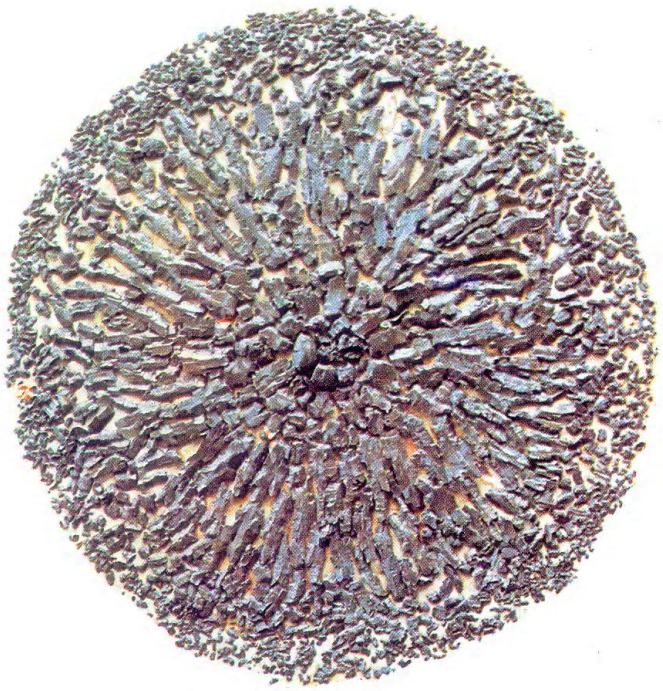

Fig.3.5 Fragmentation of mortar shell

3.3 Flight Of Fragments

The size of fragments and their initial velocity is known, as they travel through the air they are slowed down or decelerated. Two major forces act to slow down the fragments, the "face drag" due to dynamic pressure, and the "base drag" due to turbulence behind the fragment. The magnitude of these forces is a function of the projected face area of the fragment, the density of the air through which it is moving, the velocity of the fragment, and the shape factor expressed as the drag coefficient

$$F = \frac{1}{2} C_D A_f \rho_a V_f^{\,2} \quad \text{.....(3.3)}$$

Where F is the force; C_D, the total drag coefficient; A_f, the face area of fragment

ρ_a the local air density; and V_f, the fragment velocity.

The face drag coefficient, which is larger than the base drag coefficient, is generally relatively constant at low velocities, increases as velocity approaches mach 1, and then tends toward a higher constant value with further increasing velocity. The magnitude of the base drag coefficient is just the opposite, decreasing with increased velocity. The sum of these two, called total drag coefficient, C_D, is used when calculating trajectories.

From classical physics, we know that force is equal to mass times acceleration:

$$F = ma \quad \text{.....(3.4)}$$

The drag forces on a fragment slow it down or impart a negative acceleration; therefore, equation (3.4) for this case can be written as follows:

$$a = \frac{-F}{m} \quad \text{.....(3.5)}$$

Replacing F, the force, in eq. (3.4) with the drag force expressed earlier in eq. (3.3) yields

$$a = -\frac{C_D A_f \rho_a V_f^{\,2}}{2m} \quad \text{.....(3.6)}$$

From the basic definition of acceleration and gravity, $a = \frac{dV}{dt}$ and $V = \frac{dx}{dt}$ where t is time and x is distance, we have

$$VdV = adx \quad \text{.....(3.7)}$$

Combining Eq. (3.6) with Eq.(3.7), we obtain:

$$\frac{1}{V}dV = -\frac{C_D A_f \rho_a}{2m}dx \quad \text{.....(3.8)}$$

and integrating this expression between the limits V_0, X_0 and V, X, where $X_0 = 0$ yields

$$\ln\left(\frac{V}{V_0}\right) = -\frac{C_D A_f \rho_a x}{2m} \quad \text{.....(3.9)}$$

This is the velocity loss due to drag as a function of the distance traveled by a fragment along the path of its trajectory. This doesn't take into account the angle of launch and resultant slant range. Putting those factors in along with drop due to the acceleration of gravity complicates the mathematics by engineering a set of nonlinear equations. The above equations Eq. (3.9) can be used for short ranges. The full trajectory calculation will involve either graphical or finite difference calculations.

$$x = -\frac{2m\ln\left(\frac{V}{V_0}\right)}{C_D A_f \rho_a}$$

Substituting the values for the larger fragment

$$x = \frac{2*89gm*\ln\left(\frac{42.4}{959.16}\right)}{1.6*17.38cm^2*1.225*10^{-3}\frac{gm}{cm^3}} = \quad 164.29\text{m}$$

The distance covered by 1.4gm

$$x = \frac{2*1.4gm*\ln\left(\frac{338.4}{959.16}\right)}{1.6*1.32cm^2*1.225*10^{-3}\frac{gm}{cm^3}} = 11.55m$$

CHAPTER 4

4. INTERNAL BALLISTICS OF MORTAR SHELL

A projectile is an object that is placed in motion by a force acting over a very short period of time. After the projectile is set in motion by the initial impulse, during the launching phase, the projectile enters into the projectile motion phase, in which there is no longer a thrust or propulsive force acting on it. There are other forces that act on projectiles. (self-propelled "projectiles" such as rockets, since, owing to their propulsive force, they don't follow refer to as classical projectile motion until after they've expended their fuel.) Interior ballistics processes begin with the firing pin hitting the ignition system of the projectile and end when the projectile leaves the barrel.

The total effect of all interior ballistic factors determines the muzzle velocity, muzzle velocity and pressure affected by position of all-burnt, variation in charge weight, variation in propellant size, variation in projectile weight, variation in propellant shape, variation in chamber capacity, variation in bore area, variation in shot-start pressure, variation in shot-travel and the effect of not only in one quantity but simultaneous variation in charge weight, propellant size and shape. In addition, the velocity trend affected by: propellant manufacture, propellant temperature, moisture content of propellants, position of bagged propellant in the chamber, ammunition lots, non-uniform ramming, driving bands, fall-back, coppering, propellant residue, effect of barrel wear, abnormal internal ballistic effects, warmer effect, order of fire effect, hump effect, occasion-to-occasion effect (day-to-day effect), charge-to-charge propellant performance, calibration, tolerances in new equipments.

Propellant Charge: - This is a rapidly burning composition of low explosive that is burned in a barrel to propel the projectile. When suitably ignited, the propellant charge has an extremely rapid rate of burning, producing many times its own volume of gases at a high temperature and pressure. No outside agent, e.g. oxygen, is necessary for it's burning. The rate at which the contained propellant burns increases with, and is approximately proportional to, the pressure developed. The higher the pressure, the faster the rate of burning; the lower the pressure, the slower the rate of burning.

The connection between pressure and the ratio of burnt powder is called law of combustion. It is defined as follows:

$$\frac{dz}{dt} = \varphi(z).L.p \quad \ldots\ldots\ldots\ldots\ldots\ldots\ldots\ldots \quad (4.1)$$

$\varphi(z)$ stands for the form function and indicates the relationship of the momentary total surface to the initial total surface of the powder. In the case of degressive powders is $\varphi(z) < 1$ and in the case of progressive powders $\varphi(z) > 1$. Ball powders and flake powders belong to a group of degressive powders, tubular powders are neutral (when the face is neglected), and seven-hole powders are-at least at the beginning-progressive. The number L is a powder constant called dynamic vivacity that indicates the relationship between the rate of combustion and pressure. The type of propellant will alter the shape of the pressure vs. position curve. Progressive pellets raise the pressure more slowly than degressive propellants. For this reason, the peak pressure is often less. On the other hand, degressive propellants accelerate the projectile more rapidly in the initial portion of the barrel, while progressive propellants can reach higher exit velocities. Which type of propellant to use depends on the application. If the barrel cannot be made very long, it is better to use a degressive propellant to achieve the maximum exit velocity in a limited distance. As a consequence, however the barrel must be thicker to withstand the increased peak pressure. If length is not restricted, a progressive propellant can be used to minimize stress and achieve the maximum exit velocity.

4.1 The act of launching

The act of launching is a very complicated one and takes place under extreme physical conditions. High pressures occur simultaneously with high temperatures. The process is initiated by ignition of the primer system, where the hot gases and flames produced partially burn the powder surface. When the projectile weapon is launched from the barrel, it is accelerated to a high velocity by the burning of propellant. The propellant may travel with the projectile or be stationary in the barrel. The gasses produced by the burning propellant are trapped in the volume behind the projectile. The introduction of more heat into the product gasses causes the pressure to rise which in turn will accelerate the projectile. On the other hand, the movement of the projectile increases the volume

which tends to drop the pressure. With a defined extraction resistance of the projectile, the pressure in the case is responsible for a gradual ignition of the whole powder surface which increases rapidly. Thus, the projectile starts to move when the pressure has exceeded a certain value (extension pressure). At the same time the volume of the gas increases. The increase in volume and the amount of gas produced determine the course of the gas pressure that has reached its peak when both are equal. Then, the pressure decreases until the projectile has left the muzzle. The pressure remaining at this moment, called muzzle pressure, it is responsible for the processes in the muzzle.

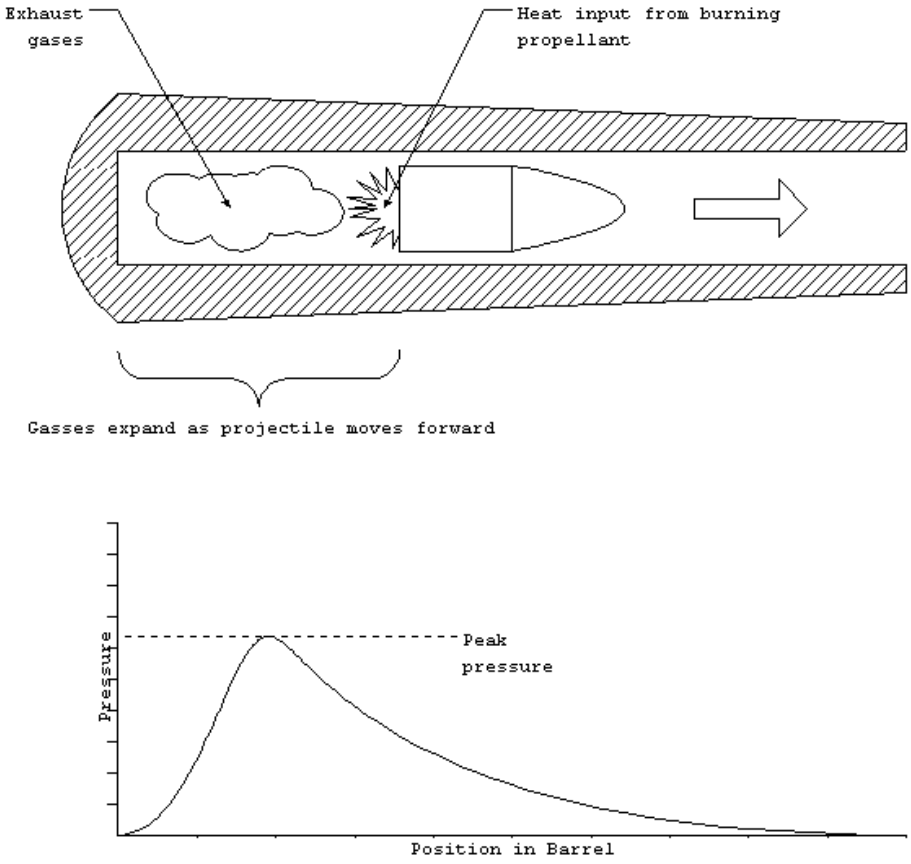

Figure 4.1 How projectiles are launched from a barrel

Initially, the pressure will rise, dominated by the introduction of heat. As the projectile gains speed, the expansion effect will get larger until a maximum pressure is reached. Afterwards, the pressure will drop rapidly.

The maximum, or peak pressure determines how much stress the barrel must be designed to withstand. Very large peak pressures require thick barrels [8].

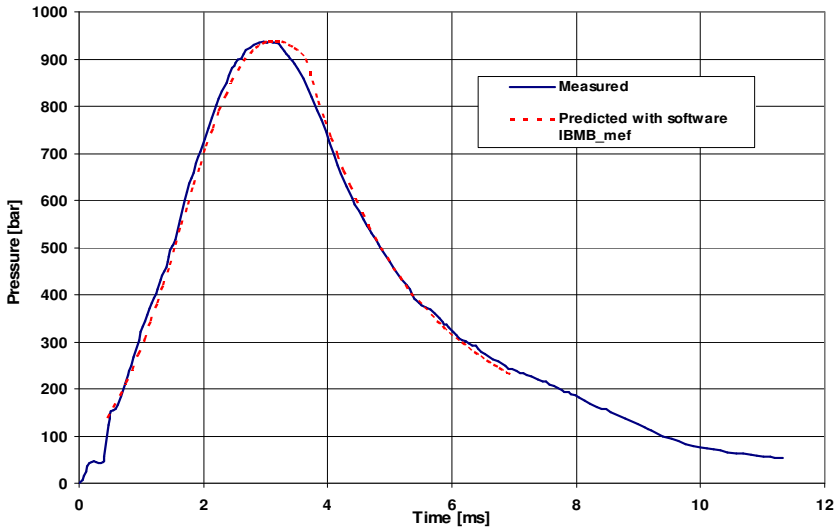

Figure 4.2 Pressure-time curve

At the moment of peak pressure, the projectile has been traveling only a short distance. Powder combustion must be controlled so that the maximum gas pressure isn't too high and so that muzzle pressure remains as low as possible. Combustion should be finished before the projectile leaves the muzzle. In addition, a maximum muzzle velocity is desirable. Short bores with light projectiles therefore need degressive powders; long bores with heavy projectiles use progressive powders.

4.2 Interior ballistics equations

The energy conservation law and the motion equation for the projectile are essential in addition to the above mentioned law of combustion. Heat energy due to burning of propellant is equal to the kinetic energy of the projectile and the interior energy gases. During the preliminary estimates, heat emission from the barrel and friction are neglected[8]:.

$$m_c \cdot Q_{ex} \cdot Z = \frac{p \cdot V_b}{\gamma - 1} + \frac{1}{2} m v^2 \quad \text{..... (4.2)}$$

Where m_c: mass of powder charge

Q_{ex}: energy of the powder per unit mass

Z: amount of burnt powder

V_b: Co volume of the gas

γ: Relation of the specific thermal capacities $\frac{c_p}{c_v}$

m: mass of the projectile

V: velocity of the projectile

The ratio of the pressure in the closed vessel to the fraction of burnt powder (z) is obtained by forming the Abel's equation for any pressure:

$$p = \frac{f \cdot m_c \cdot z}{V_B - m_c \cdot z - \frac{m_c}{\rho_c}(1 - z)} \quad \text{.....(4.3)}$$

The motion of the projectile in the barrel being one-dimensional:

$$m \cdot \dot{v} = p \cdot A \quad \text{..... (4.4)}$$

The energy equation (4.2) together with the two differential equations (4.3 and 4.4) form the interior ballistics system of equations, from which can be calculated the maximum pressure, the direction of pressure, and the muzzle velocity when necessary data on the powder and the arm are available.

4.3 Distribution of Energy

The area below the pressure-travel curve times the cross sectional area of the bore corresponds to the work done by the gases (1/2 x mass of projectile x square of MV). The heat energy liberated by the burning of the propellant can only be partly converted to kinetic energy; the remainder is lost in various ways. The total amount of energy liberated on firing is used up as follows:

Kinetic energy:

a. energy of translation of the projectile;

b. energy of rotation of the projectile;(not existing/negligible in mortar shell)

c. kinetic energy of the gases;

(The powder gases behind the projectile move at the same velocity as the projectile passing through the barrel; on the action surface, the gases are motionless. For an approximation of their kinetic energy, normally calculate one half of the projectile velocity).

Thermal energy:

d. loss of heat to the barrel, and projectile;

e. energy taken up by engraving the driving band, including frictional losses;

f. latent heat of gases leaving the muzzle.

The percentage of these energy forms can be calculated

Table 4.1 Energy Balance of 120mm

V_o = 284m/s, m_p = 0.513kg , m_c = 17.6kg , Q_{ex}= 4200J/gm

Energy breakup (produced in the barrel)	[J]	[%]
Translation energy of the projectile ($=\frac{1}{2}mv_{mv}^2-\frac{1}{2}mv_0^2$) Where *mv*: muzzle velocity, v_o= initial velocity	736,495.6	30.79
Rotational energy ($=\frac{1}{2}I\omega^2$)	265.7	≈ 0
Kinetic energy of the gases (0.5*translational energy)	368,247.8	15.39
Recoil energy of the weapon	-	-
Thermal energy at the weapon ($mc\Delta T$)	593,640	24.8
Residual energy (40% of total heat produced)	693,025	28.97
Total	2,391,741	100

4.4 Mortar Projectile's body compressive stresses

If we consider normal case of projectile motion in the barrel, main stresses on projectile body is due to inertial force as a result of translatory acceleration of projectile caused by propellant gasses force. First we have to determine acceleration of the projectile:

$$m \cdot \frac{d^2x}{dt^2} = p \cdot S$$

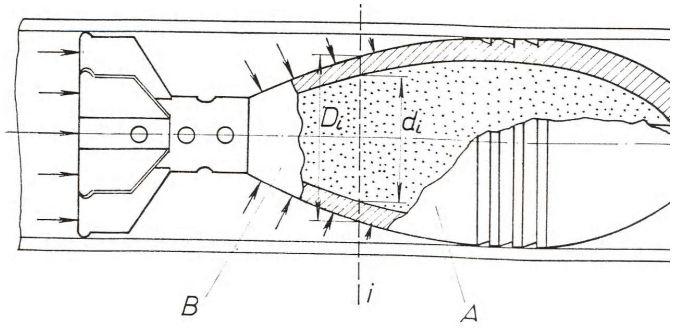

m - Projectile mass

P - Pressure in the barrel (made from propellant gasses)

S - Intersection area in the barrel

$$S = \frac{d^2\pi}{4}\ [m^2]$$

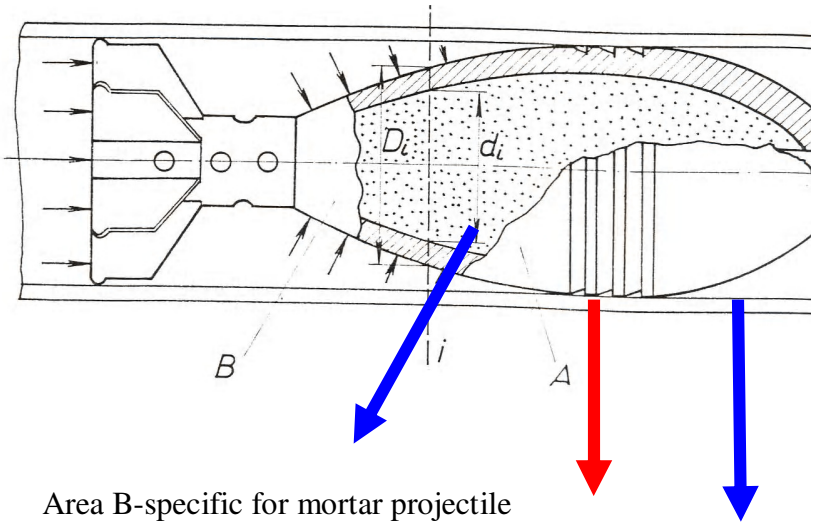

Area B-specific for mortar projectile

Frontier

Area A- same as artillery projectile

Fig.4.3 Mortar projectile in the barrel

For determination of stress on projectile body consider cross section *i-i* which divide projectile body in two parts: *A* and *B*

At the *A* part of body, it is obvious that its motion is determined with differential equation:

$$m_A \cdot \frac{d^2x}{dt^2} = F_{i-i}$$

m_A - Projectile mass in front of *i-i* cross section

F_{i-i} - Force in cross section area of *i-i*:

$$F_{i-i} = \sigma_{i-i} \cdot S_{i-i} + \left(\frac{d^2_{barrel} - D_i^2}{4} \right) \cdot \pi \cdot p$$

Maximum acceleration in mortar tube:

$$a_{\max} = \frac{d^2 x}{dt^2} = \frac{p_{\max}}{m} \cdot \left[\frac{d^2 \pi}{4} \right] \quad [Pa]$$

$$m_A \cdot \frac{p_{\max}}{m} \cdot \left[\frac{d^2_{barrel} \cdot \pi}{4} \right] = \sigma_{i-i} \cdot S_{i-i} + \left(\frac{d^2_{barrel} - D_i^2}{4} \right) \cdot p_{\max}$$

$$\sigma_{i-i} = \frac{1}{S_{i-i}} \cdot p_{\max} \cdot \frac{\pi}{4} \left[\frac{m_A}{m} \cdot d^2_{barrel} - \left(\frac{d^2_{barrel} - D_i^2}{4} \right) \right]$$

$$m = m_A + m_B \qquad S_{i-i} = \frac{\pi}{4} \cdot \left(D_i^2 - d_i^2 \right)$$

$$\sigma_{i-i} = \frac{1}{m \cdot \left(D_i^2 - d_i^2 \right)} \cdot p_{\max} \cdot \left(m \cdot D_i^2 - d^2_{barrel} \cdot m_B \right)$$

In designing the projectile we make calculations with so called calculation pressure (CP) which is greater than maximum weapon pressure in normal conditions (proof pressure). So we use equation:

$$P_{cp} = k \cdot P_{\max}$$

k – Constant of proof pressure:

k = 1,12 for projectiles with calibre greater than 40mm,

k = 1,15 for projectiles with calibre smaller than 40mm

Maximum calculated value of explosive charge compressive stress should be smaller than explosive charge critical compressive stress:

Table 4.2 Explosives critical stress values

Types of explosives	σ_{cr} (Mpa)
TNT	180
TNT-Hexogen 50:50	140
Tetril	85
Amatol 80:20	140

Table 4.3 Topology and characterstics of propellant

Bore diameter (m)	Projectile mass (kg)	Bore length (m)	Chamber volume(m^3)	Area of clearance (m^2)	Coefficient of friction
0.12	17.6	1.16	0.00309	0.000169	1.01
Propellant mass and density thermodynamic constants					
Mass (kg)	Force (J/kg)	C_p/C_v (m^3/kg)	covolume m^3/kg	Temperature (K)	Density (kg/m^3)
0.513	1099000	1.22	0.0102	3500	1640
Burning rate of propellants					
Exponent		Velocity coeff.			
1		1.30E-09 (m/s/pa)			
Propellant physical constants					
Kapa (-)	Lambda (-)	MI (-)	WEB (M)		
1.203	-0.16846	0.00895	0.00026		
Parameters of losses heat					
NI1 (-)	Sigma (wm/kgk)	HIO (-)	Temp. storage propellant (K)		
0.7	300	0.82	293		

Based on the equations of 4.1- 4.5 , the following summary of the internal ballistics of MP 120mm mortar shell is tabulated.

Table 4.4 Tabulated values of internal ballistics of mortar shell

Number of zones	Increment of propellant	Weight of propellant (gm)	Pressure developed (Mpa)	Muzzle velocity (m/sec)
1	Main charge plus one acrylic chord	133*	16	108
2	Main charge plus two acrylic chord	209	31	128
3	Main charge plus three acrylic chord	285	45.6	173
4	Main charge plus four acrylic chord	361	62	214
5	Main charge plus five acrylic chord	437	78.22	250
6	Main charge plus six acrylic chord	513	100	284

Note:- * Primary (main charge) propellant in the tube plus secondary or augmenting charge of single chord increment

4.5 Determination of shear stresses on bottom of the projectile body

In weapon barrel, during projectile motion in every moment following forces act on projectile bottom:

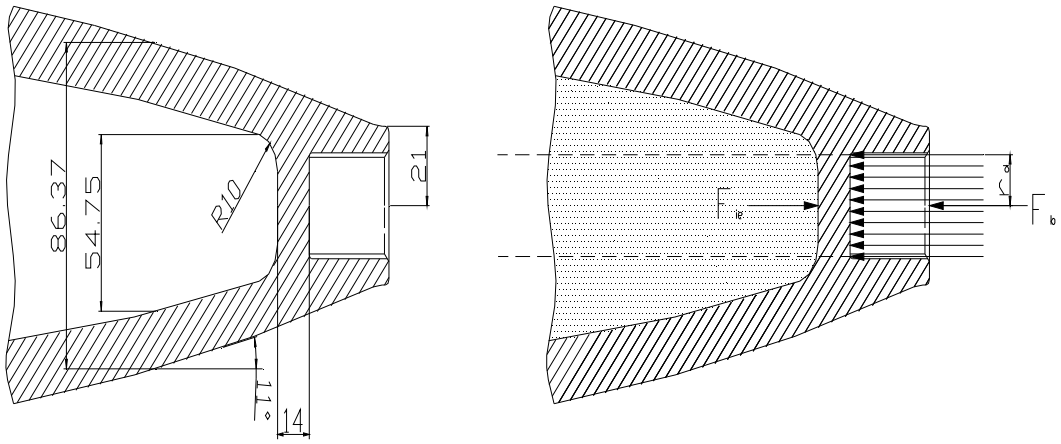

Fig. 4.4 Shear stress in mortar projectile

Shear stress on projectile bottom

$$\tau_{cp} = \frac{P_{cp}}{2 \cdot \pi \cdot r_d \cdot l_d} \left(r_d{}^2 \cdot \pi - \frac{m_e}{m} \cdot \left[\frac{d^2 \pi}{4} + \frac{e \cdot n}{2} (d_0 - d) \right] \right)$$

τ = shear stress

R_d =radius of explosivecharge

P_{cp}= calculation pressure of the propellant gases

n =number of fields per grooves

e=width of field

m=total projectile mass

m_e=explosive charge mass above projectile bottom

d_o= diameter over the grooves

d = weapon calibre

h = heght of field

$e+e'=\pi d/n$

h=(0.01-0.015)/d

Fb - Propellant gasses force and striking of the pin

Fei - Explosive charge inertial force

Projectile safety is asured if maximum calculated shear stress must be smaller than permitted (crtical) shear stress of projectile body material:

$$\tau_{cp} \leq \tau_{per}$$

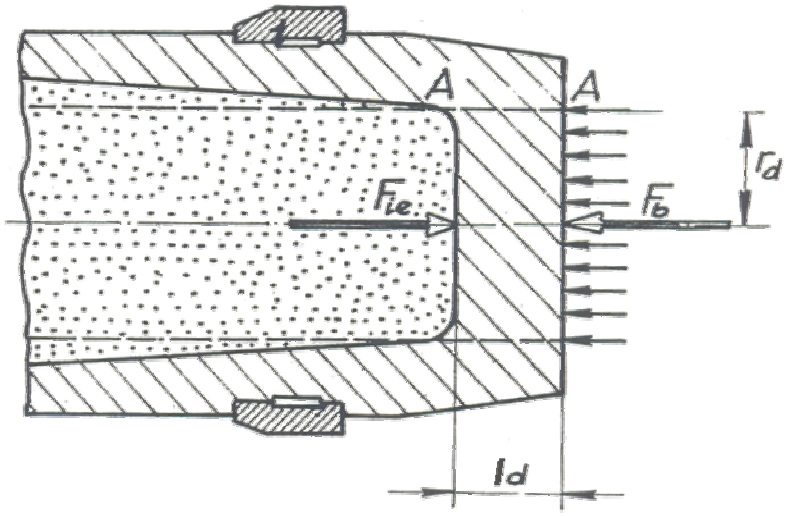

Data

$P_{max}(Mpa)$=100

K=1.12

$P_{cp}(Mpa)$=112

n =10

$e(mm)$ = 7

$h(mm)$ =1.47

$m(kg)$ =15

$me(kg)$ = 2.9

$d(mm)$ = 22mm

$d_o=d+2h$ = 22.94

For safety precautions, it isn't taking into considerations explosive charge radius

r_d(mm) = 12mm

l_d(mm)= 5.6mm

$$\tau = 126.096 \text{Mpa}$$

$$\tau_{cp} \leq \tau_{per}$$

CHAPTER 5

5.1 AERODYNAMIC FORCES AND MOMENTS ACTING ON THE PROJECTILE

Aerodynamic forces and moments acting on any projectile motion are: Drag force, Spin damping moment, lift and normal force, Overturning moment, Magnus force, Pitch damping force, Pitch damping moment, and Neglected forces and moments:- Magnus cross force and Magnus cross moment. The significant aerodynamic forces and moments which has measurable effect on a finned type projectile are the drag, lift and normal force, overturning moment and pitch damping moment are given as in their vectorial and scalar representations and calculated for the maximum yaw conditions.

Once the projectile leaves the muzzle (the end of the barrel) its trajectory is governed many forces. Primarily, gravity exerts a constant pull on the body and acts through the center of gravity *(CG)* which is determined by the distribution of weight throughout the body. Gravity always produces a uniform vertical acceleration of about 9.8 m/s^2.

Drag Force

The aerodynamic drag force opposes the forward velocity of the projectile. Drag is the classical aerodynamic force of exterior ballistics;

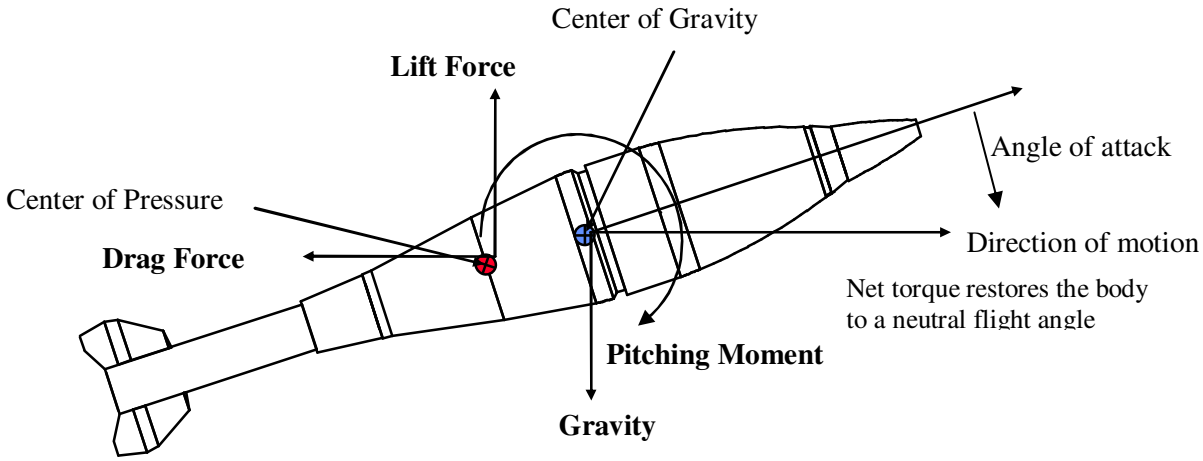

Fig. 5.1 Aerodynamic forces and moments in flight

Aerodynamic forces are generally proportional to the velocity squared. The aerodynamic forces act through the center of pressure *(CP)* which is a function of the body's shape. There are three types of drag force which apply to projectiles:

1. Skin drag- friction on the outer surface as it moves through the air
2. Shape drag- caused by low pressure behind the body due to the flow of air around its shape.
3. Wave drag - a loss of energy that is put into acoustic waves as the body passes through the air. Particularly strong near the speed of sound in air.

All drag forces act at the center of pressure and are in the opposite direction as the motion of the projectile. The drag force can be written as

Vector drag force $= \frac{-1}{2}\rho S C_D \bar{V} V = \frac{-1}{2}\rho S C_D V^2 \vec{i}$ ..... (5.1.1a)

Drag force = $\frac{-1}{2}\rho V^2 S C_D$ ..... (5.1.1b)

The quantity $\frac{1}{2}\rho V^2$ is the dynamic pressure

$S = \frac{\pi d^2}{4}$ Where d = the projectile reference diameter.

The reference diameter of a projectile is usually taken as the diameter of the cylindrical section immediately following the end of the ogive. The effect of yawing motion on drag is accounted for by allowing the drag coefficient to vary with yaw. If the total yaw angle is α_t, the drag coefficient is usually well approximated by

$$C_D = C_{D_o} + C_{D_{\delta^2}} \delta^2$$

$\delta = \sin \alpha_t$

$\alpha_t = \sqrt{\alpha^2 + \beta^2}$, a good approximation to the total yaw angle

Note that a strictly correct definition of the total angle of attack is given by the equation:

$$\sin \alpha_t = \sqrt{\left(\frac{\sin \alpha}{\cos \beta}\right)^2 + \sin^2 \beta}$$

For small total angles of attack (α_t <15 degrees), the difference between the exact and the approximate definitions is insignificant. The drag coefficient varies quadratically with total yaw angle, thus drag increases rapidly with large yawing motion. Since low drag is generally desirable, the yaw drag effect requires that the yawing motion be as small as possible. α_t varies along the trajectory, due to the epicyclic ("rosette") motion of the projectile's axis about the flight path. Consequently the drag coefficient changes during the flight path, with both velocity and yaw level.

Lift And Normal Force

Aerodynamic lift is the force perpendicular to the trajectory, tending to pull the projectile in the direction its nose is pointed. If the nose of the projectile is above its trajectory, the lift force causes the projectile to climb. The lift force is stated in vector and scalar forms:

Vector lift force = $\frac{1}{2}\rho SC_{L_\alpha}\left[\vec{V}x\left(\vec{X}x\vec{V}\right)\right]=\frac{1}{2}\rho SC_{L_\alpha}V^2\left[\vec{i}\,x\left(\vec{X}x\vec{i}\right)\right]$ …….. (5.1.2a)

Lift force = $\frac{1}{2}\rho SC_{L_\alpha}V^2\sin\alpha_t$ ……(5.1.2b)

The lift force is proportional to the sine of the total yaw angle, always acts perpendicular to the trajectory, in the plane containing both the trajectory and the projectile axis of rotational symmetry. The lift force vanishes only if the total yaw angle is zero. Aerodynamic lift is the force that produces the drift of spin stabilized projectiles at long ranges. Lift also causes such effects as aerodynamic jump and epicyclic swerve.

The lift force coefficient often exhibits nonlinear behavior, e.g., the coefficient varies with yaw level. The nonlinear lift coefficient is usually well described by:

$$C_{L_\alpha} = C_{L\ \alpha_0} + C_{L_{\alpha_2}}\delta^2$$

The coefficients $C_{L\ \alpha_0}$ and $C_{L_{\alpha_2}}\delta^2$ referred to as linear and cubic coefficients because in the lift force definition, the variation of lift force with total yaw angle includes a term proportional to ($\sin\alpha_t$), and a second term proportional to ($\sin^3\alpha_t$).

Overturning Moment

The overturning is the aerodynamic moment associated with the lift or normal force. If the projectile's nose lies above its trajectory, a positive overturning moment acts to increase the yaw angle. The overturning moment is given by the vector and scalar equations:

$$\text{Vector overturning moment} = \frac{1}{2}\rho SdC_{M_\alpha}V^2\left(\vec{i}\,x\vec{X}\right) \quad \ldots\ldots\ldots\ldots\ldots\ldots \quad (5.1.3a)$$

$$\text{Overturning moment} = \frac{1}{2}\rho SdC_{M_\alpha}V^2\sin\alpha_t \quad \ldots\ldots\ldots\ldots\ldots\ldots\ldots\ldots \quad (5.1.3b)$$

The overturning moment varies with the sine of the total yaw angle, and for a positive coefficient, always acts to increase the yaw. Thus a non-spinning projectile with positive C_{M_α} is usually unstable. If sufficiently large fins are added to the tail of a projectile, the large tail lift due to the fins overpowers the smaller lift due to nose, and the result is a negative C_{M_α}, which acts to decrease the yaw. It is intuitively obvious that such a projectile should be stable without spin. For a projectile with positive C_{M_α}, axial spin is imparted to counteract the destabilizing effect of the overturning moment.

The overturning moment coefficient usually exhibits nonlinear behavior, and the coefficient variation with yaw level is generally well described by:

$$\mathrm{C_{M_\alpha}} = \mathrm{C_{M_{\alpha O}}} + \mathrm{C_{M_{\alpha 2}}}\delta^2$$

Pitch Damping Moment

The pitch damping moment is illustrated in fig. 6.1 for a positive pitching angular velocity, it contains two parts, one proportional to q_t and one proportional to $\dot{\alpha}_t$. The total pitch damping moment is given by the vector and scalar equations:

Vector pitch damping moment

$$= \frac{1}{2}\rho Sd^2C_{M_q}V\left(\vec{X}x\frac{d\vec{x}}{dt}\right) + \frac{1}{2}\rho Sd^2C_{M_\alpha}V\left[\left(\vec{X}x\frac{d\vec{x}}{dt}\right) - \left(\vec{X}x\frac{d\vec{i}}{dt}\right)\right] \ldots\ldots\ldots\ldots\ldots \quad (5.1.4a)$$

Pitch damping moment $= \frac{1}{2}\rho V^2 Sd\left[\left(\frac{q_t d}{V}\right)C_{M_q} + \left(\frac{\dot{\alpha}_t d}{V}\right)C_{M_{\dot{\alpha}}}\right]$ …….. (5.1.4b)

q_t and $\dot{\alpha}_t$ are virtually identical in practice, and the simpler vector and scalar approximations are generally used:

Vector pitch damping moment $= \frac{1}{2}\rho Sd^2\left(C_{M_q} + C_{M_\alpha}\right)V\left(\vec{X}x\frac{d\vec{x}}{dt}\right)$ ……..... (5.1.5a)

Pitch damping moment $= \frac{1}{2}\rho V^2 Sd\left(\frac{q_t d}{V}\right)\left(C_{M_q} + C_{M_{\dot{\alpha}}}\right)$ …….. (5.1.5b)

Although the pitch damping force is generally negligible, the pitch damping moment must always be retained because of its influence on the dynamic stability. In general, a positive pitch damping moment acts to increase total transverse angular velocity, and is therefore destabilizing. For dynamic stability, the pitch damping coefficient sum, $\left(C_{M_q} + C_{M_{\dot{\alpha}}}\right)$, should be negative. Positive pitch damping moment coefficient sums have been observed for a number of projectile shapes at transonic and subsonic speeds, and usually troublesome. (Slender body theory tells us that C_{M_q} cannot ever be positive; on the other hand, the same theory shows that $C_{M_{\dot{\alpha}}}$ may be positive for some center of gravity locations. There is some evidence that the pitch damping moment can vary with yaw level at transonic and subsonic speeds; such behaviour has not been observed at supersonic speeds; In most cases where nonlinear Pitch damping has been measured, its influence on the yawing motion is much smaller than that of the nonlinear Magnus moment.

The maximum values of these forces drag force, lift force, overturning moment, pitch damping moments are calculated taking the coefficients at charge filling six (from table)

$\rho =$ 1.225kg/m^3 , $\overline{V} = 284 \, m/s$, $S = \frac{\pi d^2}{4}$ =0.01131m^2

$\delta = \sin \alpha_t$, $\alpha_t = \sqrt{\alpha^2 + \beta^2}$, $\alpha_t = \sqrt{10^2 + 4^2} = 10.77^0$, $\delta = \sin 10.77^O = 0.187$

$C_{D_O} = 0.126$, $C_{D_{\delta^2}} = 4.03$, $C_D = C_{D_O} + C_{D_{\delta^2}} \delta^2$, $C_{D_{\delta^2}} \delta^2 = 4.03 * 0.187^2 = 0.1407$,

$C_{L_\alpha} = C_{L_{\alpha_0}} + C_{L_{\alpha_2}} \delta^2$, $C_{L_{\alpha_2}} \delta^2 = 28.3 * 0.187^2 = 0.9896$,

$C_{M_\alpha} = C_{M_{\alpha O}} + C_{M_{\alpha 2}} \delta^2$, $C_{M_{\alpha O}} = 2.72$, $C_{M_{\alpha 2}} = 30.2$, $C_{M_{\alpha 2}} \delta^2 = 30.2 * 0.187^2 = 1.056$, $\left(C_{Mq} + C_{M_{\dot{\alpha}}} \right)_0 = -21.9$, $\left(C_{Mq} + C_{M_{\dot{\alpha}}} \right)_2 = -357$,

Moment /force type	Scalar notation	Non linear coefficients	Values	Angle of yaw and pitch
				$\alpha = 10^O$, $\beta = 4^O$
Drag force	$\frac{-1}{2} \rho V^2 S C_D$	$C_D = C_{D_O} + C_{D_{\delta^2}} \delta^2$	0.2667	138.4N
Lift force	$\frac{1}{2} \rho S C_{L_\alpha} V^2 \sin \alpha_t$	$C_{L_\alpha} = C_{L_{\alpha_0}} + C_{L_{\alpha_2}} \delta^2$	3.05	296.4N
Overturning moment	$\frac{1}{2} \rho S d C_{M_\alpha} V^2 \sin \alpha_t$	$C_{M_\alpha} = C_{M_{\alpha O}} + C_{M_{\alpha 2}} \delta^2$	*3.78*	44.08N
Pitch damping moment	$\frac{1}{2} \rho V^2 S d \left(\frac{q_t d}{V} \right) \left(C_{Mq} + C_{M_{\dot{\alpha}}} \right)$	$C_{Mq} + C_{M_{\dot{\alpha}}} = \left(C_{Mq} + C_{M_{\dot{\alpha}}} \right)_0 + \left(C_{Mq} + C_{M_{\dot{\alpha}}} \right)_2$	-34.21	-9.89

5.2 EQUATION OF MOTION

Newton's second law of motion for the projectile states that the rate of change of momentum must equal the sum of all the externally applied forces. The point mass trajectory, which includes the aerodynamic drag force in addition to gravity, is a very practical and accurate approximation to the actual trajectory of any projectile that flies with predominantly small yaw[15]. For constant projectile mass, Newton's second law gives the general vector differential equation of motion as:

$$m\frac{d\vec{V}}{dt} = \sum \vec{F} + m\vec{g} + m\vec{\Lambda} \quad \text{.....(5.2.1)}$$

Where m = projectile mass

$\vec{V}$ = vector velocity (relative to the ground)

t = time

$\frac{d\vec{V}}{dt}$ =vector acceleration

$\sum \vec{F}$ = vector sum of all the aerodynamic forces

$\vec{g}$ = vector acceleration due to gravity

$\vec{\Lambda}$ = vector coriolis acceleration due to the earth's rotation

Where $F = -\frac{1}{2}\rho\tilde{V}^2 SC_D$

Then $\tilde{V}^2 = \left(\tilde{V} - \tilde{W}\right) \bullet \left(\tilde{V} - \tilde{W}\right)$

$$-\hat{C}_D = \frac{\rho S C_D}{2m}$$

Coriolis acceleration has a significant effect on long range artillery fire. For the modest velocities and ranges, Coriolis effects are negligible in comparison with the acceleration due to gravity.

The vector differential equation of motion for a point mass trajectory with wind, the vector velocity, $\vec{V}$, must be replaced with $\left(\vec{V} - \vec{W}\right)$ in the aerodynamic drag force, because the drag depends on the velocity relative to the air stream, not the velocity relative to the ground.

$$\frac{d\vec{V}}{dt} = -\hat{C}^*{}_D\tilde{V}\left(\vec{V} - \vec{W}\right) + \vec{g} \quad \text{.....(5.2.2)}$$

$\vec{W}$ = vector wind velocity (relative to the ground)

The quantity $\vec{V}$ is the scalar magnitude of the projectile's velocity relative to the air stream:

$$\vec{V} = \left|\vec{V} - \vec{W}\right|$$

The vector $\vec{V}$ and $\vec{W}$ are now resolved into components along the coordinate axes velocity and acceleration are given by:

$$\vec{V} = V_X \vec{I} + V_Y \vec{J} + V_Z \vec{K} \text{ ……. ……. (5.2.3)}$$

$$\vec{W} = W_X \vec{I} + W_Y \vec{J} + W_Z \vec{K} \text{ ……. (5.2.4)}$$

$$\frac{d\vec{V}}{dt} = \dot{V}_X \vec{I} + \dot{V}_Y \vec{J} + \dot{V}_Z \vec{K} \text{ ……. (5.2.5)}$$

Where $\vec{I}$ is a unit vector along the x-axis

$\vec{J}$ is a unit vector along the y-axis

$\vec{K}$ is a unit vector along the z-axis

V_X, V_Y and V_Z are the velocity components

W_X, W_Y and W_Z are the wind components

$$\dot{V}_x = \frac{dV_x}{dt} = \text{X-component of acceleration.……(5.2.6)}$$

$$\dot{V}_Y = \frac{dV_Y}{dt} = \text{Y-component of acceleration.……(5.2.7)}$$

$$\dot{V}_Z = \frac{dV_Z}{dt} = \text{Z-component of acceleration.……(5.2.8)}$$

Substituting the velocity and wind components into the equation (5.2.2), and following the procedure, we obtain the three scalar differential equations of motion:

$$\dot{V}_x = -\hat{C}^*{}_D \tilde{V}\left(\vec{V}_X - \vec{W}_X\right) \text{ ……. (5.2.9)}$$

$$\dot{V}_Y = -\hat{C}^*{}_D \tilde{V}\left(\vec{V}_Y - \vec{W}_Y\right) - g \text{ ……(5.2.10)}$$

$$\dot{V}_Z = -\hat{C}^*{}_D \tilde{V}\left(\vec{V}_Z - \vec{W}_Z\right) \text{……. (5.2.11)}$$

The scalar is given by:

$$\tilde{V} = \sqrt{\left(\vec{V}_X - \vec{W}_X\right)^2 + \left(\vec{V}_Y - \vec{W}_Y\right)^2 + \left(\vec{V}_Z - \vec{W}_Z\right)^2} \quad \text{..... (5.2.12)}$$

A vector wind component is considered positive when it blows in the positive direction of one of the coordinate axis. Thus a tail wind, blowing from the gun toward the target will taken as a positive range wind, $W_{x.}$

Equations (5.2.9) through (5.2.11), together with equation (5.2.12) are an exact statement of Newton's second law of motion for a projectile acted on by aerodynamic drag, gravity, and wind.

The vector yaw, $\vec{\alpha}_R = \vec{i}\,x\left(\vec{X}x\vec{i}\right) = \vec{X} - \left(\cos\alpha_t\right)\vec{i}$ .....(5.2.13)

$\vec{i} = \dfrac{\vec{v}}{|v|}$, a unit vector in the direction of the velocity, $\vec{v}$

The vector yaw, $\vec{\alpha}_R$, has the magnitude ($\sin\alpha_t$), where α_t is the total angle of attack; $\vec{\alpha}_R$ is perpendicular to the trajectory, and is directed from the flight path toward the projectile's axis of rotational symmetry.

For a non-spinning, statically stable (finned) projectile, a good approximation to yaw of repose is

$$\vec{\alpha}_R = \left(\frac{C_{M_q}}{C_{M_\alpha}}\right)\left[\vec{v}x\left(\vec{v}x\vec{g}\right)\right] \text{..... (5.2.14)}$$

If the projectile is non-spinning, or very slowly rolling, then the overturning moment coefficient, C_{M_α}, must be negative for static stability. The value of the pitch damping moment coefficient, C_{M_q}, must also be negative for dynamically stable flight. If the overturning moment coefficient and the pitch damping moment coefficient are both negative, the yaw of repose of a non-spinning, statically stable projectile points slightly above its trajectory.

3-DOF trajectory of projectile at atmosphere with wind V_x = 3m/s

The ballistic coefficient =1.239

T [s]	V [m/s]	TETA [deg]	X [m]	Y [m]
0.000	284.00	45.0000	0.0	0.0
1.005	269.92	43.5273	199.2	194.3
2.000	257.02	41.9571	391.6	372.2
3.000	244.97	40.2590	580.6	537.2
4.000	233.76	38.4328	765.6	689.0
5.000	223.32	36.4706	946.9	828.0
6.000	213.60	34.3647	1124.9	954.6
7.000	204.57	32.1075	1299.7	1069.2
8.000	196.23	29.6928	1471.5	1172.1
9.005	188.52	27.1023	1641.5	1264.1
10.005	181.52	24.3588	1808.1	1344.5
11.005	175.18	21.4496	1972.3	1413.9
12.004	169.50	18.3777	2134.2	1472.7
13.004	164.49	15.1502	2294.0	1520.9
14.004	160.16	11.7788	2451.8	1558.7
15.004	156.52	8.2801	2607.6	1586.3
16.004	153.56	4.6755	2761.6	1603.8
17.004	151.29	0.9909	2913.7	1611.4
18.004	149.70	-2.7441	3064.1	1609.1
19.004	148.78	-6.4977	3212.8	1597.1
20.005	148.51	-10.2375	3359.8	1575.5
21.005	148.86	-13.9318	3505.1	1544.3
22.000	149.78	-17.5337	3648.0	1504.0
23.000	151.26	-21.0539	3790.0	1454.3
24.001	153.24	-24.4534	3930.3	1395.4
25.001	155.66	-27.7159	4069.0	1327.5
26.001	158.49	-30.8305	4205.9	1250.7
27.001	161.67	-33.7905	4341.2	1165.1
28.001	165.15	-36.5931	4474.7	1070.9
29.002	168.89	-39.2391	4606.4	968.2
30.002	172.82	-41.7316	4736.3	857.3
31.002	176.92	-44.0758	4864.3	738.2
32.002	181.13	-46.2783	4990.4	611.2
33.002	185.42	-48.3462	5114.7	476.5
34.001	189.75	-50.2876	5236.9	334.2
35.001	194.10	-52.1103	5357.1	184.6
35.900	197.98	-53.6559	5463.6	43.9
35.950	198.20	-53.7392	5469.4	35.9
36.000	198.41	-53.8223	5475.3	27.9
36.050	198.63	-53.9052	5481.1	19.9
36.105	198.86	-53.9960	5487.6	11.1
36.155	199.08	-54.0783	5493.4	3.0
36.205	199.29	-54.1603	5499.3	-5.1

5.2.1 Range

The restricted range of the 3in. and 4.2in. mortar, 2790 and 4100yards respectively, result in limited flexibility and an inability to deliver effective counter mortar fire against enemy weapons. Increased ranges may be obtained by:

a. improved aerodynamic characteristics of the shell
b. reduction of windage
c. increase in charge weight

Increase in charge weight

Higher chamber pressures will obviously be limited by the designed strength of barrel and base plate. The table below, based on the recommendations of the gun design committee and mises hencky criterion for failure, shows that the 3in. mortar charge weight could have been increased but that there is little margin for this in 4.72in mortar.

Table 5.2 3 in. and 4. 2 in mortar barrel properties

Mortar	Yield strength of barrel steel (ton/in^2)	Factor of safety	Normal working pressure (ton/in^2)	Maximum allowed pressure (ton/in^2)
3 in.	50	1.31	2.7	4.5
4.2 in	45	1.35	4.0	4.5
4.72	81	1.48	8.5	10

The need for long ranges conflicts with the requirement for high rates of fire. Barrel heating will increase as charge weight increases, the critical temperature being reached earlier with a larger charge.

Increased ranges will incur heavy and strong components unless improved materials are used. The barrel material will require to have a high yield strength with the ability to retain its yield strength at high temperatures. The base plate must have the increased flotation area necessary to prevent rapid sinking in soft ground.

Barrel heating : the rapid fall of the yield point of normal barrel steel, after the material reaches approximately 450^0 c, may cause the barrel to be stressed beyond its elastic limit with resulting permanent expansion. Prolonged firing after these conditions has caused rupture of 3in mortar barrels. Hot barrels have also been the cause of premature ignition of secondary charges resulting in every short rounds.
The increase in bore diameter will result in variable internal ballistics. (The diameter of the 3in barrel increases by 0.001in, at the shot start position, for every 5-6 rounds fired at the normal rate.)

Table 5.2 Muzzle velocity at different angles

Range of mortar 120 mm for muzzle velocity and angel of incidence 45, 55 and 65 degr.			
Velocity, m/s	45 degr	55 degr	65 degr
Propellant charge 1, 108 m/s	1102	1034.8	844.9
Propellant charge 2, 128 m/s	1495.4	1401.3	1145.3
Propellant charge 3, 173 m/s	2547.9	2383.2	1951.1
Propellant charge 4, 214 m/s	3603.2	3365.8	2762.8
Propellant charge 5, 250 m/s	4568.8	4273.6	3512
Propellant charge 6, 284 ms	5499.3	5141.5	4232

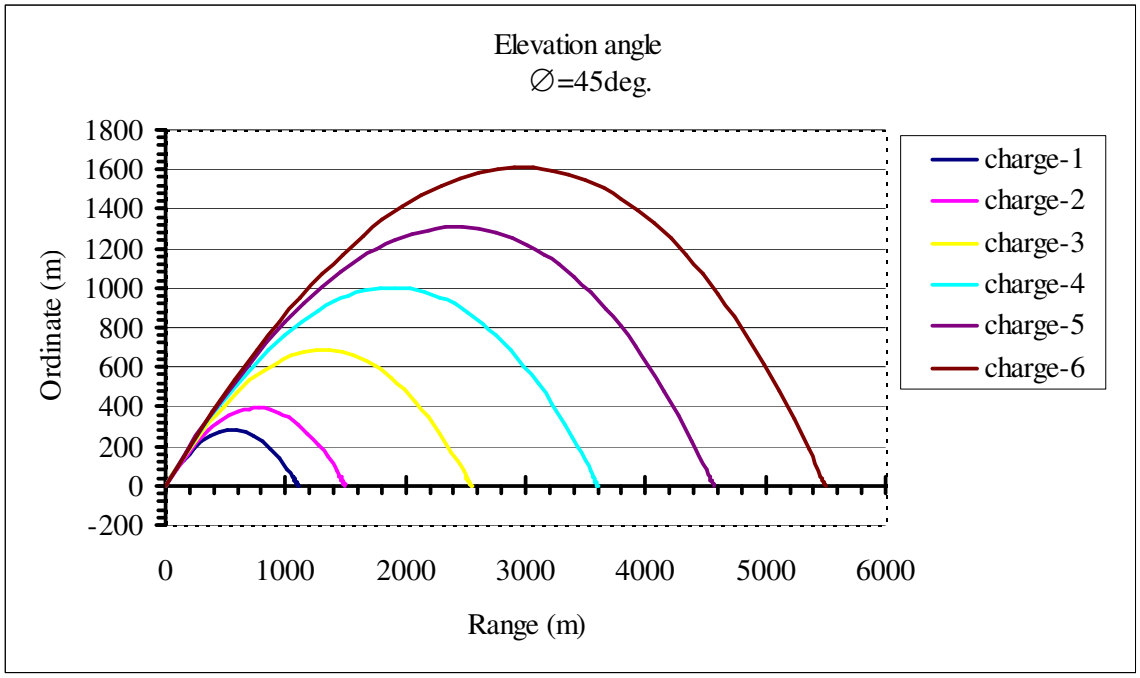

Fig. 5.2a Range versus ordinate (at elevation angle of 45)

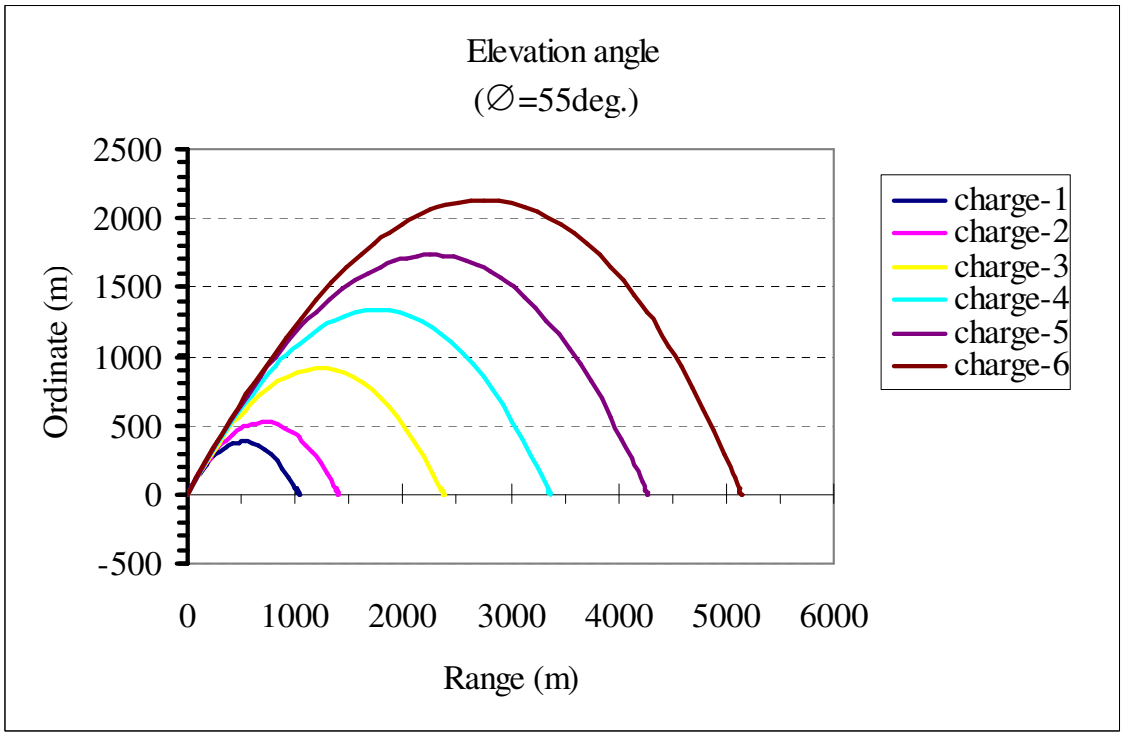

Fig. 5.2b Range versus ordinate (at elevation angle of 55)

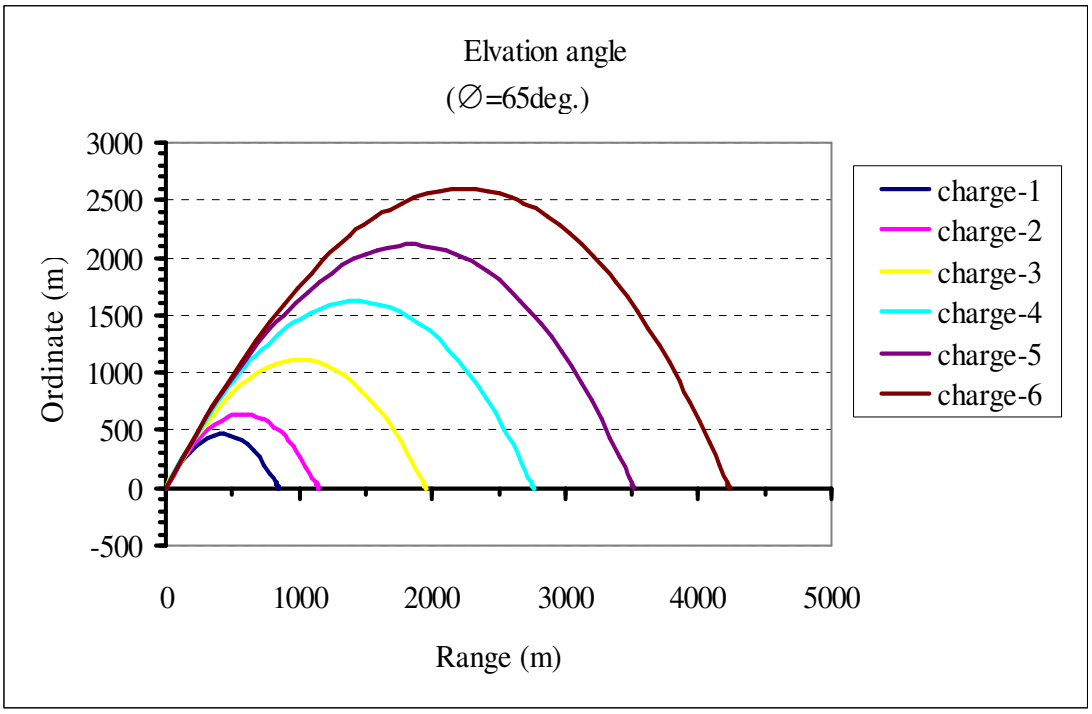

Fig. 5.2c Range versus ordinate (at elevation angle of 65)

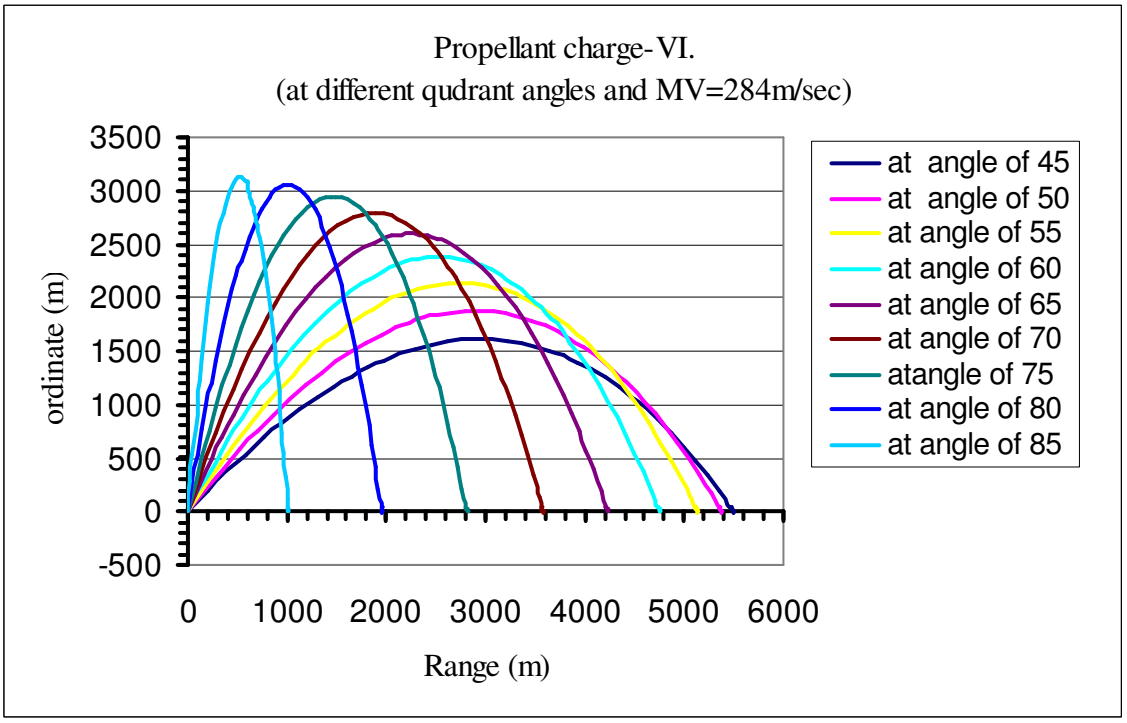

Fig. 5.2d Range versus ordinate of propellant charge-VI at different qudrant angles

5.2.2 Dispersion

Probably the most disquieting feature in the performance of mortars has been the large and sometimes unpredictable dispersion at the target. A study of dispersion patterns for various weapons shows that the mortar has had very inferior consistency when compared with other modern weapons. Fall of short patterns, as expressed by 50% Zones, have been considerably larger under similar firing conditions [26].

While area neutralization is possible, and night defensive fire tasks have been covered with good effect, attack on small targets such as m.g. positions has only been effective with a large expenditure of ammunition. This imposes a limitation which is of increasing importance as war becomes more mobile and ammunition supply more difficult. Typical dispersion figures, at maximum ranges, as shown below:-

Table 5.3 Dispersion of 2in, 3in and 4.2in mortar ammunitions

Mortars	Range	50% zones			
		For range		For line	
		(m)	(% of range)	(m)	(% of range)
2in	535	41.15	8.4	9.144	1.8
3in	2,790	137.16	5.4	22.86	0.9
4.2in	4,100	137.16	3.6	36.58	1.0

Large dispersion imposes large safety zones which restrict the use and flexibility of the weapon. Safety zones at maximum ranges for the 3in and 4.2in. mortars are:-

Table 5.4 Dispersion of safety zones

Mortars	Safety zones (m)			
	service		training	
	overhead	flanking	overhead	flanking
3in	365.76	137.16	Not	274.32
4.2in	457.2	228.6	permitted	457.2

The principal causes of dispersion

Many of the causes of the dispersion arise from the type of projectiles used. The main causes of dispersion are:

a. variation in physical characteristics of projectiles
b. internal ballistic variations
c. variations in launching conditions
d. variations in flight

Variation in physical characteristics of projectiles

3in.and 4.2in. can be produced cheaply and with the minimum use of machine tools, as a result these projectiles have cast iron bodies which are machined only at the guide bands and screw threads, short tails with spot welded vanes, secondary charges placed between the vanes and inexpensive "shot gun" type primary charges. These features result in lack of consistency and giving rise to conditions described below.

Variation in weight

The manufacturer's tolerance on the empty 3in. projectile body is 4.5oz. A difference of 1oz will alter R max by 6.5yds.

Variations in C of G and transverse movement of inertia

This will affect damping of yaw and hence the drag characteristics of individual projectiles.

Body and tail eccentricities

Inaccurate alignment of tail and body, and out-of-balance bodies will cause varying gyrations and oscillations, and varying projectile spin.

Variations in external body shape

Varying airflow will affect the aerodynamics constants.

Damage undetected before firing.

A considerable number of very rounds occurs with the current mortars. Many of these are due to damage occurring at or before ejection, but after firing. The main features have been bent or distorted tails, split tail tubes and faulty adaptors. The damages mainly arises from the fact that secondary charges are positioned between tail vanes, lack of symmetry in tail vanes, uneven support of tail vanes on firing when secondary charges are removed for lower ranges.

Internal ballistic variation

Variations in muzzle velocity caused trough:-

a. varying projectile weight
b. varying projectile shape
c. windage (gap between projectile and barrel)
d. propellant variations

Sporadic pressures and varying turbulence. Due to

a. irregular burning of propellant
b. irregular ignition "shot gun" type primary charge to moisture. Measure of ability to withstand moisture is called wet efficiency.

Wet efficiency = $\frac{MVwet^2}{MVdry^2} \times 100 = \%$ of service range likely to be achieved.

Motion of projectile in bore.

Due to varying friction, side-slap and vibrations. Chatter of guide band and tail can cause tail damage.

Variations in launching conditions

Movement of base plates. On bad ground (soft, muddy or icy) considerable base plate movement is liable to occur. This instability of base plates will cause of dispersion, particularly during rapid fire.

Jump. this is the angle between the line of departure the bomb and the axis of the bore as laid. If the angle of jump remains constant, dispersion will not be increased. (Accuracy will, however, decrease because the effect of jump on range varies with the angle of elevation)

Initial yawing impulse. This is given to the bomb when transverse movement of the barrel occurs at the moment of exit. Considerable initial yaw may be imparted to the bomb.

Disturbance to the flight intermediate zone

The propellant gases are moving faster than the shell in the region of the muzzle. The bomb is unstable in this region when it is in effect, traveling tail first relative to the

gases (a distance of about 8ft. in the 3in. mortar). This will increase any initial yaw and have a considerable weather cocking effect on the projectile.

Variation in flight

Oscillations of projectile

The drag is greater than with a steady bomb and oscillations will therefore cause a projectile to range shorter. Experimental data shown that a mean yaw of 8^0 will cause an increase in the drag varying from 30% to 60%. Projectile to projectile variations in oscillation will obviously cause dispersion.

Windage, Base Plate Stability And Spin Yaw Resonance

The close windage principle

Windage is the difference in diameters between the projectile and mortar barrel which is required to allow the muzzle loaded projectile to reach the velocity required for gravity firing. Trial firings have shown that a 0.001in. difference in windage in the 3in. mortar will alter the MV by 1-2ft/sec. Design tolerances on 3in. projectile and mortar permit windages varying from 0.036 to 0.050in. The table below compares 4.2in. mortar shells of different windage fired from the same mortar.

Table 5.5 Windage, velocity and range relation for 4.2in

Charge	Q.E.	Mean windage (in)	Mean MV (ft/sec)	Mean range (yds)	50% zones (% of ranges)	
					Range	line
2	45^0	0.035	707	4217	2.46	0.88
		0.01	755	4402	1.93	0.73

Base plate stability

Base plate stability affects both dispersion and flexibility. The sinking, tilting and sliding which occur on soft, muddy or icy ground have a detrimental effect on performance and necessitate frequent corrections for range and line. Dispersion increases with base plate movement, firepower is decreased when mortars are being dug out, as is the ability to move quickly from one base plate position to another.

5.3 STABILITY

The stability of a projectile is concerned with its motion following a disturbance from an equilibrium condition. In the vast majority of cases there is a distinct requirement for a projectile to be *stable* in flight so that it never deviates too greatly from its intended flight path following a disturbance. This has the benefit of reducing drag (yaw-dependent drag) and also inaccuracies (i.e. a reduction in dispersion of fire). The overall drag increases dramatically with α; in fact, for a tumbling round, the overall C_D rises by a factor of approximately 10.

A distinction is made between the *initial* tendency of the projectile to return to its starting position after a disturbance and any *subsequent* motion. Because the first of these can be analyzed without any reference to the resulting motion, it is termed *static stability*. Examination of the motion itself is referred to *dynamic stability* analysis. Both of these classes of stability will be considered independently below. It will also be seen that there are two classical methods for providing a projectile with inherent stability, by incorporating either *fins* or *spin*. As stated above, this relates to the *initial* response to a disturbance. There are 3 classes of static stability which are possible:

• Stable - the projectile *initially* tends to return to its starting condition.

• Neutrally stable - the projectile *initially* remains in its disturbed condition.

• Unstable - the projectile initially tends to move further away from its starting condition in the direction in which it was disturbed.

Static stability alone is not enough to ensure that a projectile returns to equilibrium after a disturbance, it merely infers that it *starts* moving back to it. Whether it actually gets there or not depends upon the projectile's *dynamic stability* characteristics.

5.3.1 Statically Stable or Not?

A projectile exhibits stable flight when its center of pressure (CP) is aft of its center of gravity (CG). The CG is the location where the net weight force acts, and the CP is the location where the net aerodynamic forces act. If the CG is aft of the CP, then a restoring torque is created whenever the projectile tilts to one side. It is usually desirable to have the center of pressure one to two projectile body diameter lengths ahead of the center of pressure (referred to as one or two calibers of stability). If the projectile has less than one

caliber of stability then the projectile could become unstable during its flight, as the CP changes when the velocity and air pressure change. If the projectile has more than two calibers of stability, then it will create too large of a restoring torque and will wobble side to side as it ascends. The center of gravity can be found by the following equation:

$$X_{CG} = \frac{1}{m_{total}} * \sum m_i * X_i$$

where x is the distance from some reference point, mi is the individual weight of each of the projectile components, and m_{total} is the total weight of the projectle.

The definition of static stability/instability now need to be able to understand which physical characteristics determine whether a projectile is statically stable, unstable or neutral.

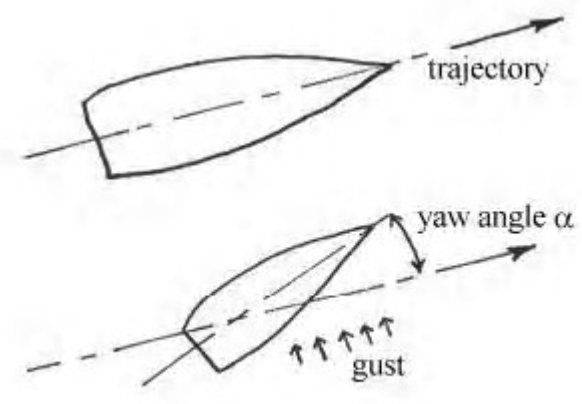

Figure 5.3.1 Gust producing yaw angle on projectile in flight

If the initial response is to move the nose back towards zero yaw (i.e. reducing the yaw angle) then it is *statically stable*. If the yaw angle initially increases as a response then it is *statically unstable* while if the disturbed yaw angle is retained the shell is *neutral*.

It is therefore clear that it is the direction or sign of the resulting yawing moment generated that defines the static stability. This depends upon the aerodynamic force produced on the body due to the yaw angle and, in particular, upon the *normal force* (i.e. the aerodynamic force component perpendicular to the body axis) and the position at which it acts along the body's axis. The point on the body through which the total aerodynamic force may be considered to act is known as its *centre of pressure* (CP). The moment produced by this normal force depends upon the moment arm of the force

relative to the body's centre of gravity *(CG)*. The important criteria which determine a body's static stability/instability are therefore the relative positions of its *CG* and *CP*. This is demonstrated in Fig 5.3.1. In the top figure, *CP* lies behind the *CG* so that a clockwise (restoring) moment is produced. This tends to reduce the yaw angle and return the body to its trajectory, therefore *statically stable*. Conversely, the lower figure, with *CP* ahead of *CG*, produces an anti-clockwise (overturning) moment which increases further and is therefore *statically unstable*. It is also possible to have a neutral case in which *CP* and *CG* are coincident whereby no moment is produced.

There is an important correspondence in the distance between the centre of pressure and the centre of gravity and the static stability of the round. This distance is called the *static margin*. By definition, it is *positive* for positive static stability (i.e. when the centre of pressure is behind the centre of gravity), *zero* for neutral stability and *negative* for negative stability (i.e. static instability).

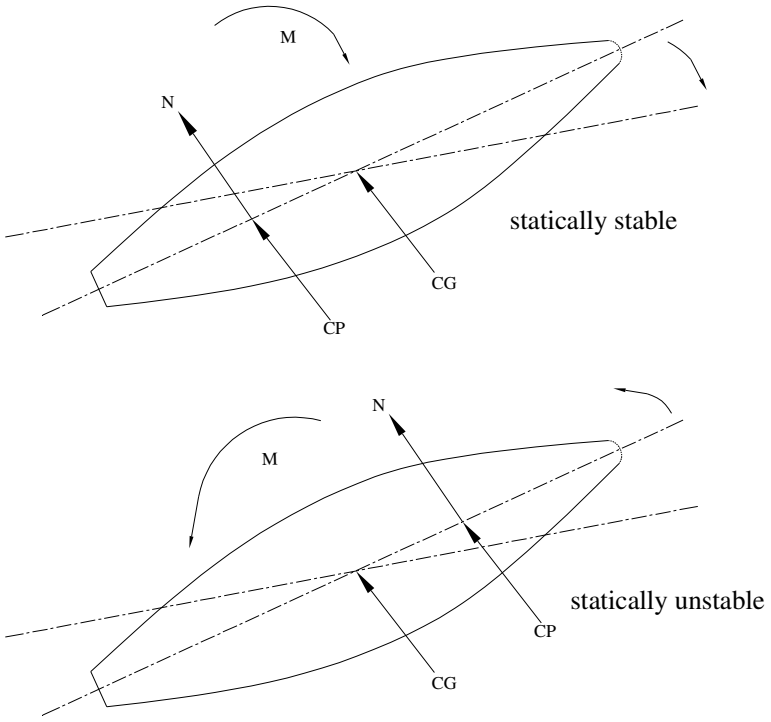

Figure 5.3.2 Static stability/instability affected by CG & CP positions

Many projectiles are inherently unstable, with the *CG* lying behind the *CP*. An artillery shell, has a thick, heavy base to withstand the launch loads and also a long, pointed nose to reduce wave drag. Both of these features lead to a rearwards *CG* position. From the earlier discussions, it is clear that some means must be found for stabilizing the round i.e. ensuring that the nose points essentially along the trajectory and that drag and dispersion effects are minimized. There are two standard techniques of generating directional stability:

a. By the use of *fins* - using natural static stability principles outlined above.

b.By the use of *spin* - using *gyroscopic* moments to overcome the aerodynamic moments.

Fin Stabilisation

It is only necessary to move the centre of pressure aft of the centre of gravity to confer static directional stability on a projectile. This may be done by providing a lifting surface aft of the centre of gravity of the round as shown in Figure 5.3.3.

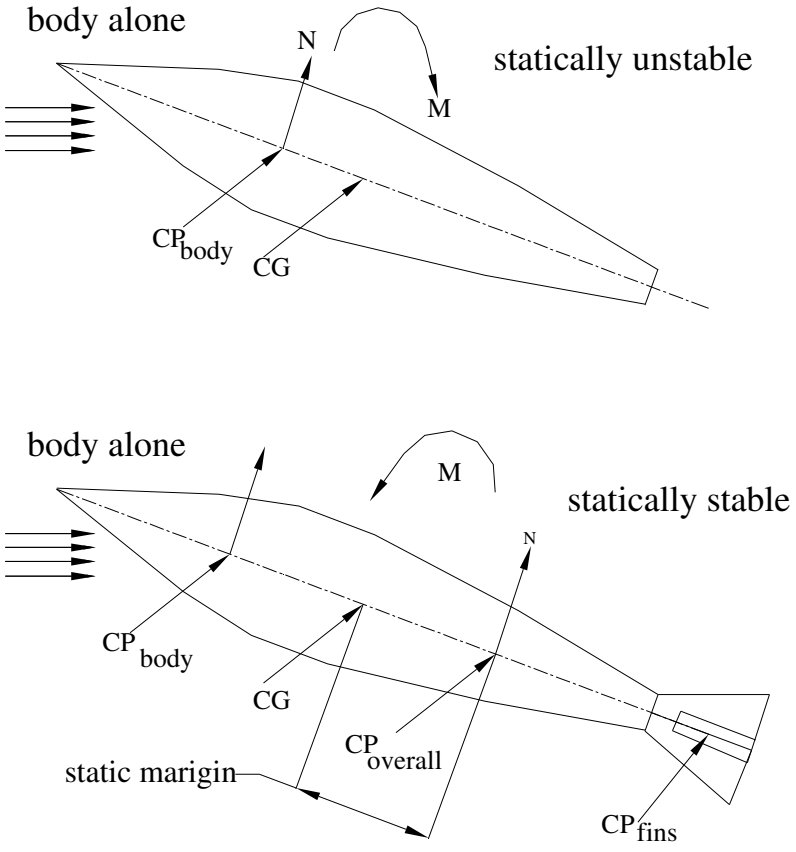

Figure 5.3.3 Fin stabilization

Here, the body lift is well ahead of the centre of gravity but is, rather small due to the fact that a typical body shape is relatively inefficient at producing lift. The lift generated by the stabilising fins is behind the centre of gravity and is also relatively large due to its relative lift effectiveness. Taking moments about, the body nose apex, produces the position for the resultant of both lift forces. This is the *overall centre of pressure* for the projectile with fins (sometimes known as the *neutral point*). If this is aft of the centre of gravity, the projectile will be directionally statically stable.

Relatively small fins at the rear of projectiles can easily stabilise them, at least up to moderate supersonic Mach numbers. The fins have to be lightweight, of course, as their inclusion at the rear will also move the *CG* rearwards which is undesirable from a static stability perspective. Fin stabilised projectiles will normally have a static margin of between 1 and 4 calibres, depending mainly on the type of target to be attacked. In general, hard targets require more stable projectiles.

The main disadvantages of fin stabilisation are that room must be found for the fins inside the barrel i.e the body of the round must be sub-calibre (and be sabot launched) or the fins must deploy after launch (thus increasing complexity of design). The fins also increase the drag of the projectile, typically by between 25% and 40%. However, the very low frontal area does give the dart configuration good penetration.

Since the fins provide stability using the same mechanism as that which produces instability in the body, i.e. from aerodynamic forces, the dart will remain stable if it enters a dense medium, as long as it stays intact. This may be contrasted with the behaviour of spin stabilised rounds [11].

Quantification of static stability

It is often convenient to be able to quantify just how stable or unstable a projectile is and there are two standard methods of doing so.

Static Margin

The first is simply to use the *static margin* method mentioned earlier. This is the linear distance between the *CG* and *CP*, though it is often non-dimensionalised with respect to the calibre. A negative static margin denotes an unstable round by convention.

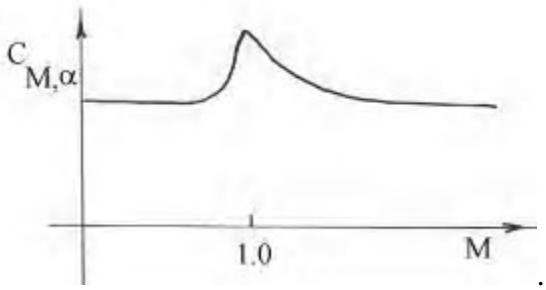

Figure 5.3.4 Variability of $C_{M,\alpha}$

$C_{M,\alpha}$ can clearly vary with anything which affects static margin, as the two parameters are intrinsically related. As a consequence, any variations in the positions of either *CP* or *CG* will directly affect the value of $C_{M,\alpha}$. The position of *CP* will certainly vary during flight if the projectile passes through the *transonic* flow regime, due to complicated shock.

Drag v Stability

There is a trade-off when it comes to the drag and stability of rounds - if the drag is improved (i.e. reduced) then the static stability will almost certainly become worse. This is well illustrated by comparing two standard mortar bombs, of 51 mm and 81 mm caliber.

The 51 mm mortar is designed to operate at low subsonic speeds (typically $M < 0.5$).

Consequently there is a relatively low requirement for reducing fore body drag, resulting in the use of a bluff-nosed nose shape which is preferable from design, manufacture and payload considerations. This also helps to stabilize the round as it moves *CG* further forwards and *CP* rearwards. This means that there is only a minimal requirement for additional fin stabilization so that the fin unit can be mounted in the poor quality dead air region produced by the separated flow from the main body. This helps to reduce the overall length of the mortar.

The 81mm mortar, in comparison, is designed to operate at transonic or low-supersonic speeds, so that there is a definite need to reduce fore body or wave drag by using a well streamlined fore body. This reduces drag but also reduces the static stability so that an enhanced contribution from the fin unit is required. This mortar therefore uses an

extended tail boom so that the dead air region is reduced in size and the fins lie outside its detrimental influence. These effects are shown below in Fig 5.3.5.

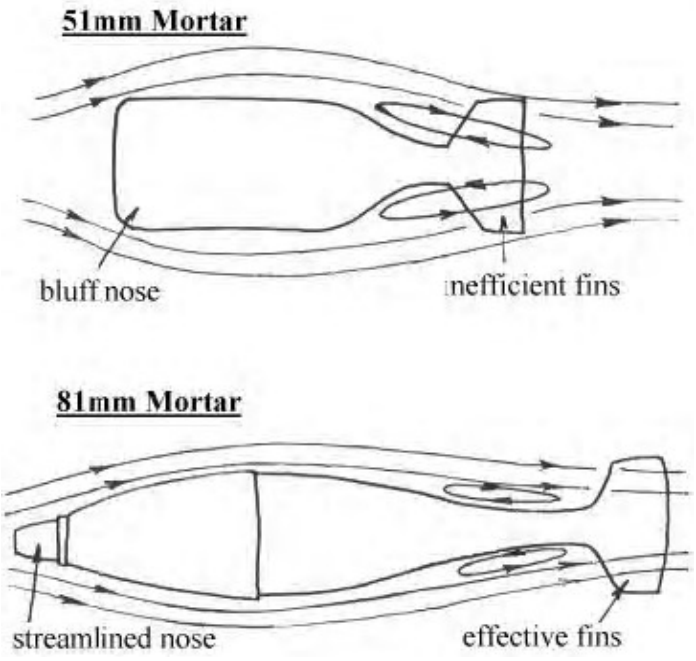

Figure 5.3.5 Comparison of different mortar bomb shapes

The barrowman equations are a common set of equations used to determine the location of the center of pressure of a finned type projectile. They are conservative and limited to conventional fin shapes.

d_0 =120mm C_{root_fin} = 60mm, C_{tip_fin} =20mm

L_N = 73.8mm, S_{fin} = 33.25mm, L_F = 66mm, X_R = 8.96mm, X_B =574mm, N_{fin} = 10,

Nose cone terms:

C_{NN} = 2 , X_N =0.666L_N = 0.666x 73.8mm= 49.15mm

Fin terms

$$C_{NF} = \left(1 + \frac{r}{r + S_{fin}}\right) \frac{4N_{fin}\left(\frac{s_{fin}}{d_0}\right)^2}{1 + \sqrt{1 + \left(\frac{2L_F}{C_{root\_fin} + C_{tip\_fin}}\right)^2}}$$

$$C_{NF} = \left(1 + \frac{73.8mm}{73.8mm + 33.25mm}\right) \frac{4 * 10 \cdot \left(\frac{33.25mm}{120mm}\right)^2}{1 + \sqrt{1 + \left(\frac{2 \cdot 60mm}{73.8mm + 26mm}\right)^2}} = 1.7996$$

$$X_F = X_B + \frac{X_R \cdot \left(C_{root\_fin} + 2 \cdot C_{tip\_fin}\right)}{3 \cdot \left(C_{root\_fin} + C_{tip\_fin}\right)} + \frac{1}{6} \cdot \left[\left(C_{root\_fin} + C_{tip\_fin}\right) - \frac{C_{root\_fin} * C_{tip\_fin}}{C_{root\_fin} + C_{tip\_fin}}\right]$$

$$X_F = 574 + \frac{8.6 \cdot (73.8 + 2 \cdot 20)}{3 \cdot (73.8 + 20)} + \frac{1}{6} \cdot \left[(73.8 + 20) - \frac{73.8 * 20}{73.8 + 20}\right] = 608.41mm$$

The center of pressure:

$$C_{NR} = C_{NN} + C_{NF} = 2 + 1.7996 = 3.7996$$

$$X_{CP} = \frac{C_{NN} \cdot X_N + C_{NF} \cdot X_F}{C_{NR}}$$

$$X_{CP} = \frac{2 \times 49.15mm + 1.7996 \times 608.41mm}{3.7996} = 314.03mm$$

X_{CP} = 314.03mm (measured from the apex)

5.3.2 Dynamic Stability Of Projectile

The dynamic stability of a projectile relates to its motions after the initial response to the applied disturbance. In a stable case the subsequent response will be damped out so that the oscillations are either oscillatory or convergent in nature or heavily damped (i.e. "*deadbeat*"). In the unstable case, the oscillations are undamped and divergent while in the neutral case the behavior is simple harmonic (neither damped nor undamped) [15].

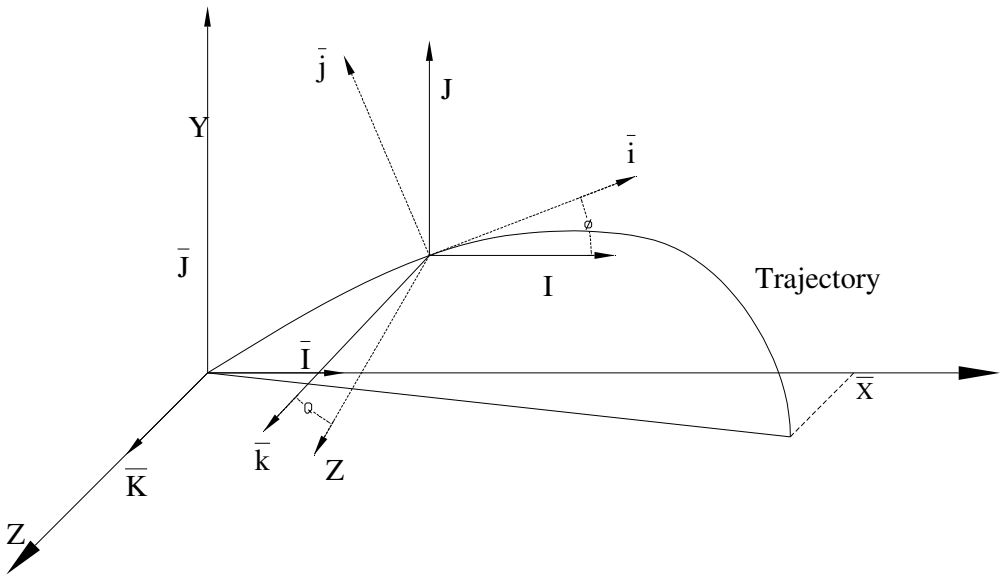

Figure 5.3.6 Non-rolling and ground fixed coordinate system of mortar in flight

The complete linearized pitching and yawing motion of symmetric projectiles:

$$\xi'' + (H - iP)\xi' - (M + iPT)\xi = -iPG \quad \ldots\ldots\ldots\ldots\ldots \quad (5.3)$$

Where

$$H = C^*_{L_\alpha} - C^*_D - K_y^{-2}\left(C_{M_q}{}^* + C_{M_\alpha}{}^*\right)$$

$$P = \left(\frac{I_x}{I_y}\right)\left(\frac{pd}{V}\right)$$

$$M = K_y^{-2}\left(C_{M_q}{}^*\right)$$

$$T = C_{L_\alpha}{}^* + K_x^{-2} C_{M_{Pq}}{}^*$$

$$G = gd\cos\Phi$$

And $\xi = \alpha + i\beta$, $C_D{}^* = \dfrac{\rho sd}{2m} C_D$ And $C_{L_\alpha}{}^* = \dfrac{\rho sd}{2m} C_{L_\alpha}$

$$K_x^{-2} = \frac{md^2}{I_X} \qquad\qquad K_y^{-2} = \frac{md^2}{I_X}$$

This differential equation contain all significant aerodynamics forces and moments that affect the pitching and yawing motion of a spinning or non-spinning symmetric projectile, and its solution give a good approximation to the complete six degrees of freedom motion, for small yaw amplitudes.

$$\lambda_F = -\frac{1}{2}\left[H - \frac{P(2T-H)}{\sqrt{P^2-4M}} \right] \text{……..….(5.4)}$$

$$\lambda_S = -\frac{1}{2}\left[H + \frac{P(2T-H)}{\sqrt{P^2-4M}} \right] \text{…….(5.5)}$$

Dynamic stability requires that both damping exponents, λ_F and λ_S, be negative throughout the projectile flight. If either damping exponent becomes (and remains) positive, that yaw mode will begin to grow, which is the definition of instability. In practice, one of the λ's can become slightly positive for a short time, then return to a negative value, with no significant adverse effect on flight.

For a non-spinning (or very slowly rolling) statically stable projectile, $M<0$, and P is either zero, or is small enough to be neglected. Equations (5.4) and (5.5) show that for this case, the only requirement for dynamic stability is that $H > 0$, for finned or flare-stabilized projectiles, the pitch damping moment coefficient sum, $\left(C_{M_q} + C_{M_\alpha}\right)$, is usually negative. The lift force coefficients are both positive, and C_{L_α} and C_D; therefore H is nearly always greater than zero, and the dynamic stability is assured.

Statically stable projectile ($M < 0$)

(1) A statically stable projectile is always gyroscopically stable, regardless of spin.

(2) If the dynamic stability, S_d lies within the interval ($0 < S_d < 2$) a statically stable projectile is always dynamically stable, regardless of spin.

$$H > 0 \text{……..…….. (5.6)}$$

$$\frac{1}{S_g} < S_d(2 - S_d) \text{……..… (5.7)}$$

Equations (5.6) and (5.7) are the generalized dynamic stability criteria for any spinning and non-spinning symmetric projectile.

Average physical characteristics of 120mm mortar projectile

Projectile diameter = 120mm

Projectile total length = 640mm

Projectile weight = 17.6kg

Axial moment of inertia = 0.03369kg.m^2

Transverse moment of inertia = 0.33458kg.m^2

Center of gravity = 25.495cm from the apex

$$C_D{}^* = \frac{\rho sd}{2m} C_D = \frac{1.1225 \frac{kg}{m^3} * \pi * (0.12m)^3 * (0.267)}{8 * 17.5kg} = 1.0366x10^{-3}$$

$$C_{L_\alpha}{}^* = \frac{\rho sd}{2m} C_{L_\alpha} = \frac{1.1225 \frac{kg}{m^3} * \pi * (0.12m)^3 * (3.05)}{8 * 17.6kg} = 1.289x10^{-2}$$

$$\left(C_{M_q}{}^* + C_{M_{\dot{\alpha}}}{}^* \right) = 0.02966$$

$$K_x{}^{-2} = \frac{md^2}{I_X} = \frac{17.6kgx(0.12m)^2}{0.03369kgm^2} = 12.099$$

$$K_y{}^{-2} = \frac{md^2}{I_y} = \frac{17.6kgx(0.12m)^2}{0.33458kg \cdot m^2} = 1.2179$$

Dynamic stability factor

$$S_d = \frac{2T}{H} = \frac{2\left(C_{L_\alpha} + K_X{}^{-2} C_{M_{pa}}\right)}{C_{L_\alpha} - C_D - K_X{}^{-2}\left(C_{M_q} + C_{M_\alpha}\right)}$$

Substituting the values

$$S_d = \frac{2T}{H} = \frac{2\left(C_{L_\alpha} + K_X{}^{-2} C_{M_{pa}}\right)}{C_{L_\alpha} - C_D - K_X{}^{-2}\left(C_{M_q} + C_{M_\alpha}\right)} = \frac{2(2.275)}{2.275 - 0.267 - 12.099(-485.355)} = 0.011$$

$M = 0.844x(-1.665) = -1.40526$ (both S_d and M are in the required range)

CHAPTER 6

6. 1 FINITE ELEMENT MODELLING AND ANALYSIS

A finite element model of an MB120mm mortar shell has been generated. The goal of analysis was to develop and validate a baseline mechanical model for a mortar casing during realistic firing conditions. This model incorporates the strength changes in the shell attributable to the variation in the hardness and microstructure produced during manufacturing. The results of the model are used to evaluate the stress and resulting deformation that a mortar case undergoes during

(i) Initial impulse force applied in the barrel for launching the shell

(ii) Impact load at the moment of hitting the target

(iii) Pressure induced due to the combustion of charge filling inside it.

The geometry of the shell, primer, barrel, barrel extension and other components was obtained from the gun design empirical and manufacturer's drawings. The drawings were entered into AUTOCAD 2007 so that they could be made proportional for application of ANSYS. The conceptual dimensions of all the components were used.

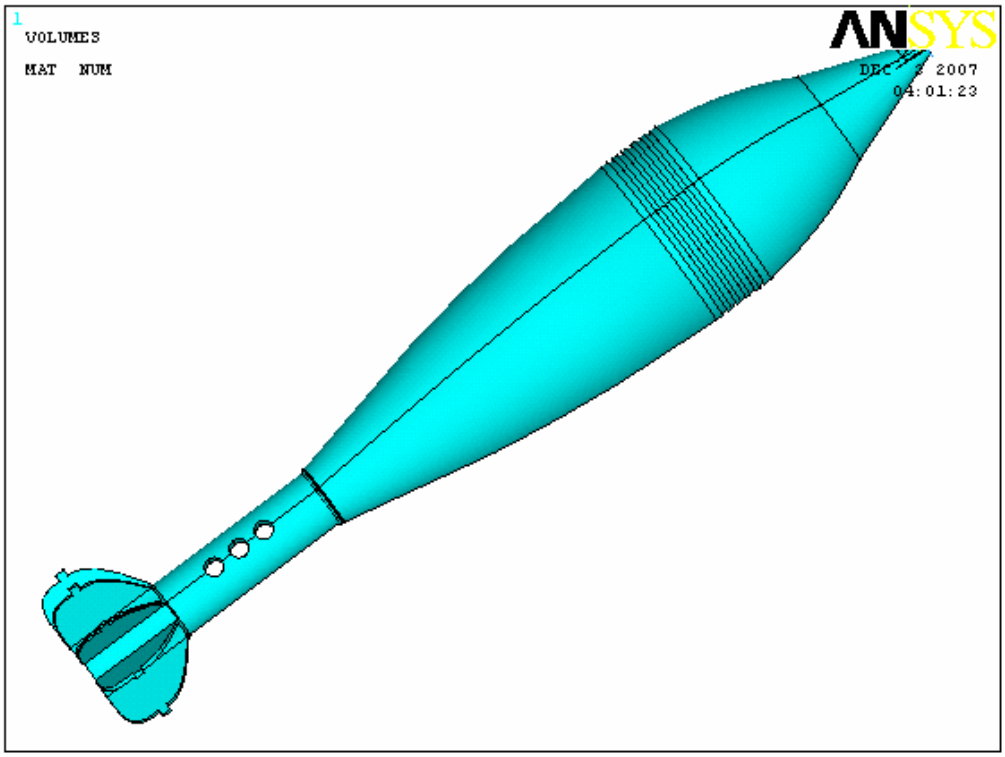

Figure 6.1 constructed modelling of complete 120mm projectile in ANSYS

Consistent with the nature of the problem, symmetry was employed to reduce the model from a full three-dimensional (3-D) analysis to a half symmetric analysis to reduce the computation time. The shell was considered to reside fully inside the chamber region so that the shoulder of the shell and the surface of the chamber were in contact.

Material Input and Model Generation

In order to develop an accurate model, realistic material properties and boundary conditions that mimic the actual shell and operating conditions were required. This information was obtained from experimental data and an empirical approach.

Material Properties

During the numerous processes casting, machining, threading, blasting and annealing steps that occur during the manufacturing of a casing, a hardness and microstructure gradient exists along the length.

The barrel and barrel extension were assumed to be linear elastic steel with a modulus of 210GPa and Poisson's ratio of 0.3. No material properties were available for the primer. It was assumed that the primer possesses the same structural characteristics as the head region of the tail tube, with a hardness of 185 HV. The overall FEA model geometry consisted of three different areas and material properties.

The input to the FEA model was solely the compressive response for the first two cases. It was assumed that the shell exhibited a homogeneous isotropic response and has an identical response in compression. This is a reasonable assumption since the data do not indicate any pre-treatment of the material such as annealing. The assumption of cast iron behaving as a homogeneous isotropic material was carried through the remainder of the modeling effort. With the geometry and the material properties established, the next step was to mesh the model.

6.2 ANALYSIS OF THE MODEL

6.2.1 Finite Element Model Mesh

The model were meshed with the solid 92 ANSYS element. This is a ten-noded tetrahedral element with plasticity, has a quadratic displacement behavior and is well suited to model irregular meshes, large strain and axisymmetric capability. The axis and plane of symmetry was the x-axis and z-x plane respectively. All four materials (the cast steel and three different mild steel) were modeled with isotropic linear elastic properties.

Meshing the model

The model needs to be meshed for finite element analysis to be carried out. The mesh density is an important factor as it varies the accuracy of the results. Increasing the mesh density gives more refined results but it increases the computational time. A balanced comprise should be reached with the accuracy of the results and the computational time, so that an appropriate mesh density can be decided.

Element type: Solid tetrahedral 10 nodes 92

No. of elements: 76851

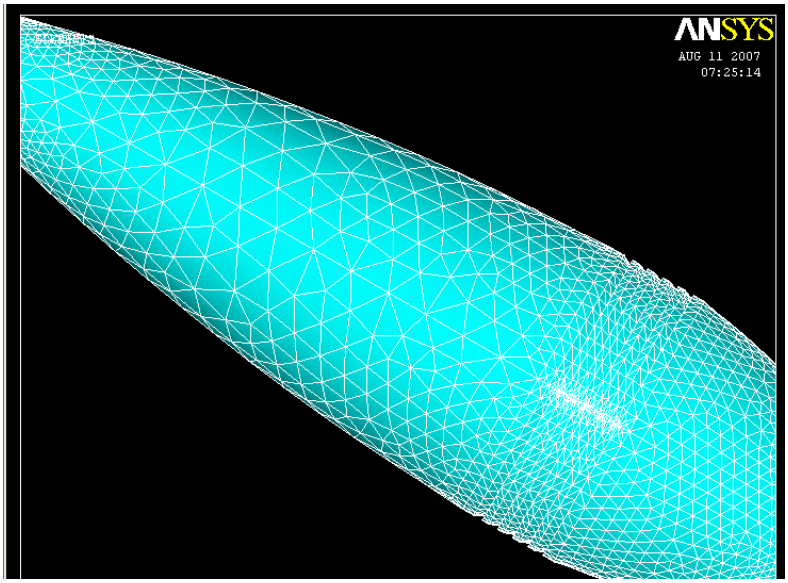

Figure 6.2 Meshing on half model of the shell using ANSYS

Figure depicts the meshed half model. The model was discretized into 76851 elements and the mesh was generated using FEA software ANSYS.

6.2.2 Applied Boundary Conditions and applied loads

Boundary conditions were applied to realistically constrain the model. Symmetric boundary conditions were applied to the plane of symmetry.

Case-I , launching load analysis. In order to fix the shell, a zero displacement constraint, in the x, y and z directions, was applied to the projectile-barrel contact and pressure on the

The interaction between the head of the striking pin and the fin face made it difficult to assign boundary conditions in this region. Initial investigations with the model used zero displacement boundary conditions and load, in all directions applied to the copper groves and external surface of the shell respectively. This assumed that continuous intimate contact existed between the barrel and the copper rings. This condition is not necessarily accurate since it does not account for any rearward motion of the shell during firing. It was determined to overly constrain the motion of the projectile.

Case-II, ground impact (of the shell). A new boundary condition was created that accounted for impact case and the load applied at the base of stiking pin. An symmetric representation of the fuse was incorporated into the model to more closely represent realistic conditions. The dimensions of the fuse were obtained from the 3-D technical data package (TDP) for the fuze UTU M78. To model the interaction between these faces, one additional contact pair was added: a pair for the shell-ground interaction.

Case-III, effect of pressure developed by the charge filling TNT, same boundary conditions of case –II were applied here. A symmetric boundary condition was applied to the fuze and zero displacement conditions were applied to the remaining free faces of the fuze and an interna pressure were applied in the internal cavity of the shell.

After assigning the material properties to the model, the boundary conditions and the loads were assigned.

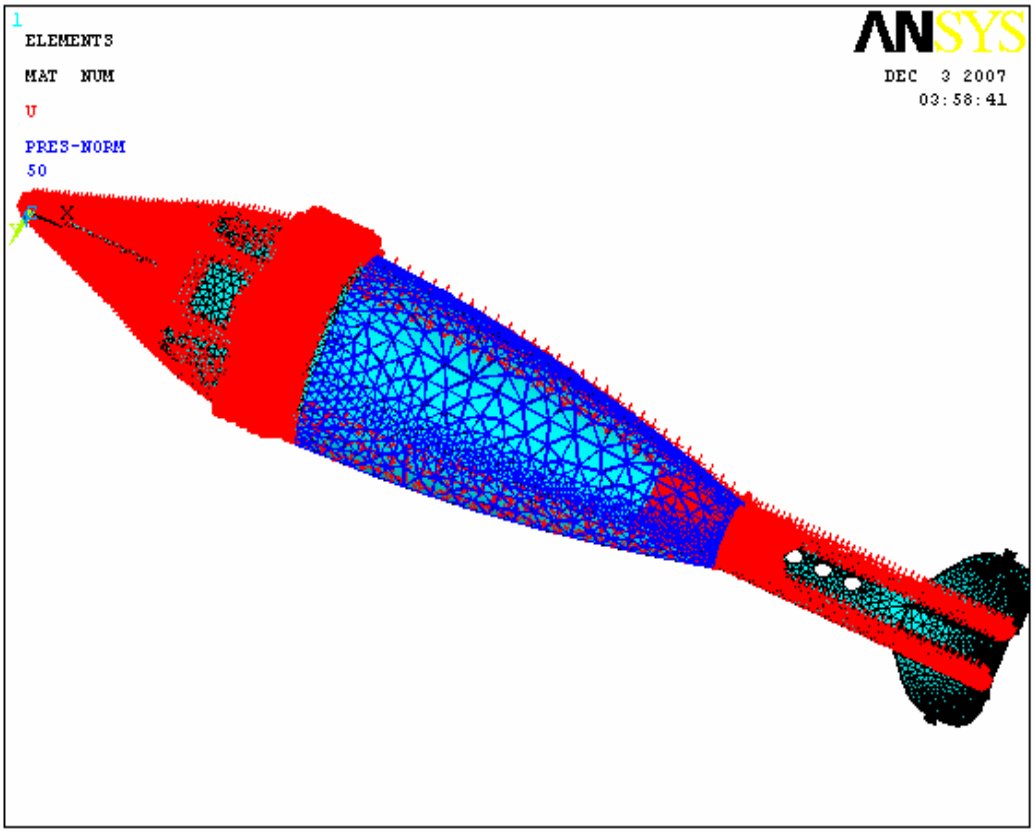

Figure 6.3 Boundary conditions and applied load on the shell model at launching (case-I)

In order to assign the boundary conditions on the shell model, the stress behavior of the model at the launching, at the moment of impact on the target and internal pressure was studied. The loading of the pressure is taken from BRL (ballistic research labratory) experimental results and calculation, by considering the maximum pressure at the base and apex points applied.

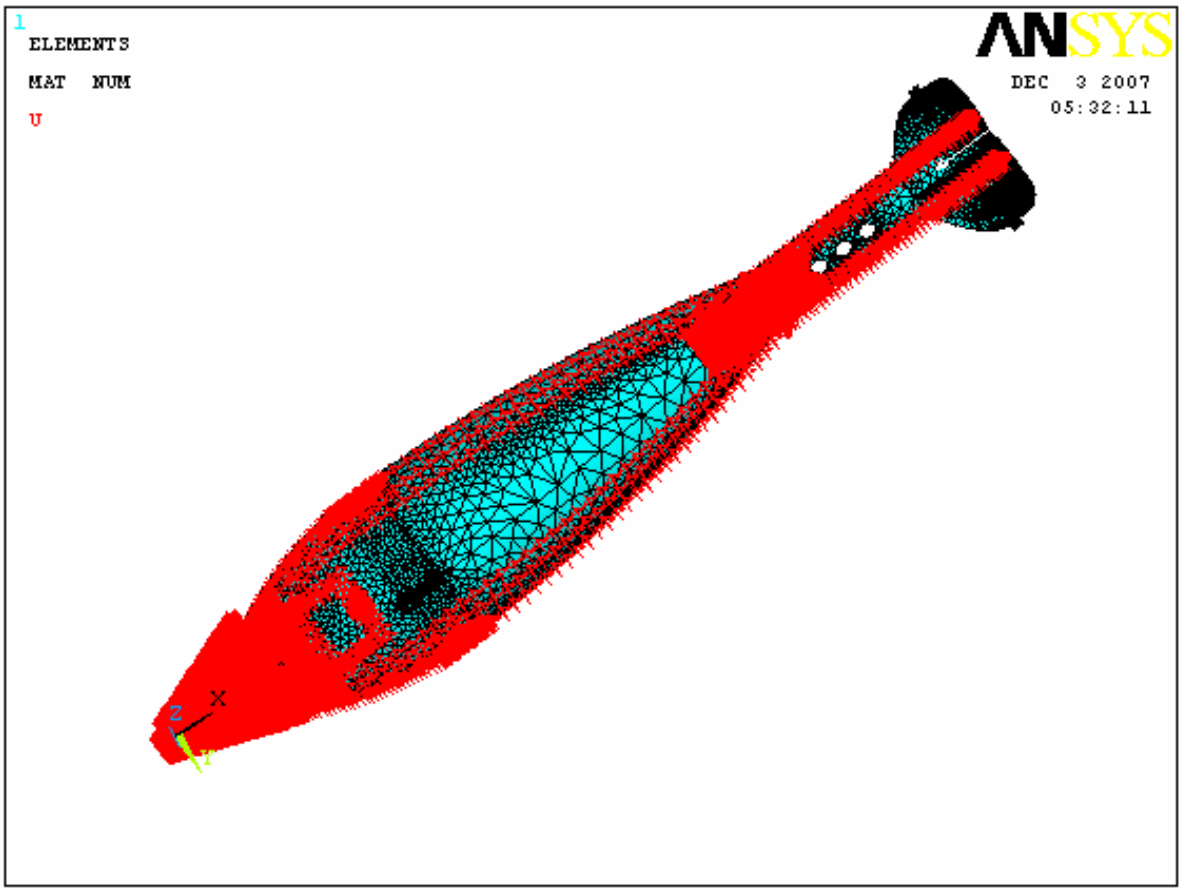

Figure 6.4 Boundary condition and applied load on the half model at impact (case-II)

The plane CD is towards the base end and the plane AB is towards the muzzle end. The planes AC and BD were constrained normal to their plane as discussed in symmetric conditions of the figure. The plane CD is also constrained in the plane normal to its plane because the obturing is fixed and the plane AB is not constrained, which is assumed to be the free end. So accordingly boundary conditions are applied.

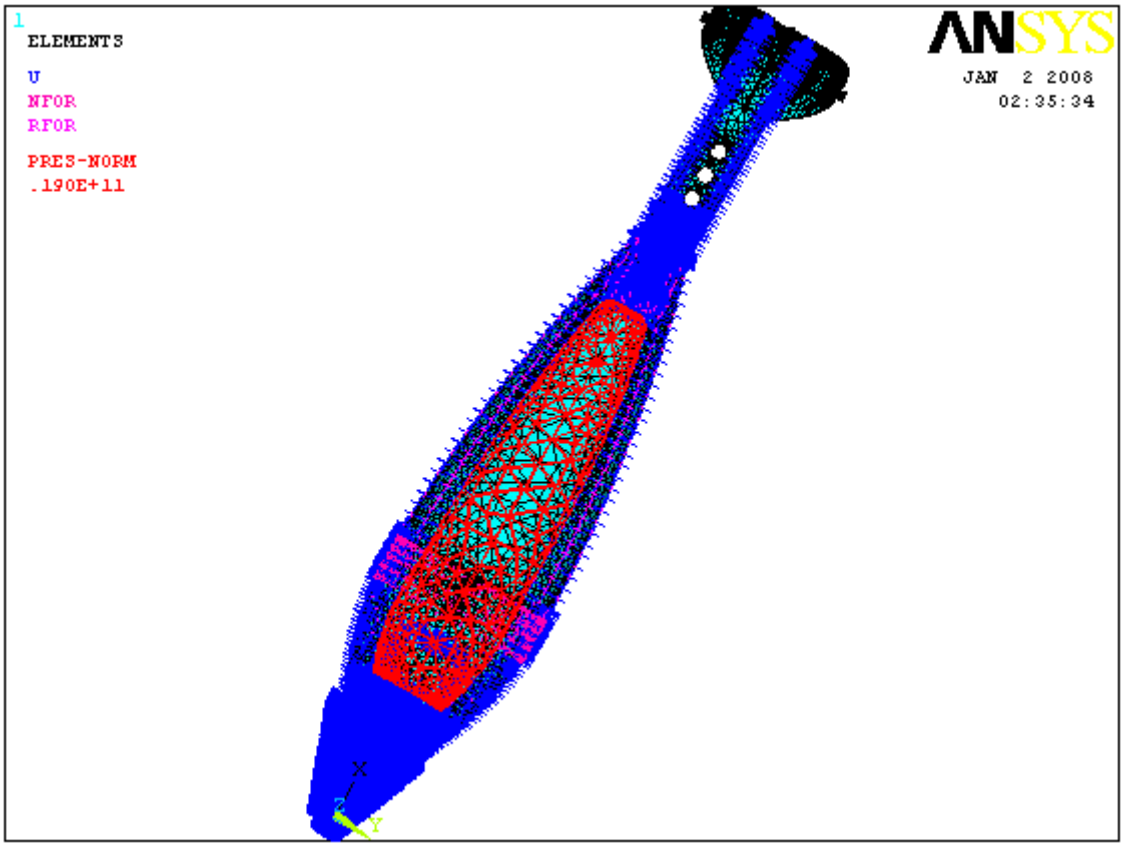

Fig. 6.5 Depicts the half model with boundary conditions and load application for charge filling 'explosion' pressure (Case-III)

The red colour that can be seen in the figure is the loads in the form of uniform internal pressure , which is applied to the internal surface of the half model.

Applied Load

Load was applied to the model as launching pressure from propellant burning gas, impact load hitting the target, bursting pressure, and forces in flight obtained from empirical formulas and ballistic experimental datas. The pressure at the base of the projectile was calculated with the Lagrangian correction for the pressure gradient down the bore. This relation is shown as equation

$$P_b = \frac{P_c}{1 + \frac{C}{2M_P}}$$

in which P_c is the pressure in the chamber, P_b is the pressure at the base of the projectile, c is the mass of the charge, and Mp is the mass of the projectile. It was assumed that the pressure in the primer cavity was less than the maximum chamber pressure because of the short duration of the pulse. As a result, the pressure in the primer cavity was chosen to be the same as the base pressure in figure 6.4. The meshed model of the shell showing the applied maximum pressure loading is presented in figure 6.5.

6.2.3 FEA results of the half model

The finite element model was post-processed to obtain the stress through the thickness of the projectile at the peak pressure as well as the plastic displacement that occurred because of the applied loads. Generalized stress plots were produced to determine the areas of high stress generated during the peak internal pressure. A maximum stress failure criterion was chosen to determine the relative distance from failure. The equation is

$$U.F.S. = \frac{\sigma_{Ultimate}}{\sigma_{in\cdot the\cdot system}} > 1$$

in which $\sigma_{Ultimate}$ is the ultimate tensile strength and σ is the stress in the system. For cases when the stress was negative, the ultimate compressive strength was used. Failure is assumed to occur when the failure criterion equals unity. The factor of safety that existed within the shell because of the applied load was determined by the equation

$$D.F.S. = \frac{\sigma_{Allowed}}{\sigma_{actual}} > 1$$

in which $\sigma_{Allowed}$. is the maximum allowable stress and σ_{actual} is the stress in the system. We obtained the stress through the thickness of the casing by plotting a nodal path midway through the thickness of the shell from the head to the tail. The stress and strains were evaluated for failure at the maximum applied internal pressure.

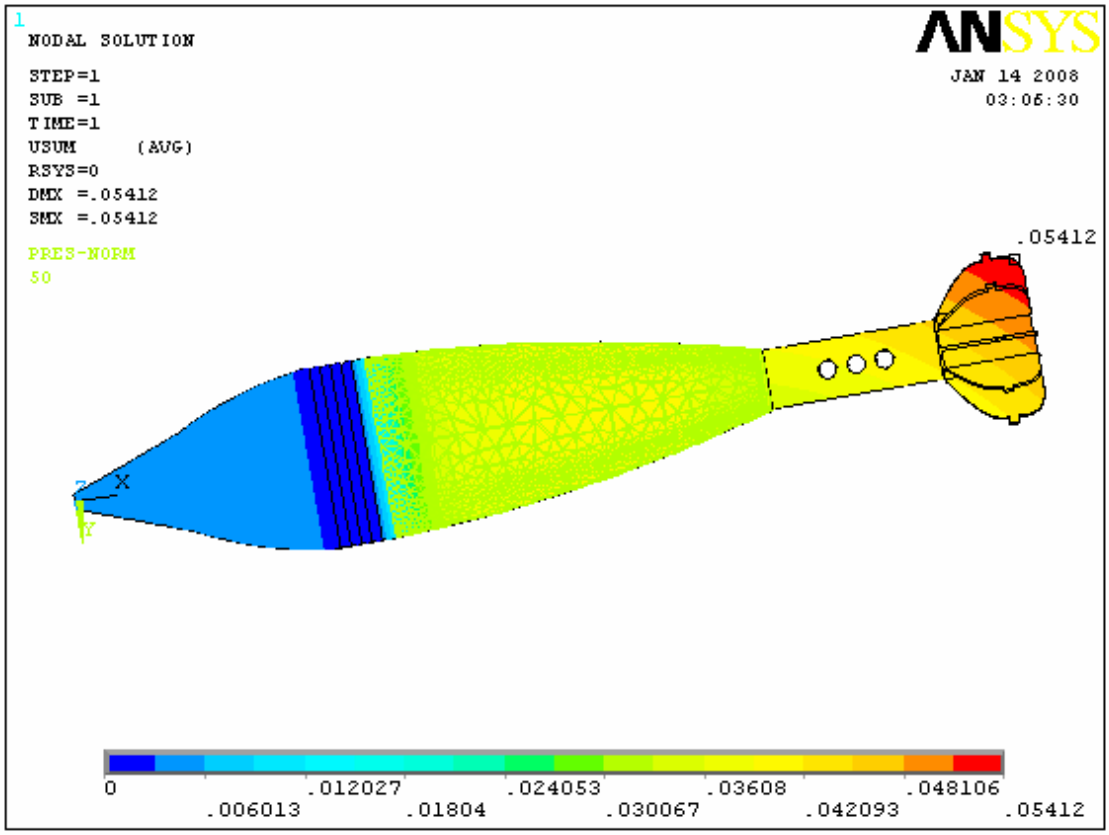

Figure 6.6 Deformation of the half model after FEA

Figure 6.6 depicts the deformation plot of the half model after FEA. It can be observed that the maximum absolute values of deformation from list result given in the table 6 below

Table 6.1 Maximum absolute value of deformation

Maximum absolute value (mm)				
Axes	U_X	U_Y	U_Z	Displacement vector
Node	96924	98200	921	96901
value	0.4254e-01	0.35373e-01	0.33207e-01	0.54123e-01

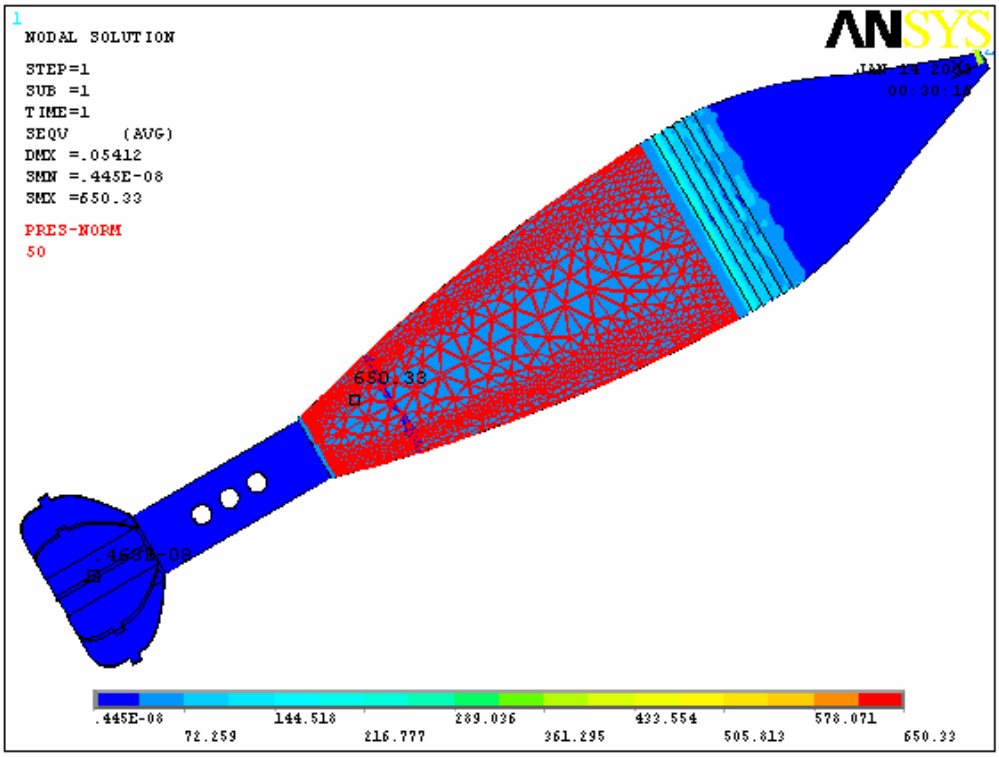

Figure 6.7 Stress distribution due to launching pressure (case-I)

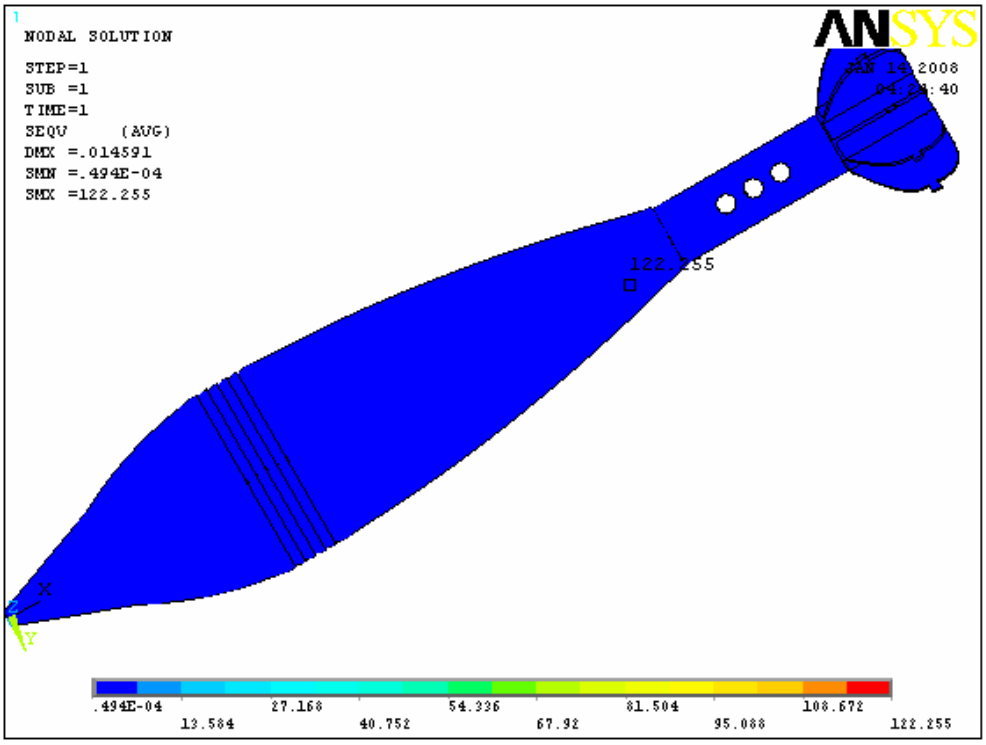

Fig. 6.8 Stress distribution due to impact hitting the target (case-II)

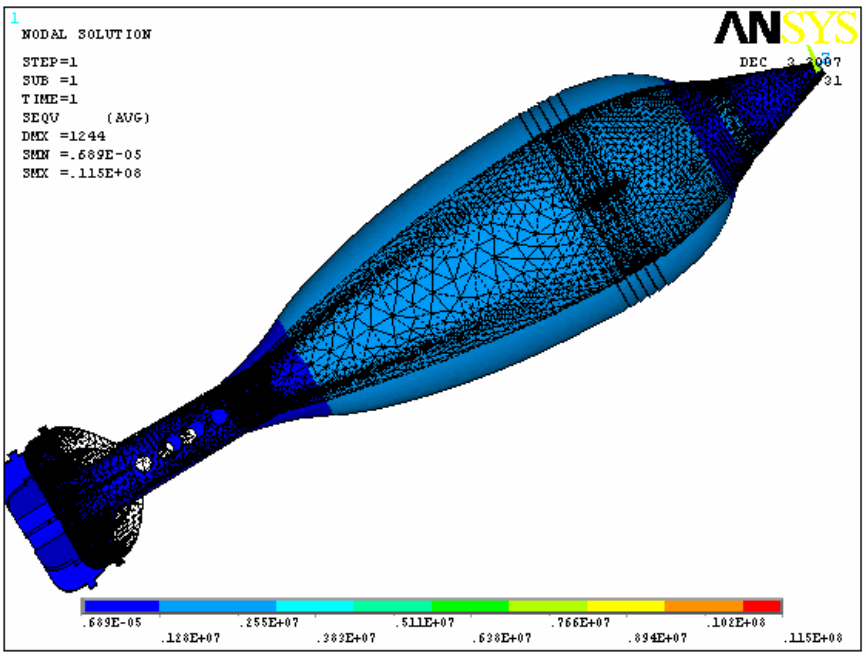

Figure 6.9 Von-mises stress distribution on the half model (deformed + undeformed) (case-III)

Figure 6.9 depicts the contour plot of the Von-Mises stress distribution on the half model after FEA. It was observed that the maximum stresses were induced in the internal surface. The stresses induced along each internal and external surfaces were uniform, which supports the boundary conditions. The list results obtained in all the cases were noted at the end. The stress values from the results at these nodes are tabulated for further study.

It can be observed that from figure the maximum stress induced was at the contact surface of tail tube with casing. The maximum stress induced was in the form of compressive stress with a magnitude of around 402 Mpa at the surface of the shell body and 650 Mpa at the interface of the casing with the tail tube.

6.2.4 Comparison of ANSYS results with high caliber artilleries stress

In this section, the stresses obtained from the analysis of the three-dimensional model using ANSYS is compared with the high explosives ammunition stress values recommended by military standards during the design of HE projectiles. Here the

analysis is carried out with different amount of pressure. The maximum compressive stresses resulted from this analytical solutions are tabulated in table 6.2.

Table 6.2 FEA stress values

Case	Stress developed due to	Pressure load (Mpa)	Max. stress value from ANSYS (Mpa)
I	Pressure due to burning of Propellant	50	on the shell body/casing only 402
			at the interface of shell-tail tube 650
II	Impact load	133N	122.55
III	CJ-pressure of TNT	19Gpa	11e+06

To verify the result obtained from ANSYS it is compared with the HE compressive stress value [1]. The maximum difference between these two outcomes is 16.8 %, therefore the developed FEA models are good enough for the stress analysis.

Table 6.3 Comparisons of maximum compressive stress on the shell

Types of stress	σ [Mpa]	$\sigma_{(ANSYS)}$ [Mpa]	Differences [%]
Compressive stress	334.27	402	16.8

(*stress comparison is based on the available data from literature on casing part only)

6.2.5 Strength failure evaluation of the ANSYS result

In the process of designing a mortar shell, the design has to take precautions to see that the shell under consideration does not fail under loading, launching, flight and impact before bursting conditions.

The failure analysis of a structure was performed by comparing stresses due to applied loads with allowable strengths of the materials. For an isotropic material, such as steel, a simple failure theory is based on finding the maximum stresses induced. These maximum stresses, if greater than that of the yield strength, indicate failure in the material before achieving the required target.

Maximum stress was observed in the bottom surface of the model when subjected to launching. The maximum stress induced was noted to be a compressive stress of 650 MPa. As the maximum stress induced in the shell model is less than the yield strength of the steel, no failure occurred in the model according to the maximum stress theory. The factor of safety of the material can be obtained by dividing the yield strength with the maximum stress induced. The factor of safety of the cast steel was calculated to be 1.47. This factor of safety was acceptable because loads taken into analysis are the projected safe working loads of the real loads.

6.3 Manufacturing a 120mm mortar shell

The final design of the mortar shell was determined with the help of FEA software ANSYS to have a HF-1 cast iron with 120mm external diameter and 17mm thickness and then the next step of this work is to propose manufacturing method with the available machinery in Ethiopia. Manufacturing tolerances and processes with first order aerodynamic forces and moments determine projectile Center of Mass Offset (Causing Torque Forces and Moments), misaligned Fin and Fuze, Offset Center of Mass with respect to Projectile Exterior should be taking into consideration.

There are five basic steps to produce 120mm mortar shell: casting, machining, drilling thread cutting and spot welding processes. And In my visit to Hormat engineering factory this all processes with the design specification can be fulfilled with the available machinery.

CHAPTER 7

7. CONCLUSIONS AND FUTURE WORK

This thesis focused on the study of structural design and analysis of the 120mm mortar shell. The summary and the conclusion of the work and the proposed future work are in the following sub-sections.

7.1 Summary

In this research the following inferences/ results are obtained.

Initially the configuration of the mortar shell was designed and fragment obtained because of Pyro charge is calculated. Using this input a detailed structural design was made and its internal ballistic and trajectory caluclations where enunciated (formulated). These calculations compare well with the existing literature [1]. The investigation on fragmentation analysis by continuum method also proves the utility of this weapon.

The last and most important part of this thesis dealt with F.E analysis of the shell for three different loading conditions. It also may be noted the available literature for stresses in the mortar shell casing is comparable with the first case analysis (which has the same boundary conditions as that of the classical values) of this thesis.

Also it may be noted that the analysis for Pyro-charge pressure (induced immediately after impact) where the whole system should shatter, is also seen in our result.

7.2 Conclusion and future work

Based on the successful result of this work, the design of the 120mm mortar will be forwarded for the fabrication of the shell. This design has the required specifications of the mortar shell needed in Ethiopia. The results of the experimental test are expected to substantiate the proposed theoretical design and analysis. This thesis could be used as a basis for future work to incorporate the other sophistications such as target acquistion, fire control, and digitization. Since mortar design incorporate ammunition and artillery behaviour it can be extended for the study of rocket and missiles design.

Future experimentation at each phase of the design is necessary to draw more definite conclusions.

Refereneces

1. Berko Zecevic, Jasmin Terzic, Alan Catovic, Sabina Serdarevic-Kadic, "Influencing Parameters on HE Projectiles with Natural Fragmentation", Journal of New Trends in Research of Energetic Materials, 2006, Mechanical Engineering Faculty, Defense Technologies Department, Sarajevo, Bosnia and Herzegovina
2. Ponder Timothy C. et.al., "Cylindrical warhead design optimization", Final rept. Jun-Aug 1971, Air Force Armament Lab. EGLIN AFB FL.
3. http://www.globalsecurity.org/militray/systms/ground/mortars.htm
4. www.boomershoot.org/general/AccuracyWind.htm ; extracted 20.06.2004
5. Moss GM, Leeming DW, Farrar CL (1995), "Military Ballistics – A basic manual, Brassey's", London 1995.
6. Beat vogelsanger, "Chemical stability, compatibility and shelf life of explosives", chimia 58 (2004) 401-408.
7. Rinker RA, "Understanding firearm ballistics" ; Mulberry House publishing, Croydon, Indiana 47112, U.S.A.; 2nd revised edition 1998.
8. Karl G. sellier, Beat P. Kneubuehl, "Wound ballistics and the scientific background", Elsevier science B.V. 1194.
9. J. A. cordes, J. kalinowski, D. carlucci, L. reinhardt, S. kerwein, "Design and development gun fired structures", Techinical report, june 2006. U.S. armamnet research, development and engineering center, Picatny arsenal, Newjersey.
10. Anthony J. Calise, Hesham A. El-Shirbiny, "An analysis of aerodynamic control for direct fire spinning projectiles", School of Aerospace, Engineering, Georgia Institute of Technology Atlanta, Georgia 30332
11. S. D Naik, "A note on stability of motion of a projectile", Institute of Armament Technology, Pune, India Vol. 26, Part 4, August 2001, pp. 379–385.
12. Jorma Jussila, "Wound ballistic simulation: Assessment of the legitimacy of law enforcement firearms ammunition by means of wound ballistic simulation", academic dissertation, University of Helsinki, Finland , January 2005.
13. Israel Military Industries ltd. (I.M.I.) ammunition group, "120-mm cargo mortar bombs -complying with the Modern battlefield needs", Motti eis, april 2001.

Bibilography

14. Military handbook, "Manufacture of projectiles, projectile components,and cartridge cases for artillery, tank main armament, and mortars" , april 1991.
15. Robert L. Mccoy, "Modern Exterior ballistics, The launch and flight dynamics of symmetric projectiles", Schoffer Military history, Atgler, PA. March 1998.
16. Lin Zhang†, Xiaogang Jin and Hongliang He, "Prediction of fragment number and size distribution in dynamic fracture", Journal Phys. D: Appl. Phys. 32 (1999) 612–615.
17. J. A. cordes, H. rand, D. carlucci, L. reinhardt, S. kerwein, "Predicting the cause of failure of 120mm mortar fin", techinical report, july 2003. U.S. Armamnet Research, Development and Engineering Center, Picatny arsenal, Newjersey.
18. Michael Dunning, William Andrews, Kevin Jaansalu, "The fragmentation of metal cylinders using thermobaric explosives", Nov 05, Defence Research and Development Canada.
19. Julian K. S. Goh, **"**Analysis of Pressurized Arch-Shells**",** Thesis , Virginia Polytechnic Institute and State University , December, 1998.
20. Explosives",http://www.globalsecurity.org/military/systems/munitions/explosives.htm (2 of 8), 2005.Manual, "82-mm Mortar"
21. "Finite element analysis theory and programming", Second edition , Mc Graw-Hill comp. 1987. Indaian institute of Technology, Madras.
22. Philip J. Magrotti, Jim Tenchune, George Barnych, "Low cost course corection (LCS) for motars information Briefing", 38th Annual Gun, Ammunition and Missiles symposium and Exhibition, 25 March 2003.
23. " Explosives Enginnering", Cooper, W. Roy, Wiley-NCH, Inc.
24. Nennstiel R , "How do bullets fly?" ; AFTE-Journal, Vol. 28, No. 2: 104-143; April 1996
25. "Proof of ordnance, munitions, Armour and explosives", Ministry of Defence Standard 05-101 Part 1 Issue 1 Publication, May 2005. London.
26. "ANSYS Reference guide", S. kariadiselvan, Jan. 2004.

Table 8. Summary of technical data

Technical data of mortar 120 mm	
Mass in flight, kg	17.6
Mass of explosive (TNT), kg	2.9
Mass of body, kg	15
Total length with fuze, mm	640
Thickness, mm	17
Primary charge M74, gm	57
Main charge M74 (6 increment), g	6 x76
Fuze PD with delay M68	UTU M78